MOLECULAR PATHOGENESIS OF VIRAL AND SUBVIRAL AGENTS IN MODEL AND CROP GRASSES

A Thesis

by

JESSE DYLAN PYLE

Submitted to the Office of Graduate and Professional Studies of
Texas A&M University
in partial fulfillment of the requirements for the degree of

MASTER OF SCIENCE

Chair of Committee,	Karen-Beth G. Scholthof
Committee Members,	Herman B. Scholthof
	T. Erik Mirkov
	Wayne Versaw
Head of Department,	Leland S. Pierson III

August 2015

Major Subject: Plant Pathology

ABSTRACT

Viral diseases cause significant agricultural yield losses globally. Because grasses constitute most of our food, forage, and bioenergy sources, the resulting economic losses caused by grass-infecting viruses are particularly devastating. However, the lack of an established genetic model for grasses has generally hindered investigation of grass-virus molecular interactions, leading to a gap in our knowledge of monocot virology.

In this study, the issue of the monocot virology knowledge gap is addressed at the levels of both the laboratory and the field. Two candidate grasses, *Brachypodium distachyon* (Brachypodium, a C_3 grass) and *Setaria viridis* (Setaria, a C_4 grass), were established as monocot model hosts for seven small RNA viruses in diverse genera. Aspects of the host disease response were characterized, including agronomically relevant phenotypic perturbations and expression profiles of defense hormone marker genes in salicylic acid, jasmonic acid, and ethylene signaling pathways. This comparative viromics approach revealed conserved and host-dependent defense hormone signaling responses to the diverse viral agents, as well as virus-specific responses between the C_3 and C_4 model hosts. Further, Brachypodium and the food crop *Panicum miliaceum* (proso millet) were utilized as laboratory models for investigating novel molecular features of *Panicum mosaic virus* (PMV), its associated satellite virus (SPMV), and satellite RNAs (satRNAs), the collective causal agents of the turfgrass disease known as St. Augustine Decline. A satRNA of PMV isolated from *Stenotaphrum* *secundatum* (St. Augustinegrass), satS, attenuates the normal disease phenotype induced by its PMV helper virus and actively acquires ~100-200 nucleotides from the 3′-end of the PMV helper virus RNA genome. This symptom attenuation and sequence acquisition is associated with host-dependent reductions in the systemic accumulation of helper virus RNA and capsid protein. Brachypodium and proso millet were also used to characterize the *de novo* polyadenylation of PMV and its subviral agents. The polyadenylated PMV RNAs resemble byproducts of a poly(A)-mediated RNA degradation pathway. Lastly, we report on the re-emergence of PMV and SPMV as the predominant viral pathogens of cultivated switchgrass in Nebraska. The Summer-based switchgrass varieties were more susceptible to PMV and PMV+SPMV infections, compared to Kanlow-based varieties. The susceptible varieties were more severely affected by the disease. Overall this study investigates questions of host-virus interactions, both in the laboratory and the field, and presents new findings on the topic of grass RNA virus biology.

DEDICATION

In loving memory of my uncle, Bill Henry

ACKNOWLEDGMENTS

I would first like to thank my committee chair, Dr. Karen-Beth Scholthof, and my committee members, Drs. Herman Scholthof, Erik Mirkov, and Wayne Versaw, for their guidance and support throughout the duration of my graduate studies.

To Karen and Herman, these past five years in the lab have been incredibly influential and formative in the development of my current interests and long-term career goals. Thank you for giving me the opportunity as a sophomore undergraduate student (with minimal knowledge of plant pathology or virology) to join your research group and discover my passion for science. I am forever grateful for the opportunity to work with such outstanding educators. Most of all, thank you for getting me hooked on the fascinating field of virology!

I would also like to recognize Dr. Kranthi Mandadi as my stupendous mentor in the lab. Kranthi and I worked side-by-side at the lab bench for several years, and he has taught me so much about proper techniques in molecular biology and the analysis, interpretation, and presentation of data. Thank you for all the great memories, as both my mentor and a good friend.

I would like to thank my close friends Will Cody, Robert Dorosky, Ken Wang, Philip Stephenson, Jennifer Graham, Matt Elliott, and Grant Brown for the fun times and for keeping me sane during my graduate studies. I couldn’t have asked for a better group of friends.

Last but certainly not least, I would like to thank my mother Janet, my father John, and my sister Sierra, for their love and encouragement throughout this process. Thank you for putting up with my countless rambling conversations about plants, viruses, and science in general. I love you all and thank you for being so supportive of me during my graduate studies.

TABLE OF CONTENTS

LIST OF FIGURES

LIST OF TABLES

Page

1. INTRODUCTION

1.1 BRIDGING THE MONOCOT KNOWLEDGE GAP

Viral pathogens have a significant impact on agricultural production each year. With the global population predicted to exceed 9.1 billion in the year 2050, the Food and Agriculture Organization estimates that global agricultural production must increase by 70% to meet growing demands for food, with developing nations almost doubling their current production (FAO, 2009; Graham-Rowe, 2011). Cereals constitute most of our staple foods including wheat (*Triticum aestivum*), rice (*Oryza sativa*), and maize (*Zea mays*). Other notable cultivated grass species, including sorghum (*Sorghum bicolor*), millets (*Panicum*, *Pennisetum*, and *Setaria* spp.), switchgrass (*Panicum virgatum*), and sugarcane (*Saccharum* spp.) provide valuable forage and biofuel resources. With the global economic importance of these monocotyledonous (monocot) crop species, the yield losses resulting from grass-infecting viral pathogens are particularly devastating. Despite these issues, we currently know very little about the field pathogenesis of grass-infecting viruses.

Historically, due to the lack of genetically amenable model monocot hosts, the molecular biology of plant viruses has been investigated using primarily dicotyledonous (dicot) plants, such as *Arabidopsis thaliana* (Arabidopsis) and *Nicotiana benthamiana*. In fact, the molecular pathogenesis of some of the most economically damaging and best-studied grass-infecting viruses has been elucidated using non-native dicot host species. As a result, there is a gap that exists in our knowledge of monocot molecular virology (Mandadi and Scholthof, 2013). While Arabidopsis continues to serve as an excellent model for the plant biology community, certain biological questions, specifically those regarding monocot host-pathogen interactions, require additional experimental systems.

Recently, akin to Arabidopsis, two grass species have been developed as laboratory models for monocot biology. *Brachypodium distachyon* (Brachypodium) is a small grass that has emerged as a system for functional genomics in the cool season grasses (Draper et al., 2001; Brkljacic et al., 2011). Brachypodium possesses many qualities of an ideal model system, including a small and sequenced genome, available yeast two-hybrid libraries, methods for *Agrobacterium*-mediated transformation, and a growing number of T-DNA insertion mutant lines (Vogel and Hill, 2008; Cao et al., 2011; Bragg et al., 2012). The diploid genome of Brachypodium is relatively small (5 chromosomes, 272 Mbp) in comparison to other sequenced grasses such as hexaploid wheat (7 chromosomes, ~17 Gbp), diploid rice (12 chromosomes, 372 Mbp), and diploid maize (10 chromosomes, ~2.5 Gbp), making Brachypodium a suitable candidate for comparative functional genomics studies (Ouyang et al., 2007; Eckardt, 2008; Brenchley et al., 2012). Additionally, Brachypodium is short in stature, has a rapid seed-to-seed generation cycle, and is easy to cultivate in the laboratory. Similar to Brachypodium, *Setaria viridis* (Setaria), commonly known as green foxtail millet, has emerged as a developing model for C_4 photosynthesis (Brutnell et al., 2010; Li and Brutnell, 2011; Bennetzen et al., 2012). Setaria also possesses many of the necessary traits of a model plant, including a small (~510 Mbp), sequenced genome, rapid generation time, ease of cultivation, and is amenable to *Agrobacterium*-mediated transformation (Brutnell et al., 2010). With the emergence of both Brachypodium (a C_3 grass) and Setaria (a C_4 grass) as model laboratory organisms, comparative evolutionary genomics studies are now facilitated for the monocots. Given the threat of viral pathogens to many economically important grasses and cereals, a comparative analysis of host responses to viral infections, using Brachypodium and Setaria, would advance our understanding of the evolution of grass antiviral defense responses.

1.2 THE *PANICOVIRUS* DISEASE COMPLEX: A MODEL FOR RNA VIRUS PATHOGENESIS

In general, many positive-sense single-stranded RNA (+ssRNA) viruses exploit similar mechanisms to hijack the host cell during infection. However, genetically diverse +ssRNA viruses can induce vastly different disease phenotypes during infection of the same host genotype, resulting in varied levels of yield losses in the field. These underlying determinants of viral pathogenicity and aggressiveness are important for understanding the mechanisms of disease induction and progression within the host plant. An interesting phenomenon for plant virology, in comparison to animal or bacterial virology, is the somewhat common occurrence of diverse subviral agents, including satellite viruses and satellite nucleic acids. We know little about the roles and mechanisms of these subviral agents in the induction of disease. The *Panicovirus* disease complex provides a unique model for the elucidation of these host-RNA virus interactions. *Panicum mosaic virus* (PMV) is a small (~30 nm) T=3 icosahedral +ssRNA virus that infects a narrow range of grasses in the *Poaceae*. PMV was first recognized as a pathogen of switchgrass in 1953, and was later identified as the causal agent of St. Augustine Decline disease of St. Augustinegrass (*Stenotaphrum secundatum*) (Sill and Pickett, 1957; Lee et al., 1973; Niblett and Paulsen, 1975). The genomic RNA of PMV is 4,326 nt in length, has six open reading frames (ORFs), and is known to lack a 5′-cap and 3′-polyadenylation sequence (Turina et al., 1998). At its 5′-most end, PMV encodes two replication-associated proteins, p48 and p112, with p112 translated as a result of a leaky amber stop codon (UAG) at position 1306 (Figure 1.1A) (Batten et al., 2006a). Downstream of the replicase complex, PMV encodes three short ORFs (p8, p6.6, and p15), collectively known as the triple gene block, which encode for proteins that are associated with cell-to-cell viral movement (Turina et al., 2000). The p26 ORF encodes for the PMV capsid protein (CP).

Interestingly, the replication machinery of PMV supports the replication of two types of subviral agents: an RNA satellite virus (SPMV) and two satellite RNAs (satRNAs) (Figure 1.1B-C). The +ssRNA genome of SPMV is 826 nt in length. SPMV encodes a CP (SPCP) as the only known gene product (Figure 1.1B) for encapsidation of its genomic RNA within ~17 nm T=1 icosahedral virions (Masuta et al., 1987). During a co-infection with the PMV helper virus, SPMV is known to induce a severe disease synergism in the host plant, characterized by exacerbated disease symptoms in the host plant and rapid systemic accumulation of the viruses, compared to infection by PMV alone (Scholthof, 1999). This is likely a result of the multifunctional role of SPCP (Scholthof, 1999; Qi et al., 2008; Mandadi and Scholthof, 2012).

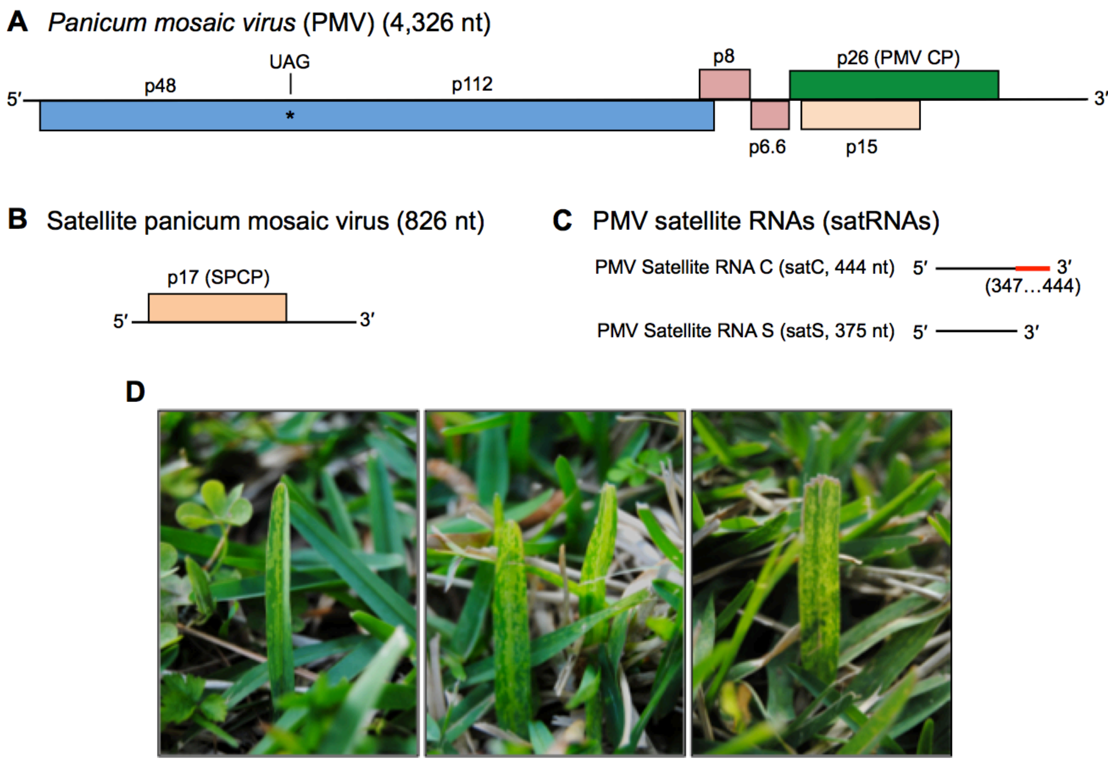

Figure 1.1. The *Panicovirus* disease complex. Illustrations of the RNA genomes of PMV (A), SPMV (B), and the PMV satellite RNAs (C) are depicted. PMV encodes two replication-associated gene products (p48 and p112), three gene products associated with cell-to-cell virus movement (p8, p6.6, and p15) and a viral capsid protein (p26). SPMV encodes its own capsid protein (p17). The PMV satRNAs do not encode any known gene products. SatC has a high degree of sequence similarity at its 3′-end (nt 347-444) with the 3′-end of the PMV genomic RNA (indicated by the red line). Together, these agents induce symptoms that are typically associated with St. Augustine Decline disease of St. Augustinegrass (D).

Two satRNAs, satellite RNA S (satS) and satellite RNA C (satC), have been identified in association with infection by PMV during natural infections of St. Augustinegrass and centipedegrass (*Eremochloa ophiuroides*), respectively (Monis et al., 1992; Cabrera and Scholthof, 1999; Cabrera et al., 2000). SatS and satC are single-stranded RNA molecules of 375 nt and 444 nt in length, respectively (Figure 1.1C). At their 5′-ends (nt 1-375), satS and satC have a high degree (73.6%) of sequence identity. Interestingly, the 3′-end (nt 347-444) of satC is nearly identical (87.6%) to the 3′-end (nt 4,229-4,326) of the PMV genomic RNA (Figure 1.1A and 1.1C, unpublished data). The roles of the PMV satRNAs during a co-infection with the helper virus remain unknown. PMV, alone or in association with either of its satellite agents (SPMV and/or satRNAs), is found ubiquitously along the U.S. Gulf Coast region as the causal agent(s) of St. Augustine Decline (Figure 1.1D) (Cabrera and Scholthof, 1999). It is estimated that homeowners in the U.S. with PMV-infected St. Augustingrass lawns waste an estimated 2.2 billion cubic meters of water annually, in attempts to revive their lawn from the viral infection–enough water to fill almost 900,000 Olympic-size swimming pools. In addition to unnecessary over-watering, PMV-infections also account for an estimated 24,000 metric tons of overused nitrogen fertilizer. Understanding the molecular pathogenicity of all members of the *Panicovirus* disease complex will be essential for controlling disease in the field and reducing the unnecessary wasting of these valuable resources.

1.3 PROJECT DESCRIPTION AND SPECIFIC AIMS

My intent is to enhance my understanding of the interactions that occur between host and pathogen, specifically in the context of grass-virus interactions. The major objective of my graduate research is the characterization of the molecular features of viral pathogens and host responses to disease, both in the laboratory and in the field. I also aim to better understand the interactions that occur between a virus and its subviral agents, along with additional molecular features that may contribute to the pathogenesis of RNA viruses. I have outlined three specific aims:

1) To establish Brachypodium (a C_3 grass) and Setaria (a C_4 grass) as model monocot hosts for studying viral diseases of grasses.
2) To utilize Brachypodium and *Panicum miliaceum* (proso millet) for the characterization of two satRNAs associated with PMV, and to investigate the role of RNA polyadenylation in the pathogenicity of PMV and its satellite agents.
3) To investigate PMV and SPMV as re-emerging pathogens of bioenergy switchgrass.

2. COMPARATIVE ANALYSIS OF ANTIVIRAL RESPONSES IN *BRACHYPODIUM DISTACHYON* AND *SETARIA VIRIDIS* REVEALS CONSERVED AND UNIQUE OUTCOMES AMONG C_3 AND C_4 PLANT DEFENSES*

2.1 OVERVIEW

Viral diseases cause significant losses in global agricultural production, yet little is known about grass antiviral defense mechanisms. We previously reported on host immune responses triggered by *Panicum mosaic virus* (PMV) and its satellite virus (SPMV) in the model C_3 grass *Brachypodium distachyon* (Brachypodium). To aid comparative analyses of C_3 and C_4 grass antiviral defenses, here we establish Brachypodium and *Setaria viridis* (Setaria, a C_4 grass) as compatible hosts for seven grass-infecting viruses including PMV and SPMV, *Brome mosaic virus*, *Barley stripe mosaic virus*, Maize mild mottle virus, Sorghum yellow banding virus, *Wheat streak mosaic virus* (WSMV) and *Foxtail mosaic virus* (FoMV). Etiological and molecular characterization of the fourteen grass:virus pathosystems showed evidence for conserved crosstalk among salicylic acid (SA), jasmonic acid and ethylene pathways in Brachypodium and Setaria. Strikingly, expression of *PHYTOALEXIN DEFICIENT4,* an upstream modulator of SA signaling, was consistently suppressed during most virus

---

* Reprinted with permission from "Comparative analysis of antiviral responses in *Brachypodium distachyon* and *Setaria viridis* reveals conserved and unique outcomes among C3 and C4 plant defenses." by Mandadi, K. K., Pyle, J. D., and Scholthof, K.-B. G., 2014. Mol. Plant-Microbe Interact. 27:1277-1290, Copyright [2014] by The American Phytopathological Society.

infections in Brachypodium and Setaria. Hierarchical clustering analyses further identified unique antiviral responses triggered by two morphologically-similar viruses, FoMV and WSMV, and uncovered other host-dependent effects. Together, this study establishes Brachypodium and Setaria as models for the analysis of plant:virus interactions, and provides the first framework for conserved and unique features of C_3 and C_4 grass antiviral defenses.

2.2 INTRODUCTION

Viral diseases of grasses cause significant losses in global agricultural production and productivity. The Food and Agriculture Organization (FAO) estimate of cereal yields for 2013 was 2,521 million metric tons (Mtons). In the US alone, *Wheat streak mosaic virus* (WSMV) is a serious threat to wheat (*Triticum asestivum*) production (French and Stenger, 2003) and is responsible for an estimated 3 Mtons of yield loss in 2012 (FAO.org). WSMV can spread quickly via its mite vector resulting in localized yield losses of up to 100% in the infected fields (Navia et al., 2013). *Barley stripe mosaic virus* (BSMV) causes yield losses up to 64% and 75% in barley (*Hordeum vulgare*) and wheat, respectively, and remains a potential threat to cultivated oat (*Avena sativa*) (Hagborg, 1954; Donald and Jackson, 1994; Jackson et al., 2009). Similarly, *Panicum mosaic virus* (PMV) causes significant grain losses in millets including proso millet (*Panicum miliaceum*), foxtail millet (*Setaria italica*) and pearl millet (*Pennisetum glaucum*). PMV is also ubiquitous along the Gulf Coast region of the US and is the causal agent of St. Augustine Decline disease of St. Augustinegrass (*Stenotaphrum *secundatum*) (Cabrera and Scholthof, 1999). Homeowners with PMV-infected St. Augustinegrass lawns waste an estimated 2.2 billion cubic meters of water annually in attempts to revive their lawns from the viral infection - enough water to fill almost 900,000 Olympic-size swimming pools. In addition to unnecessary over-watering, PMV infections also account for an estimated 54.5 million pounds of overused nitrogen fertilizer (24,000 metric tons). A recent survey of switchgrass (*Panicum virgatum*) breeding plots in Nebraska found PMV infecting upwards of 75% of switchgrass plots (Stewart et al., 2013), suggesting PMV as a potential threat to the biofuel industry. Although not much data is available for crop losses caused by other grass-infecting viruses such as *Brome mosaic virus* (BMV), *Foxtail mosaic virus* (FoMV), Maize mild mottle virus (MMMV) or Sorghum yellow banding virus (SYBV) that infect wheat, barley, maize (*Zea mays*), millets and sorghum (*Sorghum bicolor*), the cumulative economic losses due to grass viral diseases could run into hundreds of millions of dollars annually. Even with progress in identification of resistance gene loci in rice (*Oryza sativa*), barley, maize, and wheat (Trottet and Gouis, 2004; Redinbaugh and Pratt, 2009), and success in breeding resistance against some cereal-infecting viruses, there are significant gaps in our knowledge of the molecular mechanisms of monocotyledonous (monocot) host responses to virus infection (Mandadi and Scholthof, 2012, 2013).

Our knowledge of plant defense mechanisms has significantly advanced over the past decade, but much of it pertains to bacterial, fungal, and to a lesser extent viral diseases, that infect dicotyledonous (dicot) plants such as Arabidopsis (*Arabidopsis thaliana*), *Nicotiana benthamiana,* and tomato (*Solanum lycopersicum*) (Huang et al., 2005; Whitham et al., 2006; Ascencio-Ibáñez et al., 2008; Alvarado and Scholthof, 2009; Hanssen et al., 2011; Jakubiec et al., 2012; Love et al., 2012; Pacheco et al., 2012; Postnikova and Nemchinov, 2012). Only a handful of studies are related to monocot antiviral responses (Ventelon-Debout et al., 2003; Albar et al., 2006; Shimizu et al., 2007; Satoh et al., 2010; Jia et al., 2012; Mandadi and Scholthof, 2012, 2013), despite grasses being the primary sources of our food, forage, and bioenergy needs. This knowledge gap is primarily due to the lack of a tractable genetic model for monocots. Agronomic grasses including rice, maize, barley, wheat, oat, and sorghum are difficult to grow in the laboratory, require substantial greenhouse space, and have long seed-to-seed lifecycles. Recently, owing to advances in genomics and sequencing initiatives, akin to Arabidopsis, genetically tractable grasses such as *Brachypodium distachyon* (Brachypodium, a C_3 grass) and *Setaria viridis* (Setaria, a C_4 grass) have gained the status of model grasses because of their high degree of genome collinearity and phylogenetic relatedness to the field grasses (Figure 2.1) (Brutnell et al., 2010; Bennetzen et al., 2012). In addition, both Brachypodium and Setaria fulfill the requisite traits needed in a model plant, including small stature, rapid seed-to-seed life cycle, small and fully-sequenced genomes, and ease of *Agrobacterium*-mediated transformation. The functional genomic and genetic resources for Brachypodium also include diverse geographical accessions, mutant collections, and yeast two-hybrid libraries (Brutnell et al., 2010; International Brachypodium Initiative, 2010; Brkljacic et al., 2011; Cao et al., 2011; Mur et al., 2011; Bennetzen et al., 2012).

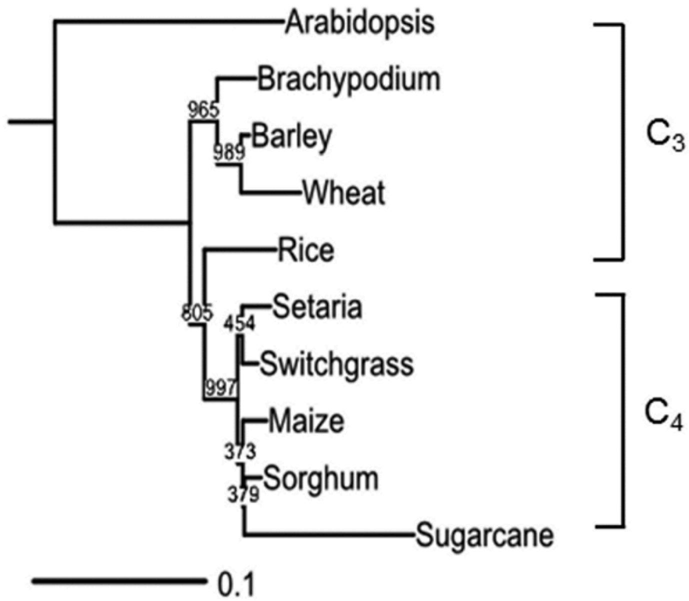

Figure 2.1. Phylogenetic relationships of the C_3 and C_4 grasses and Arabidopsis. The species tree was constructed by multiple sequence alignment of a ca. 1000 amino acid-long concatenated super sequence corresponding to six conserved proteins from the different grasses and Arabidopsis. These sequences represent SAM decarboxylase, glyceraldehyde-3-phosphate dehydrogenase, chlorophyll a/b-binding protein P26, catalase, α-tubulin, and heat shock protein70 (Vogel et al., 2006). Bootstrap results for 1000 replicates are shown at the nodes and the branch lengths indicate genetic distances.

We and others have used Brachypodium to investigate antiviral immune responses triggered by PMV (Mandadi and Scholthof, 2012) and BSMV (Cui et al., 2012). BSMV is a positive-sense, single-stranded (ss) RNA virus with a tripartite genome and is the type member of the *Hordeivirus* genus in the family *Virgaviridae* (Donald and Jackson, 1994; Bragg and Jackson, 2004; Jackson et al., 2009). Using Brachypodium as a host, Cui et al. (2012) identified the first dominant *R* gene (*BSR1*) in grasses that confers resistance against BSMV. The resistance is accompanied by a hypersensitive response and necrosis-like symptoms and is presumed to be a result of interaction between the putative Brachypodium BSR1 protein and the BSMV Triple Gene Block 1 (TGB1) movement protein (Cui et al., 2012; Lee et al., 2012).

PMV is a positive-sense ssRNA virus that is the type member of the *Panicovirus* genus in the family *Tombusviridae* and infects several *Poaceae* grasses (Turina et al., 1998; Turina et al., 2000). PMV also supports the replication of a ssRNA satellite virus, SPMV (Scholthof, 1999), and satellite RNAs (Cabrera and Scholthof, 1999; Cabrera et al., 2000). PMV+SPMV infection results in a unique synergism that is characterized by severe disease symptoms in the host plants. Taking genomic approaches, we analyzed transcriptomic changes occurring in Brachypodium in response to infection by PMV and PMV+SPMV (Mandadi and Scholthof, 2012). From this, we identified both conserved and unique grass antiviral defense responses compared to dicot antiviral responses. For example, during PMV or PMV+SPMV infection, multiple genes in salicylic acid (SA) hormone production and signaling including *SALICYLIC ACID INDUCTIONDEFICIENT2/ISOCHORISMATE SYNTHASE1, ALTERNATE OXIDASE1A* (*AOX1A*), WRKY transcription factors and pathogenesis-related (PR) proteins were up-regulated, while components of jasmonic acid (JA) and ethylene (ET) signaling *LIPOXYGENASE2* (*LOX2*), *ALLENE OXIDE SYNTHASE* (*AOS*), *FATTY ACID DESATURASE7* (*FAD7*)*, VEGETATIVE STORAGE PROTEIN1* (*VSP*) and *ETHYLENE RESPONSE FACTOR* (*ERF)* were down-regulated. These results also support the existing concept of SA-JA crosstalk, which is largely based on studies of dicot hosts (Pieterse et al., 2012; Thaler et al., 2012). Whether the SA-JA crosstalk is a conserved feature among other grass:virus interactions and among other grass clades (e.g., C_3 vs C_4 species) is not known.

To facilitate comparative analyses of antiviral defense responses, we established Brachypodium (a C_3 grass) and Setaria (a C_4 grass) as amenable host platforms for seven agronomically important grass-infecting viruses in diverse genera including PMV (Genus: *Panicovirus*) and SPMV, BSMV (Genus: *Hordeivirus*), BMV (Genus: *Bromovirus*), WSMV (Genus: *Tritimovirus*), FoMV (Genus: *Potexvirus*), MMMV (Genus: putative *Panicovirus*) and SYBV (Genus: unknown) (Table 2.1). We characterized disease etiology, phenotypic perturbations, and gene expression changes of

Virus	Genus	Family	Genome	Structure	Host range
Panicum mosaic virus (PMV)	*Panicovirus*	*Tombusviridae*	Monopartite, ssRNA (+)	Icosahedral (T=3)	Bd, Sv, foxtail, proso, pearl, wheat, maize, switchgrass
satellite panicum mosaic virus (SPMV)	NA	NA	Monopartite, ssRNA (+)	Icosahedral (T=1)	Bd, Sv, foxtail, proso, pearl, wheat, maize, switchgrass
Barley stripe mosaic virus (BSMV)	*Hordeivirus*	*Virgaviridae*	Tripartite, ssRNA (+)	Rigid rod	Bd, Sv, Nb, barley, wheat, oat
Brome mosaic virus (BMV)	*Bromovirus*	*Bromoviridae*	Tripartite, ssRNA (+)	Icosahedral (T=3)	Bd, Sv, Nb, foxtail, barley, wheat, maize, oat
Maize mild mottle virus (MMMV)	Unassigned	Unassigned	Monopartite, ssRNA (+)	Icosahedral (T=?)	Bd, Sv, foxtail, pearl, maize, wheat, barley, sorghum
Sorghum yellow banding virus (SYBV)	Unassigned	Unassigned	?	Icosahedral (T=?)	Bd, Sv, foxtail, proso, pearl, maize, sorghum
Wheat streak mosaic virus (WSMV)	*Tritimovirus*	*Potyviridae*	Monopartite, ssRNA (+)	Flexuous rod	Bd, Sv, wheat, maize, barley
Foxtail mosaic virus (FoMV)	*Potexvirus*	*Alphaflexiviridae*	Monopartite, ssRNA (+)	Flexuous rod	Bd, Sv, Nb, proso, foxtail, sorghum, barley, wheat, oat

Table 2.1. Grass viruses used in the current study. Virus names in italics have been designated as species by the International Committee for Virus Taxonomy (ICTV). Bd – *Brachypodium distachyon* (current study)*,* Sv – *Setaria viridis* (current study), Nb – *Nicotiana benthamiana*, foxtail – foxtail millet (*Setaria italica*), proso – proso millet (*Panicum miliaceum*), pearl – pearl millet (*Pennisetum glaucum*), switchgrass – *Panicum virgatum*, T – triangulation number, ? – not known, (+) – positive-sense, ssRNA – single stranded RNA.

thirteen defense markers in SA, JA, and ET signaling in the fourteen grass:virus combinations. Our analyses uncovered conserved, virus-specific and host-dependent alterations in defense responses, as well as antagonistically modulated SA-JA defense components in C_3 and C_4 grass types during virus infection.

2.3 RESULTS

2.3.1 Brachypodium and Setaria are Hosts for Diverse Monocot-infecting Viruses

The PMV+SPMV co-infection induces severe symptoms of chlorosis and necrosis on leaves, decreases seed-set and causes stunting and overall loss of biomass in Brachypodium (Mandadi and Scholthof, 2012). These symptoms mimic those of PMV+SPMV infection on field grasses such as pearl millet (Scholthof, 1999), proso millet (Buzen et al., 1984) and switchgrass (Sill and Pickett, 1957). To test if Brachypodium is a host for other grass-infecting viruses, we selected six additional viruses from diverse genera with wide host ranges. These include BSMV, BMV, MMMV, SYBV, WSMV and FoMV (Table 2.1). Brachypodium plants at the 2-3 leaf stage were inoculated with the different viruses and the disease progression was monitored up to 42 days post-inoculation (dpi). To be consistent in the interpretation of results of independent infections, we established a timeline for the disease progression based on the extent of phenotypic symptoms on systemically-infected plants. The diseased phenotypes at stages I (10 dpi), II (21 dpi) and III (42 dpi) are characterized by mild, moderate, and severe chlorosis or necrosis symptoms, respectively. In agreement with our previous findings (Mandadi and Scholthof, 2012), PMV+SPMV infection induced symptoms of chlorosis and necrosis on upper non-inoculated leaves as early as stage I and stunted the infected plants by stage II (Figure 2.2 and Supplementary Figure 2.1). Infections of BSMV, WSMV, and FoMV also induced similar symptoms of chlorosis and necrosis on leaves by stage I and reduced the overall plant height by stage II. BMV and MMMV were the most aggressive viruses causing severe necrosis on both inoculated and non-inoculated leaves by stage I and decimating the plants shortly after stage II (Figure 2.2, Supplementary Figure 2.1). In WSMV and FoMV infections, although symptoms were less severe than those caused by BMV or MMMV infections, the diseased Brachypodium plants died shortly after stage II. In contrast to the other virus infections, symptoms on SYBV-infected Brachypodium were slow to appear with only mild chlorosis at stage II, which became more prominent by stage III. The effects of SYBV infection on plant height and biomass were moderate upon visual inspection (Figure 2.2, Supplementary Figure 2.1). The infectivity rate, as determined by the presence of visual chlorosis or necrosis symptoms on the diseased plants, for BSMV,

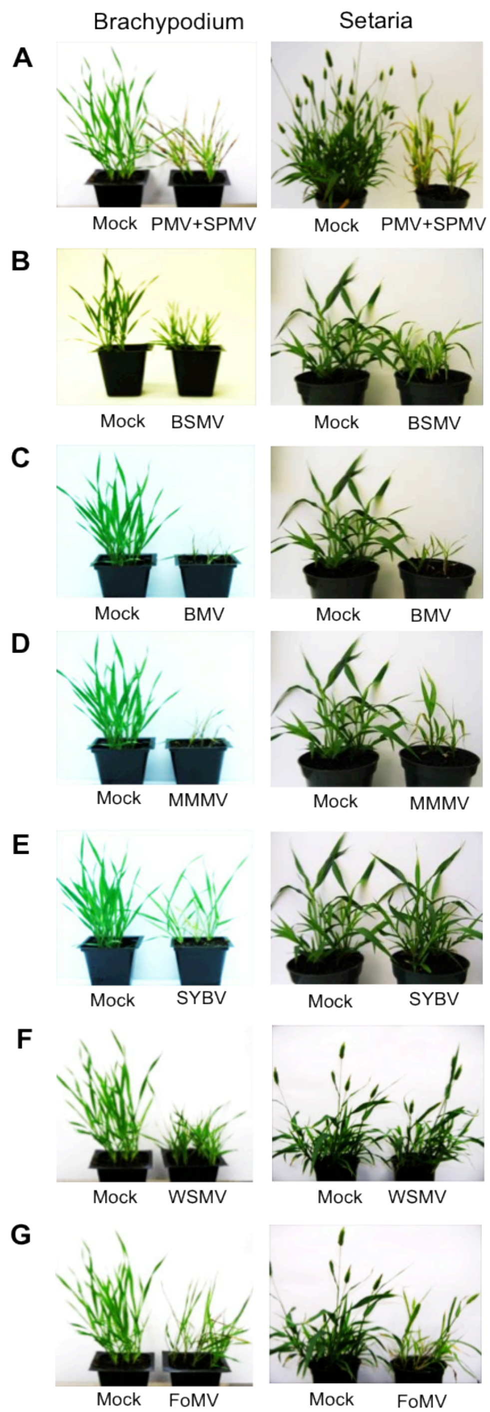

Figure 2.2. Typical disease symptoms of virus-infected *Brachypodium distachyon and Setaria viridis*. Symptoms induced by (A) PMV+SPMV, (B) BSMV, (C) BMV, (D) MMMV, (E) SYBV, (F) WSMV, and (G) FoMV in Brachypodium and Setaria at 21 days post-inoculation. All viruses, with the exception of SYBV, caused prominent chlorosis and necrosis of leaves and severe stunting of plant height.

BMV, SYBV, WSMV, and FoMV infections of Brachypodium was 100%, while PMV+SPMV and MMMV infections resulted in 95% and 90% infectivity rate, respectively.

To enable comparative analyses of antiviral responses between C_3 and C_4 grass types, we tested if *Setaria viridis* (green foxtail millet) would be a likely candidate. Setaria plants at the 2-3 leaf stage were inoculated with the seven viruses that infected Brachypodium (Figure 2.2, Supplementary Figure 2.1, Table 2.1). The disease progression was monitored at the same three stages, as described above. Surprisingly, all viruses also infected Setaria and caused similar symptoms of chlorosis, necrosis, and reduced plant height and biomass (Figure 2.2, Supplementary Figure 2.1), although with different dynamics and infectivity rates. Similar to the responses in Brachypodium, BMV infection of Setaria was 100%, and the infected plants died shortly after stage II, while SYBV-infected plants showed mild to moderate chlorosis symptoms in stage II which became more prominent by stage III. The infectivity rate of SYBV, however, varied between the two hosts. SYBV infected 100% of Brachypodium plants, yet only 9% of Setaria plants showed symptoms typical of an infection. BSMV-, MMMV-, WSMV- and FoMV-infected Setaria plants survived until stage III with 100, 100, 92, and 100% infectivity rates, respectively.

To confirm the presence of each virus in the symptomatic plants, immunoblotting analyses was performed (Figure 2.3). All of the viral capsid proteins consistently accumulated in the upper non-inoculated systemically

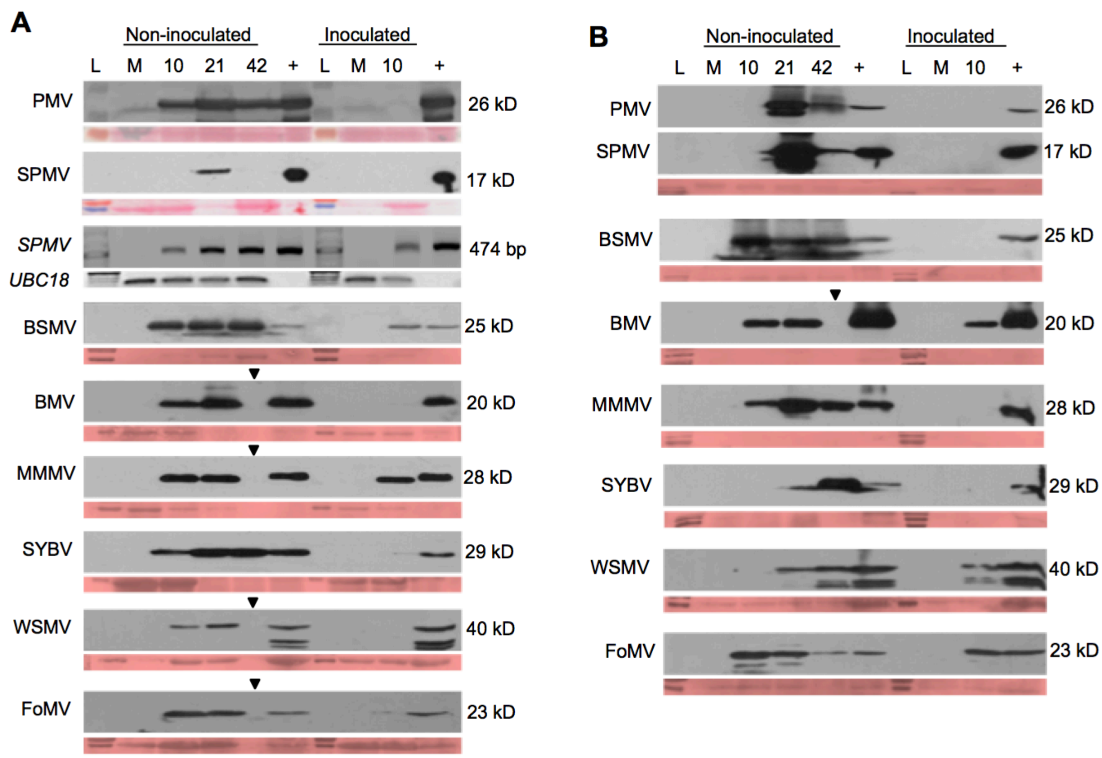

Figure 2.3. Diagnosis of virus-infected Brachypodium and Setaria plants. Immunoblot analysis was performed for capsid protein (CP) detection at infection stages I (10 dpi), II (21 dpi), and III (42 dpi) of PMV+SPMV-, BSMV-, BMV-, MMMV-, SYBV-, WSMV- and FoMV-infected (A) Brachypodium and (B) Setaria. Lane "L" represents protein molecular weight ladder, "M" represents mock-inoculated sample, and "+" indicates a positive control used as the inoculum. The black arrowheads indicate instances when no samples were collected, as infected plants did not survive through stage III. The Ponceau S-stained nitrocellulose membranes of each blot serves to indicate approximately equal protein loading among the sample lanes. The molecular weight of each viral CP is presented on the right side of each appropriate blot. Note: Because of high concentrations of some viral CPs, particularly in Setaria samples, the total protein loaded was diluted equally among the different samples which resulted in weaker Ponceau S-staining of the membranes. Because SPMV capsid protein (SPCP) accumulation was lower in the current experimental conditions, we also measured SPMV RNA in the inoculated and upper non-inoculated leaves of Brachypodium PMV+SPMV infected plants using RT-PCR and with primers specific to the 474 bp open reading frame for SPCP (See Supplementary Figure 2.2 and Materials and Methods for more details). Expression of Brachypodium *UBIQUITIN18* (*UBC18*) was used to monitor template cDNA quantities used for the different samples and SPMV plasmid DNA was used as a positive control (+).

infected leaves during the disease progression, although some were below detectable levels in the inoculated leaves at stage I. Due to environmental variables, SPMV capsid protein (SPCP) accumulation in PMV+SPMV infected Brachypodium was below detection by immunoblot assays in some stages of infection. For this, we also measured accumulation of SPMV RNA in the inoculated and upper non-inoculated leaves using RT-PCR with SPCP-specific primers. SPMV RNA consistently accumulated throughout the disease stages (Figure 2.3A) and in all three Brachypodium PMV+SPMV replicates (Supplementary Figure 2.2). Together, these results establish Brachypodium and Setaria as systemic hosts for diverse grass viruses and reveal striking similarities in symptom induction by the seven viruses in the two grass types.

2.3.2 Quantitative Effects of Grass Virus Infection on Plant Developmental and Agronomic Traits.

Plant pathogens perturb host physiology, growth, and development, which negatively affect agronomic traits such as yield and biomass. Because the seven grass viruses used here infect diverse agronomic crops (Table 2.1) and cause significant crop losses, we determined the extent of these deleterious effects in Brachypodium and Setaria. For this, we quantified agronomic parameters such as leaf length, tiller number, plant height, internode length, biomass, spikelet number and spikelet weight of the virus-infected grasses. When compared to mock-inoculated plants, virus-infected plants had significantly smaller leaves, reduced tiller numbers, shorter internodes, shorter stature (plant height) and lower shoot weight (Figure 2.4). These effects were observed in both

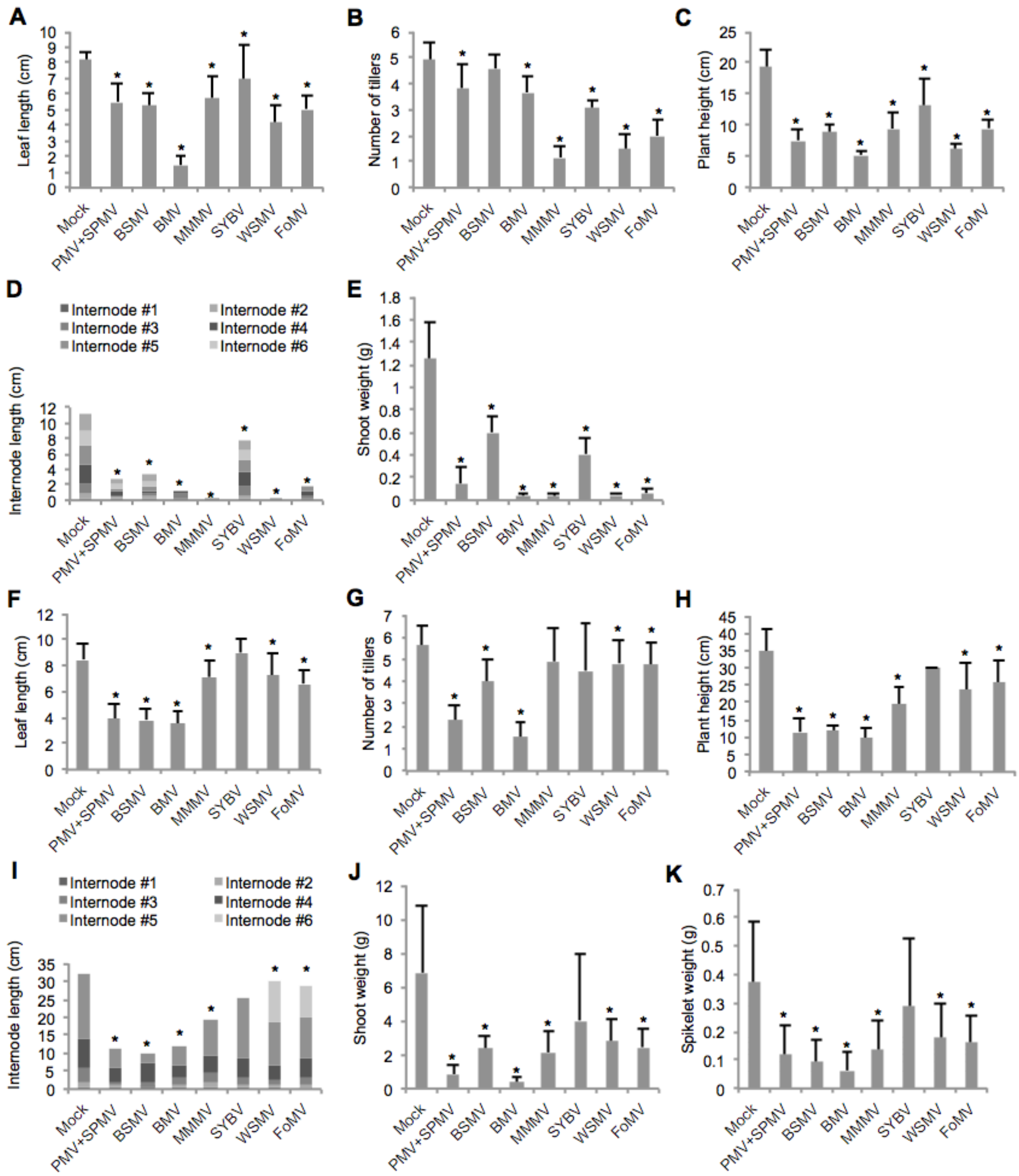

Figure 2.4. Plant growth, development and agronomic traits affected by virus infections. All virus infections in Brachypodium (A-E) and Setaria (F-K), with the exception of SYBV, significantly reduced leaf length (A, F), decreased tiller number (B, G), caused stunting (C, H), reduced internodal elongation (D, I), and decreased shoot weight (E, J) and inflorescence (spikelet) fresh weight (K). The asterisks represent statistically significant changes as determined using Student's t-test (p-value ≤0.05, n=3 to 36).

Brachypodium and Setaria and recapitulated the symptoms observed in their agronomic host plants. Although SYBV-infected Brachypodium plants upon visual inspection only exhibited mild chlorosis symptoms with no apparent effect on leaf length and plant height (Figure 2.2, Supplementary Figure 2.1), the plants had significantly shorter internodes, fewer tillers and lower shoot weight (Figure 2.4B, D and E). These negative effects of SYBV were not significant in Setaria, perhaps due to the delayed onset of symptoms and lower symptom induction (ca. 9%), when compared to Brachypodium (ca. 100%). WSMV- and FoMV-infected plants had shorter internodes and reduced height. Interestingly, WSMV- and FoMV-infected Setaria plants developed an additional internode (Figure 2.4I), compared to mock-inoculated plants. Lastly, all virus infections were associated with decreased spikelet weights and inflorescence numbers that could impact seed yield in Setaria. Because Brachypodium requires additional vernalization treatment of about 2 weeks to promote flowering, and by then most viruses (BMV, MMMV, WSMV, and FoMV) had killed the plants, we were unable to measure these parameters in Brachypodium. However, independent experiments with vernalized Brachypodium infected with PMV+SPMV showed drastic negative effects on seed set and inflorescence formation (Mandadi and Scholthof, 2012), similar to those previously observed in millets (Scholthof, 1999). Together, these experiments demonstrate that diverse viruses have similar negative impacts on agronomic traits in Brachypodium and Setaria, recapitulating their effects on the field grass hosts.

2.3.3 C_3 Antiviral Defense Hormone Responses in Brachypodium

To analyze changes in plant defense hormone signaling triggered by the diverse grass viruses in Brachypodium, we assayed the expression patterns of multiple SA, JA, and ET signaling components during the seven grass virus infections. For this, we selected thirteen candidate defense marker genes in SA (*PR-1, PR-3, PR-5, AOX1A, PAD4,* and *NPR1*), JA (*AOS, LOX2, FAD7*, and *VSP1*) and ET (*ERF1, ERF3*, and *ERF4*) signaling, whose expression was significantly altered during PMV+SPMV infection in Brachypodium (Mandadi and Scholthof, 2012). In preliminary RT-PCR analyses of a subset of virus-infected samples, we observed strong changes in the expression of several genes during infection (Supplementary Figure 2.3). In order to quantify these differences, we performed quantitative (q) RT-PCR analyses and determined the temporal expression patterns of the thirteen markers in response to the seven grass virus infections in Brachypodium. Three independent biological replicates were used for the (q) RT-PCR analyses. The (q) RT-PCR expression data was normalized to levels of a constitutively expressed gene, *UBIQUITIN18* (Hong et al., 2008), and compared to the respective expression data from mock-inoculated plants. Consistent with our previous findings (Mandadi and Scholthof, 2012), PMV+SPMV-infection in Brachypodium strongly induced expression of *PR-1* (>20-fold), *PR-3* (>3-fold), *PR-5* (>20-fold), and *AOX1A* (>100-fold) as early as stage I (10 dpi), and expression remained higher throughout sampling times, when compared to mock (Figure 2.5A and H). Expression of *PAD4*, which functions upstream in SA signaling, was downregulated (>1.8-fold) (Figure 2.5A), again consistent with our previous report.

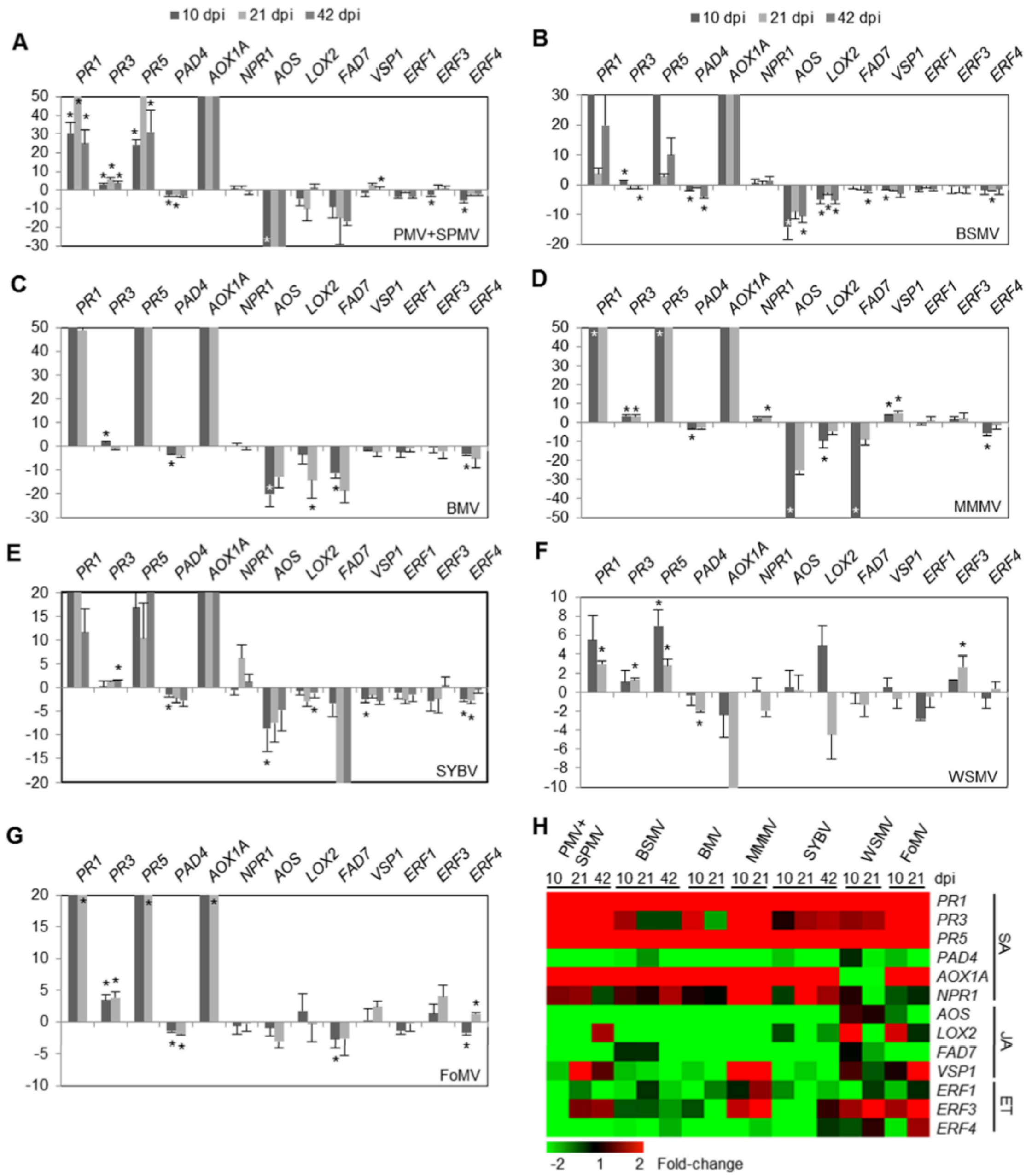

Figure 2.5. Temporal expression profiles of salicylic acid (SA), jasmonic acid (JA), and ethylene (ET) signaling components during viral disease progression in Brachypodium. Plants infected with (A) PMV+SPMV, (B) BSMV, (C) BMV, (D) MMMV, (E) SYBV, (F) WSMV, and (G) FoMV were sampled at stages I (10 dpi), II (21 dpi), and III (42 dpi) and candidate gene expressions were analyzed by (q) RT-PCR. The transcript level of *UBIQUITIN18* was used to normalize the (q) RT-PCR data. Gene expression values in individual virus panels are the average of three independent biological replicates and are relative to mock. The error bars represent standard error of the three biological replicates. The asterisks represent statistically significant changes in gene expression as determined using Student's t-test (p-value ≤0.05). Expression values higher than the maximum set on the y-axis are trimmed for visualization of smaller fold-changes. The missing time-points were instances when infected plants did not survive through stage III, and thus no samples were collected. (H) The pseudo-colored heat map represents defense gene expression during disease progression in virus-infected Brachypodium. The colors indicate fold-change in gene expression; green for ≥2-fold suppression and red for ≥ 2-fold induction when compared to mock.

Expression of *NPR1*, a key modulator of SA-JA crosstalk in Arabidopsis, did not change significantly in PMV+SPMV-infected Brachypodium (Figure 2.5A). In contrast to the SA signaling components, expression of genes in JA biosynthesis and signaling (*AOS*, *LOX2, FAD7,* and *VSP1*) and ET signaling (*ERF1, ERF3,* and *ERF4*) were downregulated during PMV+SPMV infection during stage I and, generally, remained lower throughout the disease progression (Figure 2.5A and H). Expression patterns of the thirteen marker genes during BSMV, BMV, MMMV, and SYBV infection were strikingly similar to PMV+SPMV (Figure 2.5B-E). While WSMV- and FoMV-infected plants showed similar induction of SA components (*PR-1* and *PR-5* genes) compared to the other viruses, the expression pattern of JA and ET components was different and lacked a clear trend of downregulation (Figure 2.5F and G). Hierarchical clustering (HCL) analyses of the defense gene expression among the virus groups also revealed that the expression responses triggered by SYBV, BMV, BSMV, MMMV, and PMV+SPMV clustered together and were distant to WSMV and FoMV responses (Figure 2.7A). Together, these results reveal that although most viruses similarly induce SA components and reduce JA/ET components in Brachypodium, some viruses like WSMV and FoMV trigger unique outcomes.

2.3.4 C_4 Antiviral Defense Hormone Responses in Setaria

C_4 photosynthetic pathways evolved independently at multiple times among the grasses and were accompanied by both anatomical and metabolic alterations to the cellular apparatus (Bennetzen et al., 2012; Grass Phylogeny Working Group II, 2012).

The influence of these specializations on C_4 defense hormone signaling pathways and C_4 grass:virus interactions remain largely unknown. To this end, we analyzed the expression pattern of the thirteen defense signaling genes in SA, JA, and ET signaling in Setaria (a C_4 grass) in response to the seven virus infections (Table 2.1) and compared their expression dynamics to those occurring in Brachypodium (a C_3 grass). Setaria orthologs of the thirteen Brachypodium defense markers were identified using the peptide ortholog analysis tool at Phytozome (Goodstein et al., 2012). After preliminary RT-PCR analyses of a subset of virus-infected samples (Supplementary Figure 2.3), we performed quantitative (q) RT-PCR analyses of three independent biological replicate samples of PMV+SPMV-, BSMV-, BMV-, MMMV-, SYBV-, WSMV-, and FoMV-infected Setaria plants at different stages of infection.

Similar to the expression responses in Brachypodium, PMV+SPMV-infection in Setaria induced expression of *PR-1*, *PR-5,* and *AOX1A*, while expression of *PAD4* was suppressed (Figure 2.6A and H). Expression of *NPR1* did not change significantly early during the infection (stages I and II), however, its expression was induced at stage III (Figure 2.6A). Expression of JA signaling genes, *AOS*, *LOX2,* and *FAD7*, and an ET signaling component, *ERF4*, was consistently downregulated during PMV+SPMV infection and paralleled the responses in Brachypodium (Figure 2.6A). However, we also found divergent outcomes among Brachypodium and Setaria defense gene responses. For example, in Brachypodium expression of *PR-3* was induced (>2-fold), while expression of *ERF1* and *ERF3* was suppressed (>2-fold) during PMV+SPMV infection (Figure 2.5A). Conversely, in Setaria expression of *PR-3* was strongly

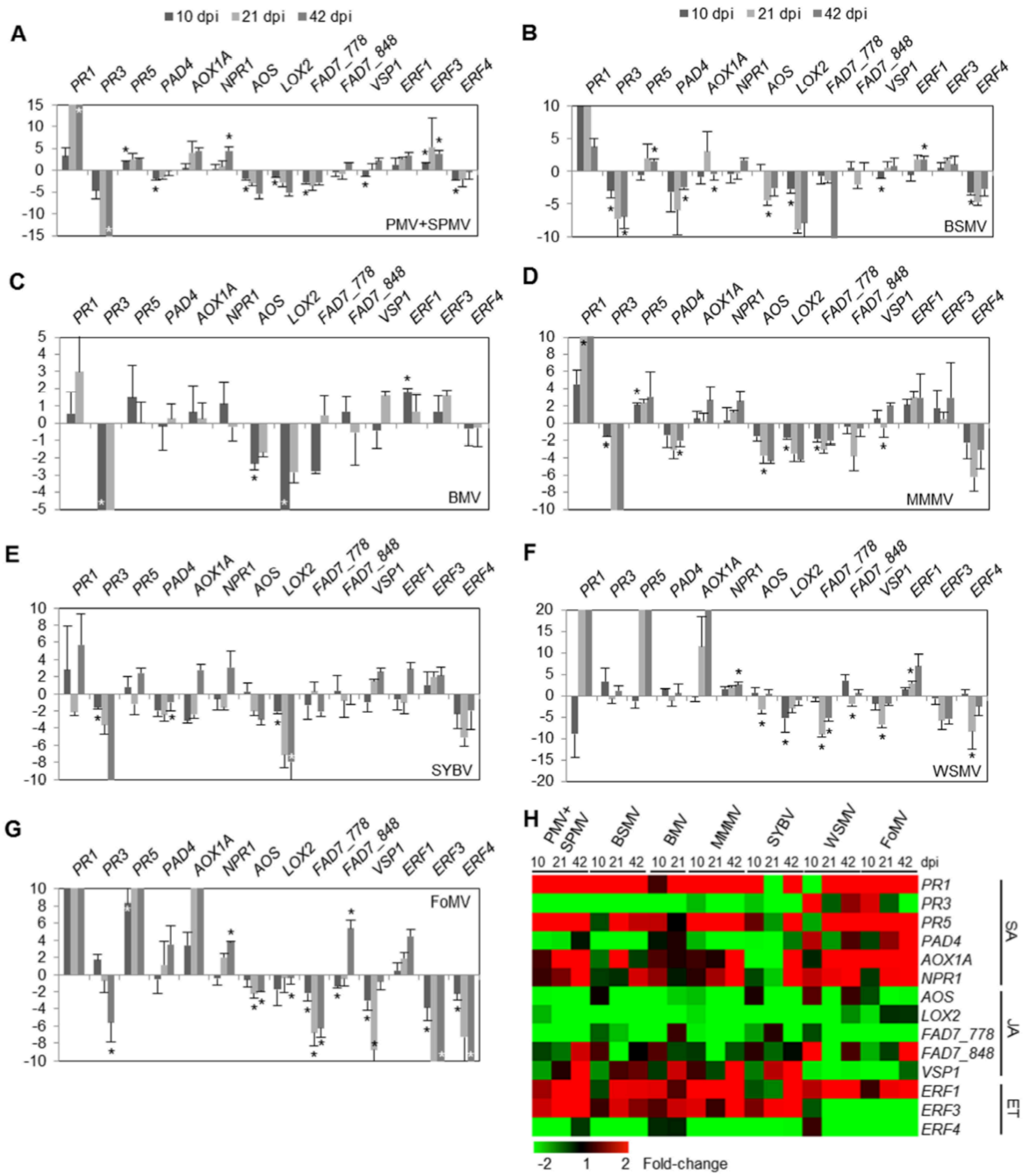

Figure 2.6. Temporal expression profiles of salicylic acid (SA), jasmonic acid (JA), and ethylene (ET) signaling components during viral disease progression in Setaria. Plants infected with (A) PMV+SPMV, (B) BSMV, (C) BMV, (D) MMMV, (E) SYBV, (F) WSMV, and (G) FoMV were sampled at stages I (10 dpi), II (21 dpi), and III (42 dpi) and analyzed by (q) RT-PCR. The transcript level of *UBIQUITIN18* was used to normalize the (q) RT-PCR data. Gene expression values in individual virus panels are the average of three independent biological replicates and are relative to mock. The error bars represent standard error of the three biological replicates. The asterisks indicate statistically significant changes in gene expression as determined using Student's t-test (p-value ≤0.05). Expression values higher than the maximum set on the y-axis are trimmed for visualization of smaller fold-changes. The missing time-points were instances when infected plants did not survive through stage III, and thus no samples were collected. (H) The pseudo-colored heat map represents defense gene expression during disease progression in virus-infected Setaria plants. The colors indicate fold-change in gene expression; green for ≥2-fold suppression and red for ≥ 2-fold induction when compared to mock. Note: The two Setaria orthologs of Bd*FAD7* are referred as *FAD7_778* and *FAD7_848.*

suppressed (>20-fold), while expression of *ERF1* and *ERF3* was induced (>2-fold) during PMV+SPMV infection (Figure 2.6A). The opposing expression patterns of *PR-3*, *ERF1,* and *ERF3* during PMV+SPMV infection of Setaria were also apparent in BSMV-, BMV-, MMMV- and SYBV-infected Setaria, although with varying degrees of fold-change (Figure 2.6A-E). Furthermore, WSMV and FoMV triggered unique responses in Setaria that were distinct from the responses induced by the other viruses. WSMV- and FoMV-induced gene expression patterns clustered together in the HCL dendrogram (Figure 2.7B), however, the clustering was less apparent compared to Brachypodium. (Figure 2.7A). Together, our results suggest that in addition to some broad parallels among Brachypodium and Setaria antiviral responses, such as upregulation of *PR-1*, *PR-5* and *AOX1A* (SA signaling) and downregulation of JA/ET components (*AOS*, *LOX2*, *FAD7* and *ERF4*), there are also unique host-dependent and virus-specific effects on defense signaling.

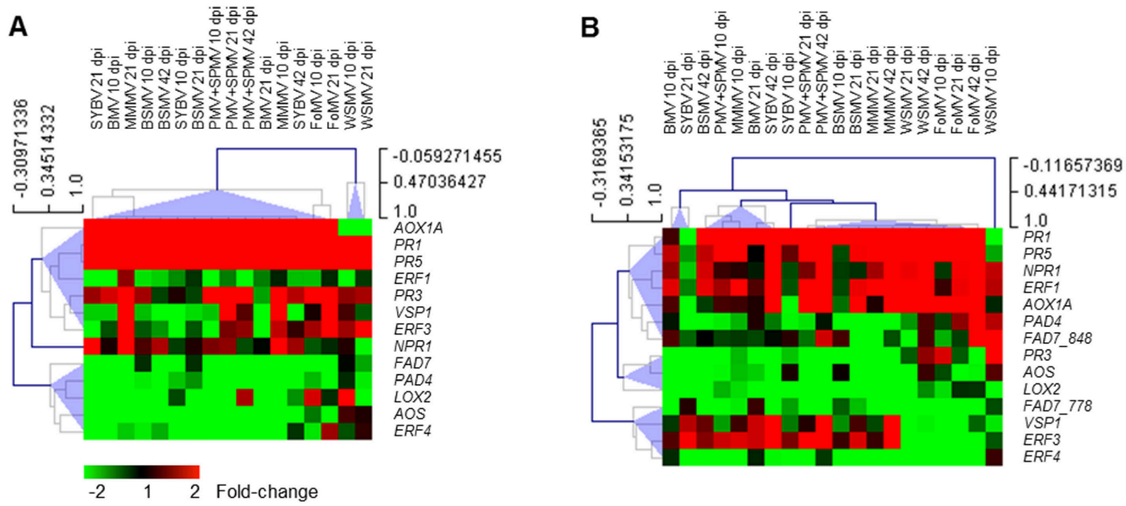

Figure 2.7. Hierarchical clustering of antiviral immune responses. Expression of thirteen defense hormone marker genes determined using (q) RT-PCR at infection stages I (10 dpi), II (21 dpi), and III (42 dpi) of PMV+SPMV-, BSMV-, BMV-, MMMV-, SYBV-, WSMV- and FoMV-infected (A) Brachypodium and (B) Setaria. The hierarchical clustering was performed using the average linkage-method and Pearson correlation metric. The node height scale is displayed beside the sample and the gene trees. The colors indicate fold-change in gene expression with green indicating ≥2-fold suppression and red for ≥ 2-fold induction when compared to mock.

2.4 DISCUSSION

Despite the significant agronomic relevance of studying grass antiviral defenses, much of the research to date has primarily focused on the epidemiology, pathogenicity and/or virulence determinants of the individual viruses, largely due to the lack of an amenable monocot host pathosystem akin to Arabidopsis. Recent genome sequencing initiatives led to the rise of Brachypodium (a C_3 grass) and Setaria (a C_4 grass) as model monocots for studying aspects of grass biology (Brutnell et al., 2010; International Brachypodium Initiative, 2010). Importantly, these model grasses are evolutionarily much closer to the agronomic grasses, having extensive genomic collinearity (Figure 2.1) (Brutnell et al., 2010; International Brachypodium Initiative, 2010). Brachypodium and Setaria both share their last common ancestor with rice ca. 40-53 million years (Myr) ago, when compared to the divergence of Arabidopsis and rice at almost ca. 150 Myr ago (Brutnell et al., 2010; International Brachypodium Initiative, 2010; Bennetzen et al., 2012).

We recently demonstrated the utility of Brachypodium for the analysis of grass defense signaling pathways through genome-wide transcriptome analyses of PMV- and PMV+SPMV-infected plants (Mandadi and Scholthof, 2012). Here, we establish Brachypodium and Setaria as amenable host platforms for seven positive-sense ssRNA viruses in diverse genera that are threats to several key grasses used for food, forage, turf and biofuel needs (Table 2.1). The seven viruses induced typical chlorosis and necrosis symptoms on the infected grass shoots and caused significant loss of agronomically-relevant traits in Brachypodium and Setaria (Figures 2.2-2.4, Supplementary Figure 2.1,

Table 2.1). Taking advantage of the fourteen host:virus combinations, we performed comparative analysis of C_3 and C_4 antiviral immune responses, pertaining to virus-triggered and hormone-mediated defenses, to uncover conserved, as well as unique host-dependent and virus-specific grass antiviral defenses.

In plants, SA, JA, and ET are the major defense hormones that mediate immune responses against diverse bacteria, fungi, and viruses (Verhage et al., 2010; An and Mou, 2011; Pieterse et al., 2012). These hormone signaling pathways often exhibit significant crosstalk with each other. SA and JA signaling pathways are usually antagonistic to each other (An and Mou, 2011; Pieterse et al., 2012), although there are examples of synergism (Mur et al., 2006). Precursors of both SA and JA are found in plants, metazoans, bacteria, fungi and algae (Gerwick, 1994; Lee et al., 2008; Brodhun and Feussner, 2011). Moreover, in metazoans, certain lipid-derived and jasmonate-like hormones such as prostaglandins are antagonized by acetylsalicylic acid (Thaler et al., 2012). However, the presence of conserved genes and molecules alone is not evidence for SA-JA crosstalk. Thaler et al. (2012) recently reviewed SA-JA crosstalk among land plants based on published experiments to date, which included genetic and biochemical analyses; measurement of SA, JA, or their derivatives and SA or JA marker gene expression after exogenous application of SA or JA and/or challenging with a biotic stress. Through ancestral-state reconstructions, SA-JA crosstalk, although not demonstrated experimentally for many land plants, was suggested to have origins dating back to the split of gymnosperms and angiosperms (Thaler et al., 2012). However, the majority of studies used for these evolutionary reconstructions primarily pertain to dicot plants. Only four studies involved monocot plants (Thaler et al., 2012), which included maize and sorghum (C_4 plants), and rice and barley (C_3 plants). Among the four grasses, evidence for SA-JA crosstalk was absent in maize (Engelberth et al., 2011) but present in sorghum, rice and barley (Weichert et al., 1999; Lee et al., 2004; Salzman et al., 2005). To our knowledge, neither these nor other studies have determined if SA-JA crosstalk occurs in response to diverse grass virus infections. We addressed this question here by analyzing defense marker gene expression in fourteen Brachypodium and Setaria viral pathosystems. The general pattern of expression changes of grass genes in the SA, JA, and ET pathways is suggestive of SA-JA crosstalk and antagonism occurring during diverse virus infections in Brachypodium and Setaria (Figures 2.5-2.8). For example, we consistently found upregulation of SA components such as *PR-1, PR-5,* and *AOX1A* and downregulation of JA components, *AOS, LOX2,* and *FAD7,* among the two grasses in most grass virus infections (Figures 2.5 and 2.6), and these components fell in distinct groups in the hierarchical clustering dendrogram (Figure 2.7).

In addition to the conserved responses, there are noticeable virus-specific and host-dependent effects between Brachypodium and Setaria, as well as among the virus types. For example, we found divergent expression patterns for *PR-3* in Brachypodium and Setaria. Expression of *PR-3* was induced by majority of virus infections in Brachypodium (Figure 2.5), while its expression was strongly down-regulated by the same virus infections in Setaria (Figure 2.6). Similarly, expression of *ERF1* and *ERF3,* which function in ET signaling, showed divergent expression patterns in Brachypodium and Setaria (Figures 2.5 and 2.6). Given that C_3 and C_4 grasses differ in their

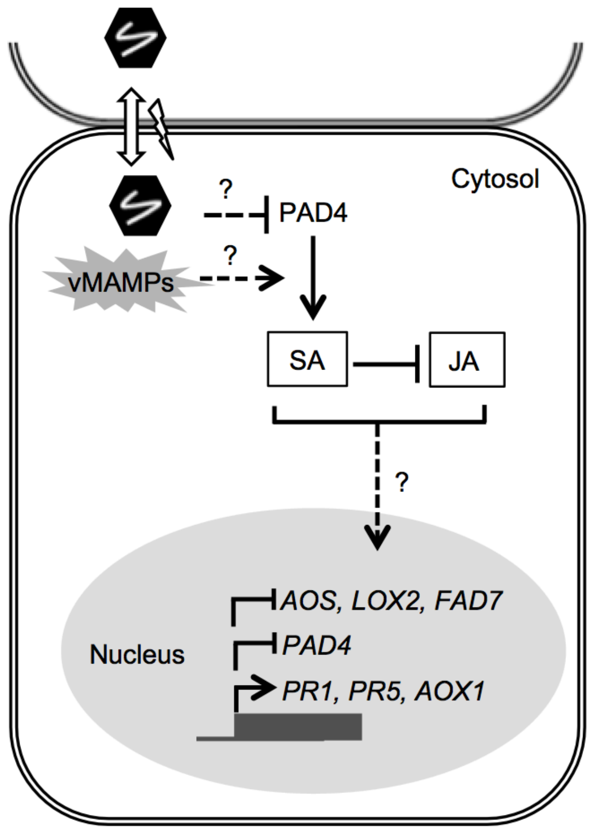

Figure 2.8. Proposed model for hormone-mediated grass antiviral responses in Brachypodium and Setaria. During virus infection, recognition of conserved virion structures, capsid protein symmetry, and/or viral nucleic acid secondary structure collectively termed as virus-associated MAMPs (vMAMPs) by the host cellular receptors trigger immune responses (Allan et al., 2001; Parker et al., 2005; Kendall et al., 2008; Chintakuntlawar et al., 2010; Hyde et al., 2014) .The defense hormone signals are transduced to the nucleus, perhaps by an NPR1-independent pathway, resulting in transcriptional reprogramming of defense-associated gene expression, although additional posttranscriptional modulations are a possibility. The relative abundance of *PAD4,* an upstream regulator of the salicylic acid (SA) signaling pathway, was consistently lower during diverse compatible grass virus infections. However, the transcript levels of multiple downstream genes in SA signaling pathway including *PR1*, *PR5,* and *AOX1* are higher, while levels of jasmonic acid (JA) signaling pathway components, *AOS*, *LOX2,* and *FAD7* are lower, providing evidence for putative SA-JA crosstalk during C_3 and C_4 compatible grass:virus interactions. The culmination of these immune responses leads to cell death- and/or systemic necrosis-like symptoms, and reflects the host's attempt to curtail virus infection. In a compatible infection, the virus triumphs over time, perhaps owing to robust virulence strategies such as suppression of *PAD4*. Unknown components or putative outcomes are presented as dotted lines and a question mark (?).

photosynthesis and metabolic carbon fixation pathways and leaf cellular anatomy (Brutnell et al., 2010), the observed differences in defense signaling components could be a consequence of C_4 specializations that occurred in Setaria. Alternatively, or in addition, differences in promoter architecture of Brachypodium and Setaria *PR-3*, *ERF1* and *ERF3* and/or their target transcription factor activities could contribute to the observed opposing expression patterns.

In Arabidopsis, PAD4 functions upstream to NPR1 in SA signaling and mediates defense responses against fungi, bacteria, and viruses (Zhou et al., 1998; Feys et al., 2001; Zhu et al., 2011). For instance, AtPAD4 is required for HRT-mediated resistance and HR against *Turnip crinkle virus* (TCV) (Chandra-Shekara et al., 2004). In our study, expression of *PAD4* was consistently downregulated in multiple grass:virus interactions in Brachypodium and Setaria, with the notable exception of WSMV and FoMV infection in Setaria (Figures 2.5 and 2.6). The predominant downregulation of *PAD4* in diverse compatible grass virus infections could have significance in establishment of disease, perhaps by evading recognition and/or suppressing PAD4-mediated resistance and HR within the infected cells.

In Arabidopsis and rice, NPR1, a nucleo-cytoplasmic protein, mediates SA signaling and SA-JA crosstalk in response to bacterial and fungal infections (Spoel et al., 2003; Dong, 2004; Chern et al., 2005; Yuan et al., 2007). Our analyses of the fourteen compatible grass:virus infections showed strong activation of SA signaling components, including *PR* genes and *AOX1A,* in both Brachypodium and Setaria as early as 10 dpi (Figures 2.5 and 2.6). However, the *PR* gene induction did not correlate to changes in

NPR1 expression throughout the early stages of infection (10 and 21 dpi). *NPR1* expression was slightly up-regulated at 42 dpi, more prominently in Setaria than in Brachypodium. Together, these results suggest that virus-triggered induction of *PR* gene expression, at least during the early stages of disease may be independent of *NPR1;* however, *NPR1* may sustain the SA signaling and *PR* gene expression in later stages of infection. Because we cannot rule out changes occurring to the NPR1 protein level or activity from the current data, dependence of SA responses on NPR1 activity during the early stages of virus infection remains a possibility. Nevertheless, our observations support those noted for dicot virus:host interactions. For example, in Arabidopsis and tomato, resistance and immune response to multiple viruses such as TCV*, Cucumber mosaic virus* (CMV) and *Oilseed rape mosaic virus* are SA dependent, yet do not require NPR1 activity (Kachroo et al., 2000; Huang et al., 2005).

The mechanism of pathogen perception by the host defense machinery is highly complex, yet the key plant immune mechanisms to detect bacterial, fungal and viral pathogens appear strikingly similar (Dodds and Rathjen, 2010; Schwessinger and Ronald, 2012; Mandadi and Scholthof, 2013). Recognition of conserved pathogen- or microbe-associated molecular patterns (PAMPs or MAMPs) at the cell surface or pathogen-encoded effector molecules inside the host cells triggers downstream defense signaling responses. Although viruses are not generally viewed as encoding MAMPs or effectors, analogous viral features do exist. Such virus-associated MAMPs (vMAMPs) include conserved viral capsid protein composition, viral nucleic-acid composition and/or secondary structures (Chintakuntlawar et al., 2010; Hyde et al., 2014), all of which can be perceived by the host defense machinery, both outside and inside the plant cells, in order to trigger host defenses (Allan et al., 2001; Mandadi and Scholthof, 2013). For example, exogenous application of *Tobacco mosaic virus* (TMV, a rigid rod tobamovirus) virions or isolated capsid protein outside of the tobacco leaf epidermis elicits a rapid intracellular oxidative burst, typically within a few seconds of application (Allan et al., 2001). This response is also triggered by related tobamoviruses with common host ranges, such as *Tomato mosaic virus* and TMV Ob strain but not by an unrelated virus, CMV (Allan et al., 2001). Our analysis here revealed WSMV and FoMV triggered distinct changes in defense signaling components in Brachypodium and Setaria, when compared to the other viruses (Figures 2.5-2.7). A noticeable feature of WSMV and FoMV is that they both form similar flexible filamentous shape virions with conserved capsid protein folds and helical symmetries that are distinct from icosahedral or rigid-rod virions (French and Stenger, 2004; Robertson and French, 2004; Parker et al., 2005; Kendall et al., 2008). It is possible that these distinct virion structural features of WSMV and FoMV contribute to the unique defense responses elicited in the infected plants (Figure 2.8) (Mandadi and Scholthof, 2013). Alternatively, or in addition, differences in WSMV and FoMV replication, movement and/or unique interactions with host components in Brachypodium and Setaria, compared to the other viruses, could trigger unique host defense responses.

Together, through establishing and extending Brachypodium and Setaria as host platforms for studying seven destructive monocot-infecting viral pathogens, this comparative analysis bridges some of the knowledge gaps that exist in the study of grass antiviral defenses, particularly relating to defense hormone-mediated responses. Our study uncovered multiple conserved, as well as unique virus-specific and host-dependent defense signaling responses triggered during compatible grass virus infections and provides the first framework of SA, JA and ET signaling components modulated during diverse C_3 and C_4 grass:virus interactions.

2.5 MATERIALS AND METHODS

2.5.1 Plant Growth Conditions

Brachypodium distachyon (Bd21-3) and *Setaria viridis* (A10) were planted in 2" x 3" pots (BWI Companies) and 4" diameter pots, respectively, with Redi-Earth soil (Sungrow Horticulture). Seeds were stratified at 4 °C for 7-10 days in the dark. Subsequently, pots were transferred into growth chambers with diurnal cycles of 14 h light (21°C) and 10 h dark (18°C). Light intensity in the growth chamber was set to 250-300 μmol/m^2s.

2.5.2 Phylogenetic Analyses

Phylogenetic species tree of C_3 and C_4 grasses (Brachypodium, barley, wheat, rice, foxtail millet [Setaria], switchgrass, maize, sorghum and sugarcane), and a dicot, Arabidopsis, was constructed using multiple sequence alignment (MSA) of a ca. 1000 amino-acid long concatenated super sequence corresponding to six conserved proteins: SAM decarboxylase, glyceraldehyde-3-phosphate dehydrogenase, chlorophyll a/b-binding protein P26, catalase, α-tubulin, and heat shock protein70 of the respective species (Vogel et al., 2006). Concatenation maximizes power to infer more accurate trees and is a common procedure to build species trees (Gadagkar et al., 2005; Vogel et al., 2006). MSA was performed with the concatenated sequences using ClustalX2 (Larkin et al., 2007) and the resulting neighbor-joining tree was generated using the interactive tree of life (iTOL) tool (Letunic and Bork, 2007). Bootstrapping with 1000 replicates was performed to indicate confidence values for the different clades. Arabidopsis was used as an out-group for the grasses and as the reference dicot.

2.5.3 Plant Infections, Sampling, Virus Inoculum and in vitro Transcription

Brachypodium and Setaria plants were rub-inoculated at the 2-3 leaf stage with virus inoculum corresponding to BSMV (strain ND18), BMV (strain M1), MMMV, SYBV, WSMV (strain Sidney 81) and FoMV (strain H93). To avoid accumulation of SPMV defective-interfering RNAs (Qiu and Scholthof, 2000, 2001), *in vitro* synthesized infectious RNA transcripts were used directly for PMV+SPMV infections. All rub-inoculated plants were stored in the dark with humid conditions overnight and then transferred to growth chambers. Leaf tissue was collected from three individual plants at 10, 21, and 42 days post-inoculation (dpi). The infections were repeated three times independently, and the three replicate samples collected were used for further analyses.

For preparing BSMV, BMV, MMMV, SYBV, WSMV, and FoMV virus inoculum, infectious tissue, that tested positive by immunoblotting, was ground in virus inoculation buffer (0.05M KH_2PO_4, 1% celite) in a 1:10 (weight/volume) ratio and was subsequently used to rub-inoculate plants. Original BSMV infectious plant sap was produced by rub-inoculating healthy Brachypodium plants with *in vitro* synthesized infectious BSMV transcripts (Petty et al., 1989). BSMV α, β and γ plasmid genomes were linearized with *Mlu*I, *Spe*I, and *Mlu*I, respectively, and were used as templates for *in vitro* transcription using T7 RNA polymerase (Fermentas), according to manufacturer's instructions. BSMV transcripts were capped *in vitro* using $m^7G(5')ppp(5')G$ cap analog (Life Technologies). Subsequently, equal amounts of BSMV α, β and γ (1:1:1) RNAs were mixed with RNA inoculation buffer (0.05 M KH_2PO_4, 50 mM glycine, pH 9.0, 1% bentonite, 1% celite) and used to rub-inoculate plants.

For preparing PMV and SPMV infectious transcripts, the respective plasmid genomes were linearized with *Eco*ICRI and *Bgl*II, and were used as templates for *in vitro* transcription using T7 RNA polymerase. Subsequently, equal amounts of PMV and SPMV (1:1) transcripts were mixed in RNA inoculation buffer and used to rub-inoculate plants.

2.5.4 Virus Diagnosis, Protein Extraction, Immunoblotting and RT-PCR

Equal amounts of tissue samples were homogenized in 5X Laemmli SDS protein extraction buffer in 1.5 ml Eppendorf tubes on ice. The extracts were then boiled for 5 min and centrifuged at 12,500 rpm for 5 min. The supernatant, containing the total protein extract, was subjected to electrophoresis for 1.5 h at 120 volts on 12.5% polyacrylamide-SDS gels. The electrophoresed proteins were then transferred onto nitrocellulose membrane (BioRad) at 300 mA for 1.5 h. Following transfer, membranes were stained with Ponceau S dye to visualize transfer efficiency. Membranes were then washed with water to remove the Ponceau S, then blocked with 5% milk in 1X Tris-buffered saline (0.2 M NaCl, 50 mM Tris, pH 7.4) with 0.05% Tween-20 (TBST) solution for 1 h at room temperature followed by primary antibody incubation with either anti-PMV (1:5000), anti-SPMV (1:2000), anti-BSMV (1:5000), anti-BMV (1:10,000), anti-MMMV (1:5000), anti-SYBV (1:5000), anti-WSMV (1:2000), or anti-FoMV (1:2000) capsid proteins. All antibodies were produced in rabbit except anti-BSMV, which was produced in mouse. All membranes were washed three times for 5 min each with TBST. For BSMV, BMV, MMMV, SYBV, WSMV and FoMV samples, membranes were incubated with horseradish peroxidase-conjugated goat anti-rabbit (Thermo Scientific) or anti-mouse (Rockland) secondary antibody (1:10,000), for 1 h at room temperature, then washed twice in TBST for 5 min, followed by 1X TBS for 5 min. Visualization of the proteins was performed using SuperSignal West Pico (Pierce) or ECL Prime (Amersham) chemiluminescence detection reagents and X-ray film (Agfa).

For PMV+SPMV samples, after primary antibody incubation, membranes were washed as described above and incubated with secondary alkaline phosphatase-conjugated goat anti-rabbit (Sigma) antibody (1:2000) for 1 h at room temperature. Membranes were subsequently washed twice in TBST for 5 min, followed by 1X TBS for 5 min. Chromageneic detection was performed by addition of nitroblue tetrazolium and 5-bromo-4-chloro-3-indolylphosphate to visualize the capsid proteins. SPMV accumulation in Brachypodium is sensitive to variations in environmental factors such as light intensity, temperature and day length (Mandadi and Scholthof, 2012). Because SPMV capsid protein detection using immunoblot assays was weaker in current experimental conditions in certain stages of infection, we also measured SPMV RNA in the inoculated and upper non-inoculated leaves of PMV+SPMV-infected Brachypodium using RT-PCR with primers specific to SPMV capsid protein open reading frame (Forward primer: 5′-ATGGCTCCTAAGCGTTCCA-3′; Reverse primer: 5′-TTATGAAGACTGAAGCTCGC-3′). SPMV RNA was consistently detectable in the inoculated leaves and its abundance accumulated throughout the disease progression in the upper non-inoculated leaves (Figure 2.3A). The presence and accumulation of SPMV was similar in all the three Brachypodium PMV+SPMV replicate samples (Supplementary Figure 2.2) and was further validated by performing SPMV bioassays (data not shown).

2.5.5 RNA Isolation, Quantitative (q) RT-PCR, and Hierarchical Clustering Analyses

Total RNA from three independent biological replicates was extracted from plant tissue and DNase treated using the Direct-zol RNA MiniPrep kit (Zymo Research), following the manufacturer's protocol. The quality and the quantity of the RNA was determined using Nano-Drop absorption values (260/280=1.9-2.1), and its visual integrity was determined by electrophoresis on a 1% agarose gel, stained with ethidium bromide. Two micrograms of total RNA was used for first-strand cDNA synthesis using SuperScript III Reverse Transcriptase (Invitrogen), following the manufacturer's protocol. For (q) RT-PCR analysis, the ABI 7500 Fast System (Applied Biosystems, Life Technologies) was used with SYBR Select Master Mix (Applied Biosystems, Life Technologies).

Brachypodium defense marker genes in SA, JA and ET pathways were selected based on BLAST and peptide ortholog analysis (Goodstein et al., 2012) and phylogenetic analyses (Mandadi and Scholthof, 2012). To identify *S. viridis* orthologs of candidate Brachypodium genes, we used the peptide homolog (PH) tool available through Phytozome (Goodstein et al., 2012) and searched against the annotated genome of its closest domesticated relative, *S. italica* (foxtail millet). *S. viridis* and *S. italica* genomes are highly syntenic, with little difference among the gene sequences as determined by Bennetzen et al. (2012). Further, the PH tool employs "all-against-all Smith-Waterman alignment" (Smith and Waterman, 1981), which is considered superior to BLAST or FASTA based alignments for recovery of orthologous peptides to a query sequence (Pearson, 1991; Shpaer et al., 1996). Genes that were difficult to call as direct orthologs, or that had multiple homologs within Brachypodium and Setaria, are indicated as "-like". For example, Setaria has two *FAD7*-like genes (referred as *FAD7_778* and *FAD7_848*) with close similarity to Bd*FAD7* (Supplementary Table 2.2) and were both included in the study. All primers were verified for specific matches in the *S. viridis* raw sequence libraries using SRA-BLAST analyses and were further tested by RT-PCR (Fig. S3). Primer sequences without significant BLAST hits and those that did not produce a specific RT-PCR amplicon were eliminated from the analyses. Of the fifteen Setaria genes chosen initially for the study, only one gene homolog of the two *AOX1A*-like genes, Si010566m, did not pass the BLAST and RT-PCR tests and was removed from the study.

All gene specific primers used for quantitative (q) RT-PCR were designed using QuantPrime (Arvidsson et al., 2008) (Supplementary Table 2.1 and 2.2). With the exception of Setaria *PAD4* (Si026081m), all genes have only one annotated primary transcript. The primer sets were tested for specificity by separating the resulting RT-PCR products on 1% agarose gels via electrophoresis, as well as, by analyzing the dissociation curves after the (q) RT-PCR (Supplementary Figures 2.3 and 2.4). Expression of *UBIQUITIN18* (Bradi4g00660) was used for normalization. The fold-changes in gene expression were calculated following the $^{\Delta\Delta}C_T$ method (Livak and Schmittgen, 2001) and are presented as relative to mock-inoculated plants that are set to 1. Student's t-test was used to determine statistical significances. Fold-changes in expressions were also represented as pseudo-colored heat maps using the Multi-experiment Viewer (MeV) (Saeed et al., 2003), with green color indicating ≥2-fold suppression and red color for ≥ 2-fold induction when compared to mock. To determine correlated expression patterns among the gene and virus groups, hierarchical clustering (HCL) analysis was performed using MeV HCL tool using the average linkage-method and Pearson correlation metric. The node height scale was adjusted to display the major gene- and virus-clusters.

3. DYNAMIC 3’ MODIFICATIONS TO VIRAL AND SUBVIRAL RNA GENOMES *IN VIVO* REVEAL NOVEL FACTORS THAT INFLUENCE PATHOGENESIS

3.1 OVERVIEW

Panicum mosaic virus (PMV) is an emerging pathogen of cultivated *Panicum virgatum* (switchgrass) and is well established as the causal agent of St. Augustine Decline disease of *Stenotaphrum secundatum* (St. Augustinegrass). A unique feature of PMV is its support for multiple species of subviral agents, including a satellite virus (SPMV) and satellite RNAs (satRNAs). The genomes of PMV and its satellite agents are all positive-sense, single-stranded RNAs (+ssRNAs) that lack a 5′-cap and 3′-poly(A) sequence. Here, we describe diverse, *in vivo* modifications that occur at the 3′-ends of PMV, SPMV, and a satRNA of PMV, designated satS. When co-inoculated with the genomic RNA of PMV, satS moves systemically in host grasses and attenuates the normal disease symptoms induced by PMV alone in the model grass *Brachypodium distachyon* (Brachypodium) and the food crop *Panicum miliaceum* (proso millet). The 375 nt RNA genome of satS actively acquires an additional ~100-200 nts from the terminal 3′-end of the PMV genomic RNA *in vivo* during infection and systemic movement, with non-specific recombination junction sites and varying sequence lengths. Additionally, the presence of satS RNA results in a striking reduction in the overall accumulation of PMV genomic RNA and capsid protein in the non-inoculated leaves of infected proso millet by 10 days post-inoculation, but not in Brachypodium. This suggests that the satS-PMV RNA chimeras can act as a unique type of defective-interfering RNA during the infection cycle, and that the mechanism of interference may be host-specific. The satS-PMV chimeras were also detected in native infections of cultivated switchgrass from Nebraska. Of the samples tested, satS was only detected in plants that were also infected with SPMV, suggesting an evolutionary role for retention of the three agents during natural co-infections. We also report the serendipitous discovery that the genomic RNAs of PMV and SPMV undergo *de novo* 3′ polyadenylation during infection of Brachypodium, and that a population of PMV, SPMV, and satS RNAs are polyadenylated in native infections of St. Augustinegrass. The polyadenylated RNAs of PMV are mostly truncated at the 3′-terminus and resemble byproducts of a relatively uncharacterized RNA degradation pathway. These findings shed light on the diversity of modifications that occur at the 3′-ends of RNA viruses and their subviral agents during infection. The role of these dynamic modifications in the ongoing cellular arms race between host and virus are discussed.

3.2 INTRODUCTION

Viruses are generally regarded as the most fundamental and functionally condensed pathogens, entirely dependent on their host cell for every step of the Central Dogma and employing elaborate strategies for completion of their disease cycle. However, many viruses possess the ability to support the existence of even smaller entities, known collectively as satellite agents. Satellites are separate biological entities that consist of a nucleic acid genome, and are completely dependent on their corresponding helper viruses for replication in the infected host cell (Murant and Mayo, 1982; Hull, 2002; Krupovic and Cvirkaite-Krupovic, 2011; International Committee on Taxonomy of Viruses, 2012). Some satellites, referred to as satellite viruses, encode a capsid protein (CP) for packaging of their genomes, while others, known as satellite nucleic acids, are encapsidated by the CP of their helper viruses. Much like viruses, the nucleic acid composition of the satellite genomes is incredibly diverse, including both single-stranded and double-stranded RNA and DNA, protein coding and non-coding, linear and circular (International Committee on Taxonomy of Viruses, 2012). Satellite viruses and nucleic acids have been found in association with viruses that infect diverse ranges of eukaryotic hosts, including algae, protozoa, fungi, and animals, however most of the known satellites, satellite nucleic acids in particular, are associated with viral infections of higher plants (Hull, 2002; Krupovic and Cvirkaite-Krupovic, 2011; Desnues and Raoult, 2012).

Plant RNA viruses, in particular, frequently support the replication of diverse exogenous, non-genomic RNAs, including satellite RNAs (satRNAs), satellite RNA viruses, sub-genomic RNAs (sgRNAs), defective RNAs (D-RNAs), and defective-interfering RNAs (DI-RNAs) (Hull, 2002). The support of these RNA entities by the helper virus machinery is dependent upon dynamic, and largely undetermined, interactions between helper, satellite, and host factors. The role of true RNA satellites (e.g., satellite RNA viruses and satRNAs) in the progression of disease in not well understood, and their biological origins are equally as enigmatic (Scholthof et al., 1999; Simon et al., 2004). The impact of satellites on the normal disease development induced by their helpers is diverse, including attenuation, no symptom alteration, and exacerbation, and many of these satellite-induced disease effects are host-dependent (Scholthof, 1999; Simon et al., 2004; Hu et al., 2009).

The interaction between the replication machinery of RNA viruses and their subviral agents, at the genomic level, in many cases appears to be largely dependent on the sequence and secondary structure of the 3′ RNA terminus. Several satellite agents share conserved 3′ sequence identity with the 3′-end of their helper viruses. For example, a 355 nt satellite RNA of *Turnip crinkle virus* (TCV), satC, shares approximately 150 nts of sequence similarity (>90%) at its 3′-end with the 3′ terminus of its helper virus (Simon and Howell, 1986). The genome of satellite tobacco mosaic virus (STMV) has multiple 3′ regions of conserved sequence with the 3′-end of several *Tobacco mosaic virus* (TMV) strains and other *Tobamovirus* members (Dodds, 1998). The retention of these helper virus sequences in the 3′-end of their satellite genomes suggests a functional role for helper-satellite interactions. Similarly, the 3′ sequences of viral genomes are often retained in the generation of replicating DI-RNAs (White and Morris, 1999; Pathak and Nagy, 2009). In particular, this is true for DI-RNAs of multiple members of the *Tombusviridae* including *Tomato busy stunt virus* (TBSV), *Cymbidium ringspot virus* (CyRSV), and TCV (Hillman et al., 1987; Li et al., 1989; Rubino et al., 1990). This 3′ sequence retention has also been documented in the generation of DI-RNAs of the satellite panicum mosaic virus (SPMV) (Qiu and Scholthof, 2000, 2001).

In addition to the important roles of the 3′-end of RNA satellite genomes, the 3′-ends of viral RNA genomes are diverse and serve important functional roles in virus replication, gene expression, and genome packaging. Many viruses rely on key structural or sequence-based regulatory features of their 3′ genomic RNAs for efficient pathogenesis, including tRNA-like structures, RNA packaging signals, and virus-encoded polyadenylation sequences (Weiner and Maizels, 1987; Dreher, 1999; Barr and Fearns, 2010).

RNA polyadenylation is a process that occurs primarily in the nucleus of eukaryotic cells to aid in mRNA nuclear export, cytoplasmic protection, and recognition by ribosomes (Dreyfus and Régnier, 2002). It is well established that nuclear-replicating viruses, primarily DNA viruses and some minus-sense RNA viruses, exploit host factors within the nucleus to promote polyadenylation of transcribed viral mRNAs (Martín-Benito and Ortín, 2013; Schmid et al., 2014). It is also known that many cytoplasmic-replicating +ssRNA viruses of both plants and animals encode a stretch of adenine bases at their at the 3′-end of their RNA genomes to mimic a poly(A) tail of host mRNAs, which presumably helps to prevent cytoplasmic degradation of viral RNAs and promote recognition of viral RNAs by host ribosomes (Gallie, 1996; Barr and Fearns, 2010). Thus, polyadenylation of viral mRNAs, either host-directed or viral-encoded, serves as an important pathogenicity factor for many viruses.

While some viruses encode poly(A) sequences as part of their terminal genomic 3′-ends, many other viruses do not, and must rely on alternative mechanisms for effective gene expression and cytoplasmic RNA protection. RNA viruses are known to exist in the infected host cells as a ‘quasispecies’, with the genomic composition defined by a general consensus sequence, but with many, if not most, individual RNA genomes exhibiting a mosaic of individual mutations that differ from the consensus (Domingo et al., 2012; Andino and Domingo, 2015). This is largely a result of the error-prone RNA-dependent RNA polymerase used by RNA viruses for genome replication. Outside of the established quasispecies hypothesis, major changes to the viral RNA genome *in vivo* (large insertions, deletions, etc.) are not often observed, and generally remain unknown or uncharacterized. One of these major genomic modifications that has been documented in only a handful of previous studies is the *de novo* polyadenylation of viral RNA genomes that lack an encoded 3′ poly(A) sequence (Jupin et al., 1990; Guilford et al., 1991; Hill et al., 1997; Raju et al., 1999; van Leeuwen et al., 2006).

Panicum mosaic virus (PMV) is the type member of the *Panicovirus* genus in the family *Tombusviridae*, and is well established as the causal agent of the ubiquitous turfgrass disease, known as St. Augustine Decline (Batten and Scholthof, 2004b). PMV is a +ssRNA virus that lacks a known poly(A) sequence at the 3′-terminus of its genome (Turina et al., 1998). Replication of PMV RNA occurs in the cytoplasm, possibly on the membranes of peroxisomes (Batten et al., 2006a). PMV is somewhat unique, in that the virus is able to support the replication of two distinct satellite agents, a +ssRNA satellite virus (SPMV) and satRNAs during native infections of *Stenotaphrum secundatum* (St. Augustinegrass) and *Eremochloa ophiuroides* (centipedegrass) (Cabrera and Scholthof, 1999; Batten and Scholthof, 2004b). The satellite agents of PMV also do not encode poly(A) sequences at the 3′-ends of their genomic RNAs and presumably replicate in the cytoplasm using the replication machinery of the PMV helper virus (Masuta et al., 1987; Monis et al., 1992). Additionally, PMV and its satellite agents do not encode the characteristic AAUAAA eukaryotic polyadenylation sequence in their genomes.

In this study we report novel and dynamic rearrangements of the 3′-ends of PMV and its satellite agents, including *de novo* acquisition of helper virus sequences by a satRNA during infection, and *in vivo* polyadenylation of PMV, SPMV, and a PMV satRNA in multiple host grasses. A satRNA of PMV previously isolated from St. Augustinegrass, designated satS, actively acquires ~100-200 nucleotides (nts) from the 3′-end of the PMV genome during infection of the model grass *Brachypodium distachyon* (Brachypodium) and the food crop *Panicum miliaceum* (proso millet). These satS-PMV chimeras were also detected in naturally infected St. Augustinegrass and *Panicum virgatum* (switchgrass) hosts. The systemic accumulation of the satS-PMV chimera RNAs results in attenuated disease symptoms in Brachypodium and proso millet, and induces host-specific effects on the systemic accumulation of the helper virus. Additionally we present the serendipitous discovery that PMV, SPMV, and satS-PMV chimera RNAs are polyadenylated during laboratory infections of Brachypodium and native infections of St. Augustinegrass. The polyadenylated genomic RNAs of PMV are characterized by significant truncations of the viral 3′-untranslated region (UTR), often followed by U-rich linker sequences upstream of the added poly(A) sequence. These results demonstrate that the 3′-end sequences of PMV and its satellites are dynamic and prone to major changes *in vivo*, including deletions, additions and helper-satellite recombination events.

3.3 RESULTS

3.3.1 Host Symptom Attenuation during a PMV+satS Co-infection

Over 20 years ago, two species of PMV satRNAs were isolated and cloned from infected St. Augustinegrass and centipedegrass, and designated satS and satC, respectively (Monis et al., 1992). The cloning and sequencing of these satRNAs will be reported elsewhere. We initially sought to determine the infectivity of both satS and satC during co-infections with PMV in Brachypodium and proso millet hosts, and characterize the impact of these satRNAs on the normal helper virus-induced disease. The plants were inoculated and co-inoculated with full-length *in vitro* transcripts of PMV, PMV+SPMV, PMV+satS, and PMV+satC, and the progression of disease was monitored over a two-week period. The PMV+SPMV co-infections were included for comparison, as the synergism induced by these two agents has been well studied using these host grasses (Scholthof, 1999; Mandadi and Scholthof, 2012, 2013; Mandadi et al., 2014). At 14 days post-inoculation (dpi), the symptomology of plants inoculated with PMV+satC closely resembled those that were inoculated with PMV alone (Figure 3.1). These symptoms included moderate stunting and prominent systemic chlorotic mottling, compared to Mock-inoculated plants. The PMV+SPMV co-infections resulted in the typical disease synergism phenotype of severe stunting and chlorotic streaks on upper, non-inoculated leaves. However, co-infections of PMV+satS clearly attenuated the symptoms normally induced by PMV alone, resulting in a phenotype that was indistinguishable from the Mock-inoculated plants (Figure 3.1).

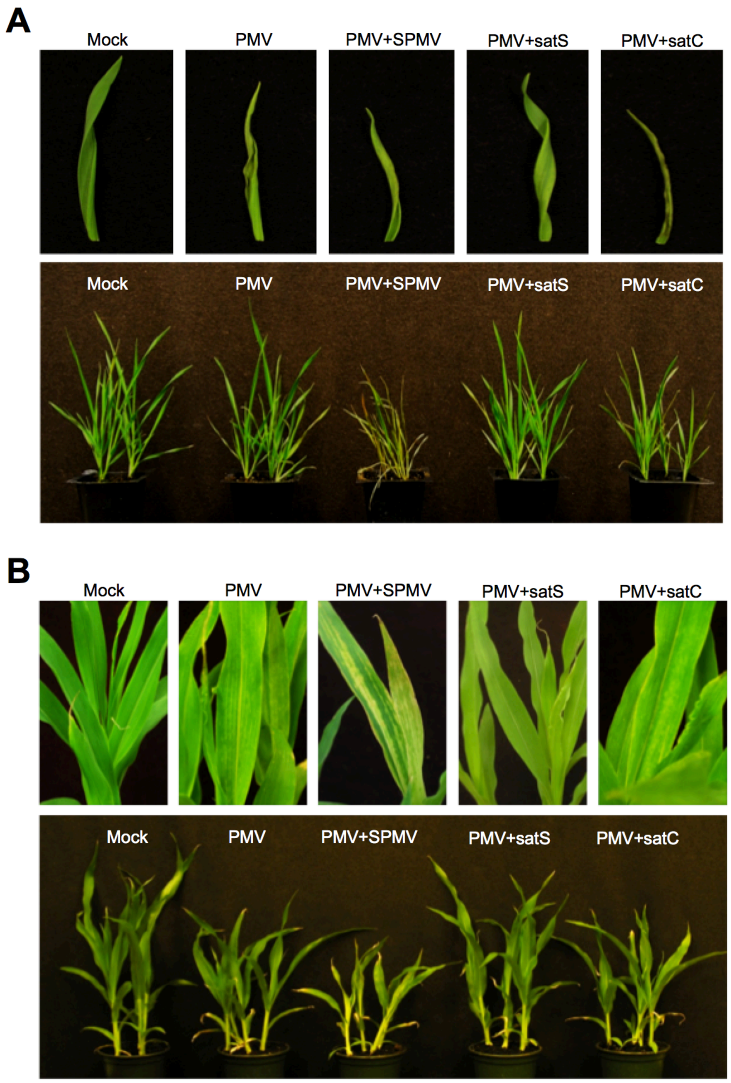

Figure 3.1. Symptoms induced by PMV and its satellite agents on Brachypodium (A) and proso millet (B). Plants were rub-inoculated with PMV alone, and in combination with SPMV and its satRNAs (satS and satC). Photographs of symptoms on upper, non-inoculated leaves (upper panels) and whole-plant stunting (bottom panels) were taken at 14 days post-inoculation (dpi).

This attenuation was more prominent for proso millet than Brachypodium. These findings suggest that the subviral agents of PMV can have diverse effects on the normal helper virus-induced disease phenotype, ranging from synergism (SPMV), to no effect (satC), to attenuation (satS).

3.3.2 Replication and Spread of satS During Infection of Brachypodium and Proso Millet

In order to determine the systemic infectivity of PMV and its subviral agents in Brachypodium and proso millet, samples were collected at 14 dpi from upper, non-inoculated leaves for reverse transcriptase-polymerase chain reaction (RT-PCR) and western blotting analysis. Reverse primers for the satRNA RT-PCRs were designed to selectively amplify satS or satC, taking advantage of the extended 3′-end of satC and the internal sequence heterogeneity between the two satRNAs (Supplementary Figure 3.1). RT-PCR analysis revealed that the PMV genomic RNA was present in all samples except Mock (Figure 3.2). As expected, the SPMV primers only amplified a product for the PMV+SPMV inoculated plants. Primers for satS amplified cDNA from the PMV+satS plants, validating that satS had accumulated in the non-inoculated tissues of both Brachypodium and proso millet by 14 dpi (Figure 3.2). Surprisingly, the satC-specific primers only amplified cDNA from the PMV+satS co-inoculated tissues, indicating that satS had acquired the additional 3′ sequence for recognition by the satC reverse primer during systemic accumulation (Figure 3.2, Supplementary Figure 3.1).

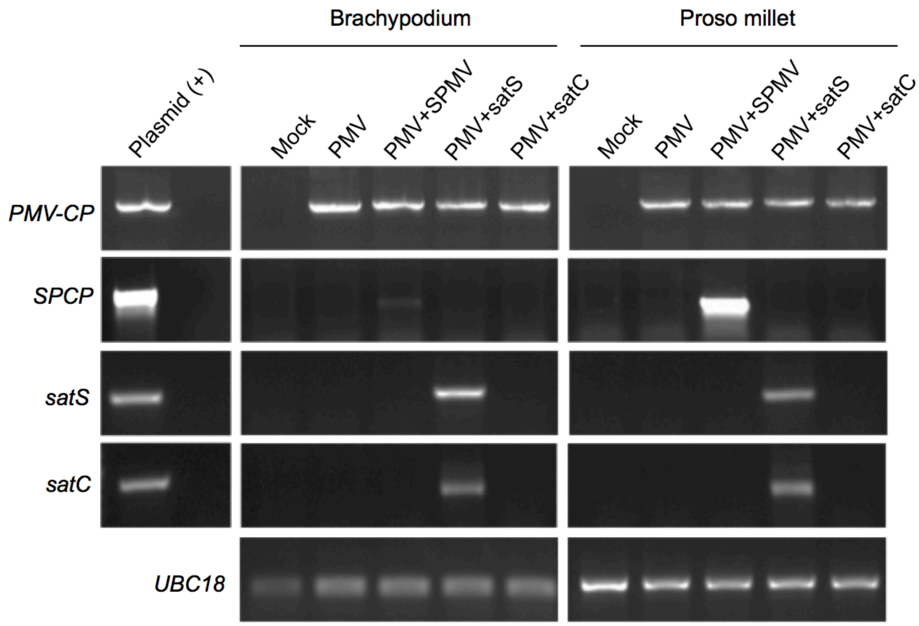

Figure 3.2. RT-PCR diagnostics of Brachypodium and proso millet inoculated with PMV and its satellite agents. Plants shown in Figure 3.1 were sampled at 14 dpi for total RNA isolation and RT-PCR analysis. All cDNA samples were prepared using random DNA hexamers for first-strand synthesis. Primers were selected to amplify the *PMV-CP* and *SPCP* ORFs from the PMV and SPMV genomic cDNA, respectively. The satRNAs were amplified using satS- and satC-specific primers (Supplementary Figure 3.1). RT-PCRs for satS and satC were performed at high cycle numbers (>30 cycles) to achieve sufficient amplification. *UBIQUITIN18* (*UBC18*) was amplified to show approximate equal cDNA concentrations among the samples.

These findings suggest that satS actively acquires the 3′-end of the PMV genomic RNA during systemic accumulation in Brachypodium and proso millet. The apparent lack of systemic infectivity of the satC clone was not investigated further in this study.

3.3.3 In Vivo *Acquisition of PMV 3′ Genomic RNA by satS*

The amplification of a PCR product from PMV+satS plants using satC primers prompted us to investigate the nature of the modified 3′-end of satS. Since the original clone of satC contains an additional ~100 nts with 90% sequence identity to the 3′-end of the PMV genome, serving as the basis for design of the satC-specific reverse primer, we hypothesized that satS was actively acquiring some portion of the PMV genomic 3′ sequence. The product amplified from satC-specific primers displayed a slight smear at a higher molecular weight than the primary band (Figure 3.2A-B), suggesting sequence heterogeneity among the hypothetical satS-PMV chimeras.

In order to address this further, we cloned and sequenced 18 near full-length isolates of the satS-PMV chimeras from PMV+satS-inoculated Brachypodium and proso millet, using the satS forward and satC reverse primers (Supplementary Figure 3.1). As expected, based on the estimated PCR product size, all clones were much longer than the originally inoculated 375 nt satS *in vitro* RNA transcripts, ranging from 70-180 nt longer in sequence length (Table 3.1). All isolates from both Brachypodium (Bd) and proso millet (Pm) consisted of a 5′ sequence of approximately 310-375 nt with 100% sequence identity to the original satS clone, with the exception of isolate PmL which had a shorter identical sequence of 238 nt. Additionally, these isolates all contained 3′ sequences of varying length with 100% sequence identity to the 3′-end of the PMV genome, ranging

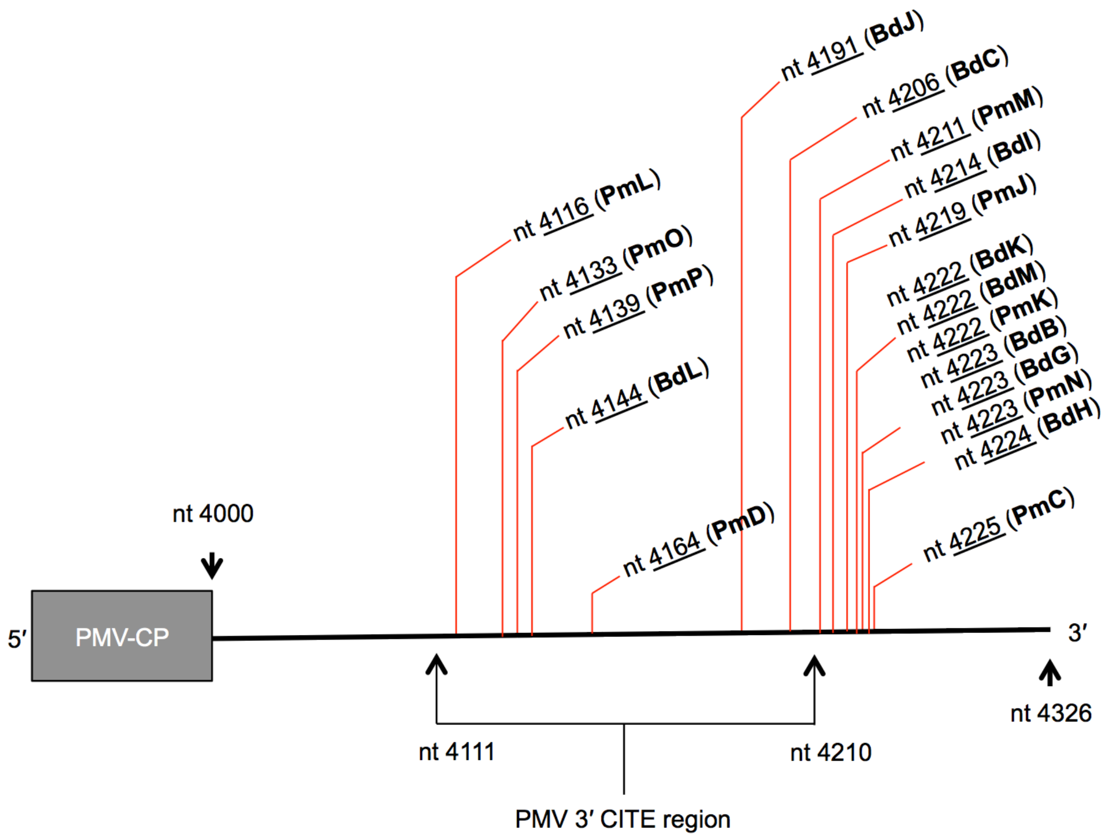

Figure 3.3. Mapping of the satS-PMV recombination junction sites to the 3′-UTR of the PMV genome. Isolated clones of the satS-PMV chimera RNAs from Brachypodium (Bd) and proso millet (Pm) are illustrated according to the specific sites of sequence acquisition from the PMV genomic RNA. The gray box indicates the 3′-terminal region of the *PMV-CP* ORF ending at nt position 4,000. The position of the PMV 3′ cap-independent translational enhancer (CITE) is indicated with arrows from nt positions 4111-4210. Individual clone labels are bolded in parentheses. Underlined numbers indicate the specific recombination nt position on the PMV genome.

Brachypodium

Isolate	Length (nt)	Recombination Junction Site
BdB	482	satS$_{370}$-G**UACUUUU**G-PMV$_{4223}$
BdC	496	satS$_{375}$-C**UU**C-PMV$_{4206}$
BdG	482	satS$_{370}$-G**UACCUUUU**G-PMV$_{4223}$
BdH	479	satS$_{370}$-G**UACCUU**U-PMV$_{4224}$
BdI	491	satS$_{370}$-G**UACCUUU**U-PMV$_{4214}$
BdJ	514	satS$_{370}$-G**UACCUUU**C-PMV$_{4191}$
BdK	483	satS$_{373}$-C**UUAUU**A-PMV$_{4222}$
BdL	556	satS$_{370}$-G**UAC**C-PMV$_{4144}$
BdM	480	satS$_{375}$-CA-PMV$_{4222}$

Proso millet

Isolate	Length (nt)	Recombination Junction Site
PmC	452	satS$_{341}$-C**GAGGGUCC**A-PMV$_{4225}$
PmD	539	satS$_{375}$-C**U**U-PMV$_{4164}$
PmJ	447	satS$_{338}$-CC-PMV$_{4219}$
PmK	485	satS$_{375}$-C**UUUUU**A-PMV$_{4222}$
PmL	446	satS$_{238}$-GU-PMV$_{4119}$
PmM	492	satS$_{375}$-C**U**U-PMV$_{4211}$
PmN	465	satS$_{357}$-G**UUAU**G-PMV$_{4223}$
PmO	547	satS$_{358}$-C**UUUUU**G-PMV$_{4133}$
PmP	492	satS$_{314}$-AC-PMV$_{4139}$

Table 3.1. Description of isolated satS-PMV chimera clones. The satS-PMV RNAs were amplified from Brachpodium (Bd) and proso millet (Pm) cDNAs, cloned, and sequenced. The total nt length of each isolate accounts for the full 5′- and 3′- termini of the original satS and PMV clones, respectively, as these complete ends were not amplified by the primer sets used (Supplementary Figure 3.1). The numbers in subscript represent specific nt sites of recombination on the satS and PMV genomic RNAs. Bolded and underlined sequences represent the heterologous, U-rich linker regions that separate the 5′ satS and 3′ PMV sequences.

from 101-207 nts. Interestingly, with the exception of 4 isolates (BdM, PmJ, PmL, and PmP), most of the satS-PMV chimeras contained heterologous, U-rich linker sequences at the recombination junction sites between the 5′ satS sequence and the 3′ PMV sequence (Table 3.1). These sequences varied, in terms of both length and nucleotide composition, however 5 isolates from Brachypodium (BdB, BdG, BdH, BdI, and BdJ) had linker regions of near-identical sequence with the general motif 5′-UACCUUU-3′. The origin of this linker sequence remains unknown, however a very similar sequence of 5′-UACCUU-3′ is found from nt positions 2762-2767 in the sub-genomic promoter region PMV genomic RNA. Most of the acquired PMV sequences could be mapped back to a primary "hot spot" region from nt positions 4219-4225 at the 3′-end of the PMV genome. This region is immediately downstream of the PMV 3′ cap-independent translational enhancer (CITE) domain (Figure 3.3) (Batten et al., 2006b).

Taken together, these findings demonstrate that the original satS RNA acquires varying lengths (~100-200 nts) of sequence from the terminal 3′-end of the PMV genome during systemic accumulation in Brachypodium and proso millet hosts. The integrity of the satS 5′ and PMV 3′ sequences are retained in the satS-PMV chimera RNAs, however most isolates also contained short U-rich linker regions at the recombination junctions sites. The common sequence motif found in the linker regions of some isolates, combined with the genomic mapping of the recombination sites, suggest roles for both the PMV sub-genomic RNA promoter and 3′ CITE in the generation of the satS-PMV chimera RNAs.

3.3.4 Impact of satS on Accumulation of Helper virus RNA and CP

In order to further characterize the attenuation effect of satS during co-infections, we conducted temporal assays for the accumulation of the PMV RNA and CP in infected Brachypodium and proso millet tissues over the course of two weeks. Samples for RNA and protein analysis were collected at 7, 10, and 14 dpi for Mock-, PMV-, and PMV+satS-inoculated plants. Inoculated tissues were collected at 7 dpi, and non-inoculated tissues were collected at all three time points. RT-PCR analysis revealed that the PMV RNA was present in the inoculated tissues and gradually accumulated in the non-inoculated tissues of PMV-inoculated Brachypodium and proso millet (Figure 3.4A-B). In proso millet, PMV and satS were present in both the inoculated and non-inoculated tissues by 7 dpi. Interestingly, the PMV+satS co-infection resulted in a striking depletion of both PMV and satS RNAs in the non-inoculated tissues by 10 dpi, to below detectable levels (Figure 3.4A). This suggests that satS significantly interfered with the normal accumulation of its helper virus, to the point where both agents were unable to persist in host cells. In Brachypodium, PMV and satS were only detected in the non-inoculated leaves by 7 dpi, and continued to accumulate by 10 dpi (Figure 3.4B). However, in contrast to proso millet, the PMV RNA continued to accumulate to 14 dpi, while satS was below detectable levels at the two-week time point. These results were recapitulated during analysis of the PMV CP accumulation (Figure 3.5A-B). The striking reduction in CP accumulation was observed by 10 dpi for PMV+satS-inoculated proso millet but not for Brachypodium. Taken together, these results suggest that the PMV and satS-PMV chimera RNAs gradually accumulate in the non-inoculated tissues of

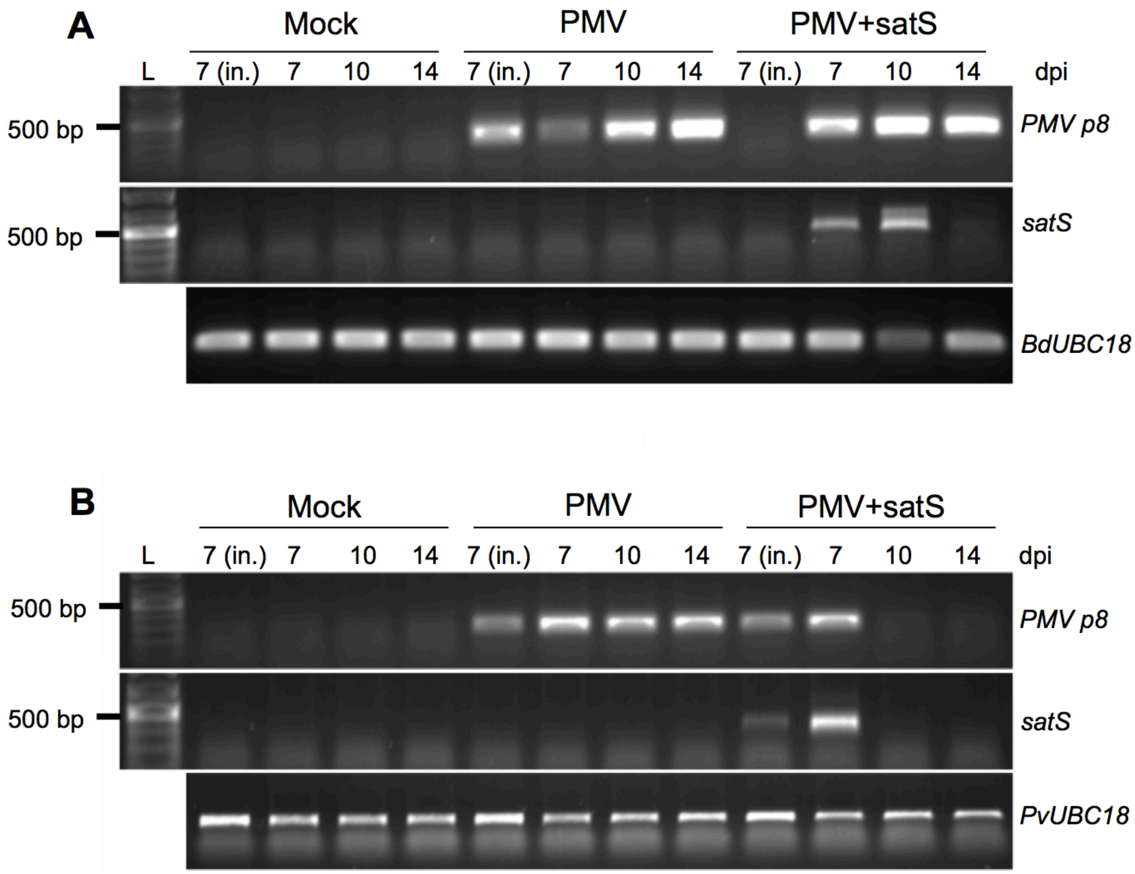

Figure 3.4. Temporal RT-PCR analysis of PMV and satS-PMV chimeras from infected Brachypodium (A) and proso millet (B). Samples from Mock-, PMV-, and PMV+satS-inoculated plants were collected for total RNA isolation and RT-PCR analysis at 7, 10, and 14 dpi. At 7 days post-inoculation (dpi), samples were collected from both inoculated (in.) and non-inoculated leaves. All cDNA samples were prepared using random DNA hexamers for first-strand synthesis. PMV RNA was detected using primers specific for the *PMV p8* ORF. satS was detected using the satS/C-specific forward primer and satC-specific reverse primer (Supplementary Figure 3.1). As a result, the observed satS RT-PCR products represent amplified satS-PMV chimera RNAs. *UBIQUITIN18* (*UBC18*) was amplified to show approximate equal cDNA concentrations among the samples. Switchgrass primers for *UBC18* (*PvUBC18*) were used to amplify *UBC18* from proso millet, since there is no reference genome currently available for proso millet.

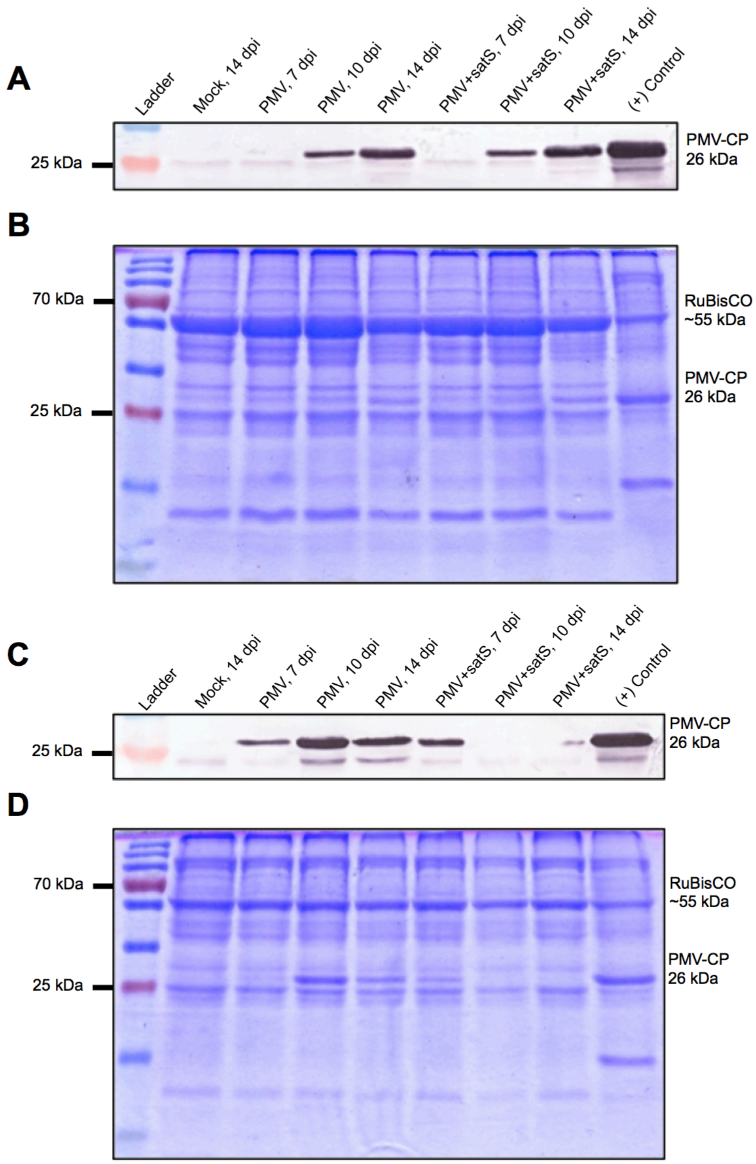

Figure 3.5. Immunoblot analysis of the PMV CP from PMV- and PMV+satS-inoculated Brachypodium (A-B) and proso millet (C-D). Samples from Mock-, PMV-, and PMV+satS-inoculated plants were collected for total RNA isolation and RT-PCR analysis at 7, 10, and 14 dpi. Accumulation of the PMV CP was determined by immunoblotting (A and C). Gels stained with Coomassie Brilliant Blue (B and D) are shown to illustrate approximate equal loading of the protein samples (RuBisCO, ~55 kDa), and show the high accumulation of the PMV CP.

Brachypodium and proso millet, and that satS has a host-dependent interference with the systemic accumulation of PMV RNA and CP. These results correlate with the more noticeable disease phenotype attenuation in proso millet by 14 dpi, compared to Brachypodium (Figure 3.1A-B).

3.3.5 Detection of satS-PMV Chimeras during Native Infections of Switchgrass

As part of a separate study in collaboration with the group of Dr. Gary Yuen at the University of Nebraska-Lincoln, investigating the presence of PMV and SPMV in cultivated switchgrass, we were curious to determine whether satS could also be detected during co-infections of this bioenergy crop (Stewart et al., 2015). The current hypothesis is that the PMV satRNAs may be geographically limited due to various environmental factors, as the satRNAs have only been found in association with co-infections of St. Augustinegrass and centipedegrass in the Gulf Coast states of the U.S. (Cabrera and Scholthof, 1999; Batten and Scholthof, 2004a). To investigate this further, we performed RT-PCR on a subset of switchgrass samples using satS- and satC-specific primers (Supplementary Figure 3.1). Of the eight selected switchgrass samples, six had previously tested positive for PMV via ELISA (#5, #6, #9, #10, #11, and #12), three tested positive for the additional presence of SPMV via western blotting (#6, #9, and #10), and two did not test positive for PMV via ELISA (#16 and #19) (Stewart et al., 2015). RT-PCR analysis revealed that three of these samples (#6, #9, and #10) also tested positive for the satRNAs using both satS- and satC-specific primers (Figure 3.6). As shown in previous experiments (Figures 3.2 and 3.4A-B), the PCR products from

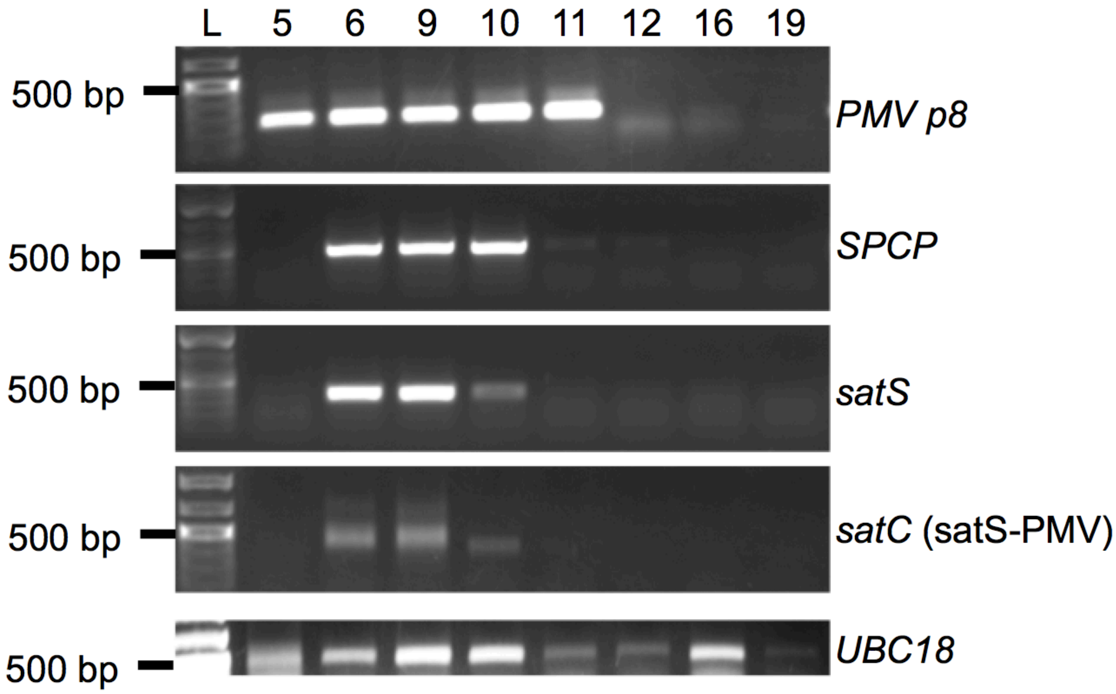

Figure 3.6. RT-PCR analysis of PMV and its satellite agents in 8 selected switchgrass samples from Nebraska breeding plots. Switchgrass samples from a previous study that were not serologically positive for PMV (#16 and 19), or were serologically positive for PMV (#5, 6, 9, 10, 11, and 12) and SPMV (#6, 9, and 10) were selected for total RNA isolation and RT-PCR analysis (Stewart, et al. 2015). All cDNA samples were prepared using random DNA hexamers for first-strand synthesis. Primers were selected to amplify the *PMV p8* and *SPCP* ORFs. The satRNAs were amplified using satS- and satC-specific primers (Supplementary Figure 3.1). As a result, the observed satC RT-PCR products represent amplified satS-PMV chimera RNAs. *UBIQUITIN18* (*UBC18*) was amplified for total cDNA comparisons among the samples.

satC-specific primers displayed a smear on the agarose gel, indicating sequence length heterogeneity among the satS-PMV chimeras. These results present the first documented evidence of the PMV satRNA species in cultivated switchgrass in regions of higher latitude than the Gulf Coast states. Interestingly, of the eight samples tested, the satRNAs were only detected in samples that also tested positive for both PMV and SPMV. These results correlate with a previous study, demonstrating preferential packaging of the satRNAs by SPMV (Desvoyes and Scholthof, 2000).

3.3.6 De Novo *Polyadenylation of PMV and SPMV*

The RNA genome of PMV, like all members of the *Tombusviridae*, is thought to be uncapped and non-polyadenylated (International Committee on Taxonomy of Viruses, 2012). Many RNA viruses encode a 3′ genomic poly(A) sequence, which likely functions as a cellular mRNA mimic, facilitating translation of the viral gene products and protecting the viral RNAs from cytoplasmic degradation (Dreyfus and Régnier, 2002; Barr and Fearns, 2010). As part of a separate study, we serendipitously discovered that the genomic RNAs of PMV and SPMV undergo *de novo* polyadenylation during infection in Brachypodium. Total RNA was extracted from PMV+SPMV-inoculated Brachypodium, and cDNA was prepared using oligo-dT primers for host gene expression analyses (Mandadi et al., 2014). Subsequently, these cDNA samples were used to confirm the effectiveness of primer sets for multiple PMV and SPMV open reading frames (ORFs). To our surprise, all primer sets amplified PCR products from the Brachypodium cDNAs (Figure 3.7A). Using oligo-dT primers, we did not expect reverse-transcription to occur for the genomic RNAs of PMV and SPMV, which supposedly lack 3′ poly(A) sequences. To investigate this phenomenon further, we extracted total RNA from St. Augustinegrass displaying the characteristic symptoms of St. Augustine Decline (Figure 3.7B), and prepared cDNA using oligo-dT primers. Following RT-PCR analysis, the presence of polyadenylated PMV and SPMV RNAs was also confirmed in the native St. Augustinegrass infections (Figure 3.7B). Additionally, these analyses revealed that satS-PMV chimeras were also amplified from the oligo-dT St. Augustinegrass cDNAs, suggesting that the satRNAs are also present in a polyadenylated state.

To investigate the nature of these polyadenylated RNAs, we focused on the genomic RNA of PMV. To confirm that the genomic RNA of PMV was polyadenylated, we performed RT-PCR using primers specific to the p48 PMV ORF (Supplementary Figure 3.2). The amplified p48 product from the oligo-dT-primed cDNA suggests that the genomic RNA of PMV is polyadenylated, since the p48 ORF is only present in the full-length genomic RNA and not the PMV sgRNA. Using a strategy similar to the approach taken by Li et al. (2014), we selectively amplified and cloned the polyadenylated 3′-ends of the PMV RNAs. The selective amplification of polyadenylated PMV 3′-ends involved an adapter-modified oligo-dT primer for first-strand cDNA synthesis, followed by RT-PCR using a PMV CP ORF-specific forward primer and a reverse primer specific to the oligo-dT adapter (Supplemental Figure 3.3). These RT-PCR products were cloned and sequenced to determine the nature of the polyadenylated PMV 3′-ends.

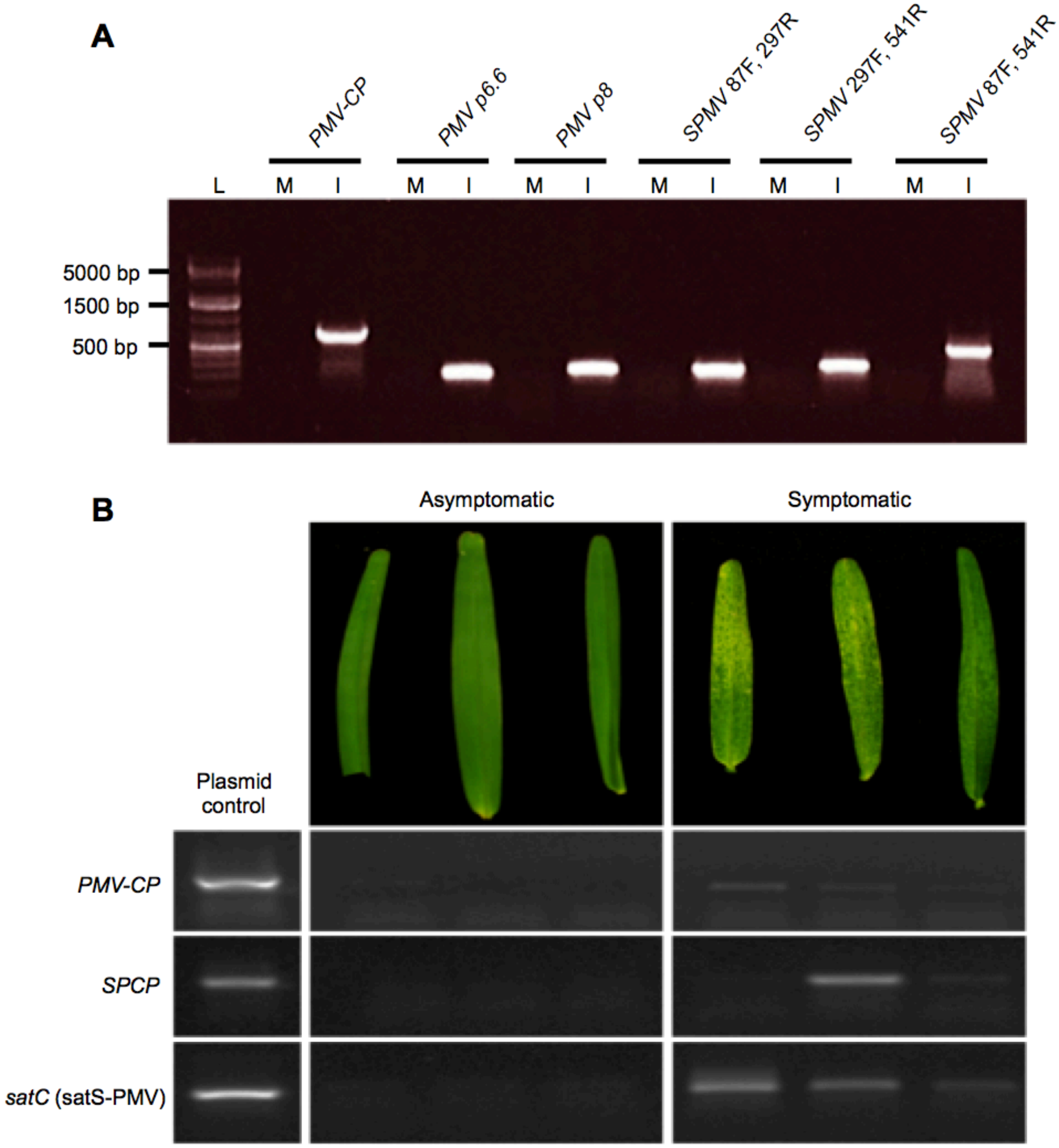

Figure 3.7. Evidence for RNA polyadenylation of PMV and its satellite agents in Brachypodium and St. Augustinegrass. Total RNA was extracted from PMV+SPMV-infected Brachypodium plants at 42 days post-inoculation for RT-PCR viral diagnostic analysis (A). Plants were previously rub inoculated with *in vitro* synthesized infectious viral transcripts Additionally, six St. Augustinegrass leaf samples were collected from the Texas A&M University campus and total RNA was extracted for RT-PCR diagnostic analysis of native infections by PMV and its sub-viral agents (B). First-strand cDNA synthesis for all samples was performed using oligo-dT primers. RT-PCRs were performed using primers for three PMV open reading frames (*PMV-CP*, *p6.6*, and *p8*), three SPMV amplicons (nt 89-297, nt 297-541, and nt 87-541), the *SPCP* open reading frame, and *satC*. “M” represents mock-inoculated plants while “I” represents virus-infected plants. Lane “L” contains a DNA molecular weight ladder. St. Augustinegrass samples were collected based on the presence or absence of symptoms typically associated with St. Augustine Decline. Plasmid cDNA clones for PMV, SPMV, and satC were used as positive controls.

The results from 12 clones revealed that most of the sequenced polyadenylated PMV RNAs were significantly truncated at the 3′-end (Table 3.2). Many of the clones lacked most of the 3′-UTR, which may have been a skewed result of selective amplification from the terminal codons of the CP ORF. Despite this, several clones contained long stretches of adenine bases at the 3′-ends, prior to the modified oligo-dT adapter primer sequence (Table 3.2). These poly(A) sequences were not long enough to resemble the true poly(A) tails of eukaryotic mRNAs (Dreyfus and Régnier, 2002). However, due to the use of oligo-dT primers for first-strand cDNA synthesis, which can bind anywhere along a poly(A) tail, we cannot rule out that the viral poly(A) sequences may have been longer than what was cloned. Interestingly, 4 of the 12 clones had heterologous, U-rich linker sequences in between the 3′ viral sequence and the added poly(A) sequence (Table 3.2). One of the 12 clones had a heterologous, U-rich sequence, followed by the oligo-dT primer sequence, at the terminal 3′-end of the PMV genome (nt position 4,326), suggesting that some full-length RNAs are polyadenylated. The presence of these linker sequences resembles those that have been reported previously with other plant and animal RNA viruses that acquire poly(A) sequences *in vivo* (Jupin et al., 1990; Hill et al., 1997; Raju et al., 1999; van Leeuwen et al., 2006; Li et al., 2014). Taken together, these results indicate that the polyadenylated RNAs of PMV are mostly truncated at the 3′-end and would likely be non-functional in the infected host cell. The inconsistency of the added 3′ U-rich and poly(A) sequences, combined with the significant loss of PMV 3′ viral sequence, suggests that the active polyadenylation is not

Isolate	Sequence
PMV-A	PMV_{4289}-A**AAAA**-[AAAAAx30 + adapter]
PMV-B	PMV_{4326}-C**UUAUUU**-[AAAAAx30 + adapter]
PMV-C	PMV_{4000}-A**AAAAAAAAAAAAAAAAAAAA**-[AAAAAx30 + adapter]
PMV-D	PMV_{4042}-G**UAAGAAAAUAA**-[AAAAAx30 + adapter]
PMV-E	PMV_{4000}-A**GU**-[AAAAAx30 + adapter]
PMV-F	PMV_{4000}-A**AAAAAAAAAAAAAAAAAA**-[AAAAAx30 + adapter]
PMV-G	PMV_{4000}-A**AAAAAA**-[AAAAAx30 + adapter]
PMV-H	PMV_{4000}-A**GUUUUCAUGUCCCAAAAAAAAAAAAAAAAAAAAAAAAA**-[AAAAAx30 + adapter]
PMV-I	PMV_{4000}-A**AAAAAA**-[AAAAAx30 + adapter sequence]
PMV-J	PMV_{4060}-G-[AAAAAx30 + adapter sequence]
PMV-K	PMV_{4005}-G**AAAAAAAAAAAAAAAAAAAAAAAAAAAAAAAAAAAAAAAAAAAAAAAAA**-[AAAAAx30 + adapter sequence]
PMV-L	PMV_{4000}-A**AAAA**-[AAAAAx30 + adapter sequence]

Table 3.2. Sequencing results from polyadenylated PMV RNAs. Total RNA was extracted from PMV-infected Brachypodium plants at 42 dpi. The PMV 3′-UTR was selectively amplified and cloned using a modified oligo-T-adapter primer for first strand cDNA synthesis, followed by RT-PCR amplification using PMV-specific forward and adapter-specific reverse primers (Supplementary Figure 3.3). The numbers in subscript represent specific nt sites of sequence addition on the PMV genomic RNA. Additional 3′ sequences that were not part of the PMV genome or the oligo-dT-adapter sequence are underlined and bolded. The text in brackets represents the reverse complement of the oligo-dT-adapter primer for first-strand cDNA synthesis (Supplementary Figure 3.3).

a pathogenicity factor utilized by the virus, and may represent a form of host-mediated RNA degradation.

3.4 DISCUSSION

RNA viruses of both plants and animals have been studied in great detail with regard to viral replication, gene expression, and antagonism of host defense systems. However, our knowledge of the dynamic modifications to viral RNA genomes during infection is currently lacking. Previous studies have indicated that the 3′-ends of viral RNAs are susceptible to a variety of active modifications, many of which are likely detrimental to the genomic integrity of the virus. Here, we present multiple pieces of experimental evidence suggesting a variety of active modifications to the 3′-ends of viral and subviral genomes in the infected host cell. We demonstrated that a satRNA of PMV actively acquires varying lengths of the PMV 3′ RNA sequence during systemic accumulation, and has host-specific influences on disease, both at the molecular and phenotypic levels. This study reports the systemic presence of the satS-PMV chimeras in four diverse grass hosts, during both native and laboratory infections, raising questions about the host-dependent roles of satS in disease. We also report the *de novo* polyadenylation of PMV and SPMV in Brachypodium, and the presence of polyadenylated viral and subviral RNAs in native infections of St. Augustinegrass. However, the majority of polyadenylated PMV RNAs are likely non-functional due to major truncations at the 3′-end of the viral genome. Our findings have implications for the RNA-RNA interactions that are likely occurring between helper viruses, their satellite agents, and host cellular factors. These findings also present intriguing hypotheses for our understanding of the molecular arms race between virus and host, and the series of events that ultimately results in disease progression or a successful host defense response.

During our initial analysis of the PMV satRNAs, we found that satS accumulated systemically in both Brachypodium and proso millet, resulting in altered disease symptoms, while satC appeared to be non-infectious (Figures 3.1 and 3.2). This apparent non-infectivity of the original satC clone is interesting, considering that the sequences of the isolated satS-PMV chimeras look very similar to the original satC, with regard to the additional 3′ PMV sequence (Monis et al., 1992). However, a sequence alignment of the original satS and satC clones reveals many sequence differences between the two satRNAs, particularly in the middle of satS and 5′-end of satC (Supplemental Figure 3.1). These differences in sequence, combined with overall differences in secondary RNA structure, may result in the inability of satC to accumulate systemically in the same manner as satS. Alternatively, host-specific factors could play a role in sequence composition and systemic accumulation, since satS and satC were originally isolated from different grass hosts. It is yet to be determined whether removal of the 3′-end of satC, with sequence similarity to the PMV genomic RNA, would allow for systemic accumulation of satC in Brachypodium and proso millet.

In our analysis of the satS-induced effect on the accumulation of helper virus RNA and CP, we found host-specific differences between Brachypodium and proso millet (Figures 3.4 and 3.5). In proso millet, satS induced a striking attenuation in the disease phenotype normally associated with PMV alone, which was directly correlated with a significant reduction in the overall accumulation of PMV RNA and CP (Figures 3.4B and 3.5B). In contrast, PMV supported the replication of satS during early stages of infection in Brachypodium, but appeared to overcome the attenuating effects of satS in later stages. This was demonstrated by the temporal accumulation of helper RNA and CP in the non-inoculated tissues and the reduced accumulation of satS RNA by 14 dpi (Figures 3.4A and 3.5A). This was also reflected by a less apparent attenuation in the disease phenotype, compared to the loss of symptoms seen on proso millet (Figure 3.1A-B). These findings reflect the host-specific nature of the role(s) for satS in the progression of disease.

Sequence analysis of the satS-PMV chimera RNAs revealed significant sequence variability among the isolates (Table 3.1). On average, the chimera RNAs had acquired approximately 100-200 nucleotides from the 3′-end of the PMV genome during systemic accumulation. Most of the chimeras had unique 5′ and 3′ recombination sites between the satS and PMV RNAs, however two primary sequence hot spots were identified on the PMV genome (Figure 3.3). These recombination hot spots were found flanking the PMV 3′-CITE (Batten et al., 2006b). We were intrigued to discover the presence of heterogeneous, U-rich linker sequences in most of the clones that were isolated from Brachypodium and proso millet (Table 3.1). Surprisingly, more than half on the Brachypodium isolates contained the linker motif 5′-UACCUUU-3′, which has sequence identity to the region near the sgRNA promoter on the PMV genome. Many questions remain regarding the role(s) of the PMV 3′-CITE and sgRNA promoter in the generation of the satS-PMV chimeras during infection. It seems likely that these recombination events are partially influenced by the complex secondary RNA hairpin structures present in the 3′-end of the PMV genome (Batten et al., 2006b; Miller et al., 2007). We are currently investigating the infectivity of the satS-PMV chimeras that were isolated from Brachypodium and proso millet, and whether their pathogenesis, or lack thereof, resembles that of the original satC clone.

This study also provides the first report of PMV satRNAs in cultivated switchgrass (Figure 3.6). For many years, we had hypothesized that the PMV satRNAs may be limited to lower latitude regions of the U.S., since they had only been detected in infected turfgrass samples from the Gulf Coast states (Cabrera and Scholthof, 1999; Cabrera et al., 2000; Batten and Scholthof, 2004a). However, these findings challenge that hypothesis, and show that PMV+satRNA co-infections are more geographically widespread than previously observed. We were interested to find that satS and the satS-PMV chimeras were only amplified from samples that also contained SPMV (Figure 3.6). These findings correlate with a previous study from our lab, demonstrating that the CP of SPMV can specifically bind to the satRNAs, and that the satRNAs are preferentially packaged by SPMV during a triple co-infection (Desvoyes and Scholthof, 2000). This would suggest that, despite the antagonistic role of satS in laboratory inoculated hosts, there may be some evolutionary advantage for retaining both satS and SPMV during native co-infections. We are currently investigating the outcomes of a triple co-infection of PMV+SPMV+satS-inoculated Brachypodium and proso millet.

Many questions remain regarding the molecular events that result in the generation of these satS-PMV chimeras. Perhaps these subviral agents represent a novel form of hybrid DI-satRNAs, which would imply that they are primarily a product of virus replication errors. This hypothesis was originally proposed for one satRNA of TCV, satC, which possesses characteristics very similar to those of the satS-PMV chimeras observed in this study (Simon and Howell, 1986; Simon et al., 1988; Cascone et al., 1990; Zhang et al., 1991). However, it has since been determined that co-infections of TCV+satC result in exacerbated symptoms in host plants (Sun and Simon, 2003). Alternatively, these satS-PMV chimeras could represent a novel host-directed, RNA-mediated antiviral response. More detailed molecular studies investigating the specific interactions between host, viral, and subviral factors are needed to address and test these hypotheses. These studies would also reveal clues about the enigmatic, potentially host-derived, origins of satRNAs.

The host-specific nature of satS suggests that fundamental differences must exist in either i) host factors that interact directly or indirectly with the replication machinery of PMV, resulting in differential accumulation of the DI-satS-PMV chimeras and helper virus factors, or ii) host defense factors that are preferentially activated in the presence of satS-PMV chimeras, resulting in depletion of the virus and satRNA from the infected host cells.

Additionally, we present multiple pieces of evidence demonstrating that PMV and each of its satellite agents are polyadenylated *in vivo* during infection of multiple host grasses. This novel feature was observed for PMV- and PMV+SPMV-infected

Brachypodium in the laboratory and during native infections of St. Augustinegrass (Figure 3.7A-B). Interestingly, in the case of Brachypodium, this appears to be an active mechanism of polyadenylation, as the *in vitro*-synthesized transcripts of PMV and SPMV do not have poly(A) tails. Similar features of active polyadenylation of viral RNAs have been observed in only a handful of earlier studies for both plant (*Beet necrotic yellow vein virus*, *White clover mosaic virus*) and animal (*Hepatitis C virus*, *Sindbis virus*) +ssRNA viruses (Jupin et al., 1990; Guilford et al., 1991; Hill et al., 1997; Raju et al., 1999; van Leeuwen et al., 2006). More recently, Li et al. demonstrated that several +ssRNA plant viruses known to lack poly(A) tails acquired a heterogeneous, adenine-rich sequence at the 3′-ends of their genomic RNAs *in vivo* through a currently unknown mechanism (Li et al., 2014). The significance of this *de novo* polyadenylation remains poorly understood.

Our initial hypothesis was that the addition of a poly(A) tail could protect viral RNAs from RNase-mediated degradation and facilitate translation of the viral gene products. In this sense, the *de novo* polyadenylation of +ssRNA viruses may be a critical pathogenicity factor. However, the sequencing results presented in this study show that the polyadenylated PMV RNAs resemble cellular by-products resulting from cytoplasmic RNA degradation pathways (Slomovic et al., 2010; Moon et al., 2012). This is apparent from the presence of major 3′-end truncations in the isolated PMV sequences, often followed by heterogeneous U-rich sequences and relatively short poly(A) sequences (Table 3.2). This RNA degradation pathway could represent a novel form of RNA-mediated antiviral defense response conserved among eukaryotes. It is well established in mammalian systems that preformed cytoplasmic RNA receptors stand as a first line of defense for specific recognition of viral RNAs and activation of downstream interferon-mediated defense responses (Chan and Gack, 2015; Sparrer and Gack, 2015). Questions remain about whether this predicted RNA degradation pathway could be specifically acting on viral RNAs in diverse eukaryotes, or if the pathway is a general post-transcriptional control mechanism employed by the host to control levels of cellular RNAs (Dreyfus and Régnier, 2002; Reinisch and Wolin, 2007; Barr and Fearns, 2010; Moon et al., 2012).

Given that most of these clones are lacking in critical 3′-end sequences, including the PMV 3′-CITE and other genomic regulatory elements, we hypothesize that these isolates would not produce infectious virus progeny. However, we are currently in the process of testing the infectivity of select polyadenylated isolates, including the one isolate that was polyadenylated at the terminal 3′ sequence of the PMV genome (Table 3.2). We are also interested in determining whether PMV, SPMV, and the satS RNAs are packaged into virions in a polyadenylated state. This would indicate that polyadenylated viral and subviral RNAs could be successfully transmitted to new host plants. As a component of this, we are also curious about the subcellular location of the viral and subviral RNA polyadenylation. Most polyadenylation in eukaryotes occurs in the nucleus, however PMV and its satellites are predicted to replicate in the cytoplasm (Batten and Scholthof, 2004b; Batten et al., 2006a). We know that the CPs of PMV and SPMV localize to the nucleus and nucleolus/Cajal body-like structures, respectively, and that the CPs have an affinity for their corresponding genomic RNAs and the satRNAs

(Desvoyes and Scholthof, 2000; Qi et al., 2008). Thus, the PMV and SPMV CPs could act as chaperones for the nuclear/nucleolar import of the viral and subviral RNAs for polyadenylation. Alternatively, a family of monocot-specific poly(A) polymerases (PAPs), which lack a nuclear localization domain, could add poly(A) sequences to the viral and subviral RNAs in the cytoplasm (Hunt et al., 2012). These experiments are currently underway, and should reveal more information about the nature of the polyadenylated viral and subviral RNAs.

3.5 MATERIALS AND METHODS

3.5.1 Plant Growth Conditions and Sampling

Brachypodium distachyon (accession Bd21-3) and *Panicum miliaceum* were planted 3 seeds to a pot in 2×3-in. rectangular and 4-in. circular pots, respectively (BWI Companies). Seeds were planted in Redi-earth soil (Sungrow Horticulture), covered, and stratified in the dark at 4°C for 5-7 days to allow for equal germination times. Following the cold treatment, plants were moved to growth chambers programmed for diurnal cycles of 14 hr daylight (~250-300 $\mu mol/m^2s$), 10 hr dark at 21°C and 18°C, respectively. Plants were fertilized weekly with Peters 15-5-15 micronutrient fertilizer (BWI Companies), and allowed to grow for approximately 2 weeks before inoculation.

Brachypodium and proso millet were sampled for total RNA and protein extractions at 7, 10, and 14 dpi. At 7 dpi, samples were collected from both the inoculated and the upper, non-inoculated tissues for all mock-inoculated and transcript-inoculated plants. At 10 and 14 dpi, samples were only taken from the upper, non-inoculated tissues. Leaf tissues from three individual plants were pooled during sampling to constitute each individual sample. For the PMV and SPMV polyadenylation experiments (Figure 3.2A), the non-inoculated tissues of three individual Brachypodium plants were pooled at 42 dpi for total RNA isolation and subsequence cDNA preparation.

Panicum virgatum (switchgrass) samples were collected as part of a separate study from a breeding nursery located near Mead, NE (41.166103°N, 96.482938°W) during the summer of 2012 (Stewart et al., 2015). Field samples were kept in coolers and delivered to the University of Nebraska in Lincoln, NE, where they were stored at -75°C for approximately one year. Samples were then sent on ice to Texas A&M University in College Station, TX, where they were stored at -80°C until processing. Symptomatic and asymptomatic St. Augustinegrass samples for the polyadenylation experiments (Figure 3.2B) were collected from a 10 m^2 lawn area on the Texas A&M campus (30.615481°N, 96.338344°W) and stored at -80°C until processing.

3.5.2 Synthesis of RNA Transcripts and Inoculations

Full-length cDNA plasmid clones of PMV (pPMV85), SPMV (pSPMV1), satS (psatS3), and satC (psatC4) were used to generate genomic RNA transcripts for inoculation of Brachypodium and proso millet hosts (Masuta et al., 1987; Monis et al., 1992; Turina et al., 1998). Plasmids were linearized using the restriction endonucleases *Eco*ICRI for pPMV85, *Bgl*II for pSPMV1 and psatS3, and *Xba*I for psatC (New England Biolabs), and RNA was synthesized for each using T7 polymerase (Fermentas). *In vitro* transcribed RNAs were separated and observed on 1% agarose gels by electrophoresis and ethidium bromide staining to assess transcript quality and relative abundance. Inoculum was prepared by mixing each of the co-infecting transcripts in a 1:1 (v:v) ratio, and combining the transcript mixture with an equal volume of RNA inoculation buffer (0.05 M KH_2PO4, 50 mM glycine, pH 9.0, 1% bentonite, 1% celite) as described previously (Mandadi and Scholthof, 2012; Mandadi et al., 2014). Each individual Brachypodium and proso millet plant was inoculated with 8 μl of the transcript/buffer mixture and kept in the dark at room temperature overnight. After the overnight waiting period, the plants were returned to the normal growth chamber conditions for the remainder of the infection cycle.

3.5.3 Total RNA Extractions, cDNA Preparations, and RT-PCRs

Total RNA was isolated from Brachypodium, proso millet, switchgrass, and St. Augustinegrass samples as described previously using Direct-zol RNA MiniPrep kits (Zymo Research) with TRI Reagent (Ambion), following the manufacturers protocol (Mandadi et al., 2014). The quantity and quality of the total RNA was assessed using Nano-Drop absorption values and by electrophoresis on 1% agarose gels, followed by ethidium bromide staining. Approximately 1 μg of total RNA from each sample was used as the template for cDNA preparation using M-MLV Reverse Transcriptase (Invitrogen). Total cDNA was primed using random DNA hexamers and oligo-dT primers for the satRNA and polyadenylation experiments, respectively. RT-PCRs were performed using standard *Taq* DNA polymerase (New England Biolabs) and appropriate primer sets (Supplementary Table 3.1).

3.5.4 Immunoblot Detection of the PMV CP

Immunoblotting was performed as described previously (Mandadi et al., 2014). Briefly, tissue samples were homogenized in liquid nitrogen, and total soluble proteins were extracted using 5X Laemmli extraction buffer. Samples were boiled and subjected to centrifugation (12,000 × g) for 5 min each, immediately prior to electrophoresis. The total protein extracts were separated on 12.5% polyacrylamide-SDS gels and transferred to nitrocellulose membranes using standard SDS-PAGE equipment (BioRad). To assess approximately equal protein loading, replicate gels were stained in Coomassie Brilliant Blue. Membranes were blocked in 5% milk in 1X Tris-buffered saline (TBS) (0.2 M NaCl, 50 mM Tris, pH 7.4) with 0.05% Tween-20 (TBST) for 1 hour at room temperature. After blocking, membranes were incubated in the primary antibody:milk-TBST solutions for anti-PMV (1:5,000) overnight at 4°C, washed twice with 1X TBST for 5 min each, then incubated in the secondary alkaline phosphatase (AP)-conjugated, anti-rabbit antibody:milk-TBST solution (1:10,000) for one hour at room temperature. Following the secondary incubation, the membranes were washed twice with 1X TBST and once with 1X TBS for 5 min each. The blots were developed by exposure to nitroblue tetrazolium (NBT) and bromo-4-chloro-3-indolylphosphate (BCIP) in 1X AP buffer (100 mM NaCl, 5 mM $MgCl_2$, 1M Tris pH 9.5).

3.5.5 Cloning and Sequencing of satS-PMV Chimeras and Polyadenylated RNAs

Amplified RT-PCR products, using primers for the satS-PMV chimeras or polyadenylated PMV RNAs (Supplementary Table 3.1), were directly ligated into pGEM-T vector plasmids (Promega) according to manufacturers protocol. Plasmids were transformed into electrocompetent DH10B *E. coli* cells, and the transformed cells were subjected to X-gal blue-white screening. Single colonies were selected and the plasmids were isolated using QIAprep Spin Miniprep kits (Qiagen). Inserted amplicons were prepared for sequencing using the chain-termination ABI BigDye reaction mix (Applied Biosystems) with M13 forward primers (Supplementary Table 3.1), and Micro Bio-Spin clean-up columns (BioRad). Sequencing was performed by the Texas A&M Gene Technologies Laboratory (http://www.idmb.tamu.edu/gtl/) using an ABI 3100 automated sequencer (Applied Biosystems).

4. MULTI-YEAR PATHOGEN SURVEY OF BIOFUEL SWITCHGRASS BREEDING PLOTS REVEALS HIGH PREVALENCE OF INFECTIONS BY *PANICUM MOSAIC VIRUS* AND ITS SATELLITE VIRUS[*]

4.1 OVERVIEW

Switchgrass (*Panicum virgatum* L.) cultivars are currently under development as lignocellulosic feedstock. Here we present a survey of three established switchgrass experimental nurseries in Nebraska in which we identified *Panicum mosaic virus* (PMV) as the most prevalent virus. In 2012, 78% of 139 symptomatic plants tested positive for PMV. Of the PMV-positive samples, 17% were co-infected with PMV and its satellite virus (SPMV). Less than 14% of all sampled plants in 2012 were positive for four additional viruses known to infect switchgrass. In 2013, randomized sampling of switchgrass individuals from the same 2012 breeding plots revealed that infection by PMV or PMV+SPMV was both more prevalent and associated with more severe symptoms in the cultivar Summer, and experimental lines with Summer parentage, than populations derived from the cultivar Kanlow. A three-year analysis, from 2012-2014, showed that previously uninfected switchgrass plants acquire PMV or PMV+SPMV between harvest cycles. In contrast, some plants apparently did not maintain PMV

[*] Reprinted with permission from "Multi-year pathogen survey of biofuel switchgrass breeding plots reveals high prevalence of infections by *Panicum mosaic virus* and its satellite virus." by Stewart, C. L., Pyle, J. D., Jochum, C. C., Vogel, K. P., Yuen, G. Y., and Scholthof, K.-B. G. 2015. Phytopathology. In press. http://dx.doi.org/10.1094/PHYTO-03-15-0062-R. Copyright [2015] by The American Phytopathological Society.

infections at detectable levels from year-to-year. These findings suggest that PMV and SPMV should be considered important pathogens of switchgrass and serious potential threats to biofuel crop production efficiency.

4.2 INTRODUCTION

In the past decade public and private efforts have focused on developing high lignocellulosic biomass crops as feedstock for generation of biofuels (McLaughlin and Kszos, 2005; Somma et al., 2010; Perry, 2012). One promising North American crop is switchgrass (*Panicum virgatum* L.), a warm-season C_4 perennial grass native to the region east of the Rocky Mountains (Vogel, 2004; McLaughlin and Kszos, 2005). Switchgrass is a high yielding perennial biomass plant that can be grown on marginal cropland with total net energy production outputs of more than 500% of total resource input (Sanderson et al., 1996; Hill et al., 2006; Bouton, 2007; Schmer et al., 2008). In terms of biofuel production, cultivated switchgrass is estimated to match current ethanol yields derived from maize, and will likely exceed these production amounts as switchgrass cultivation, development, and processing technologies continue to advance and develop (Bouton, 2007; Schmer et al., 2008).

The emergence of pathogens in newly established switchgrass agro-ecosystems, and concomitant production losses, is a matter of concern for plant pathologists, plant breeders and agronomists. Current switchgrass cultivars deployed in the field for forage and erosion control are typically described as tolerant or unaffected by most types of microbial pathogens (Vogel, 2004; Bouton, 2007), yet our knowledge of pathogens of switchgrass is limited. Several species of plant-pathogenic fungi including *Bipolaris oryzae* (leaf spot), *B. spicifera* (spot blotch and root rot), *Colletotrichum graminicola* (leaf spot), *C. navitas* (anthracnose), *Elsinoe panici* (leaf spot), *Puccinia emaculata* (rust), *Rhizoctonia cerealis* (sharp eyespot), *Tilletia pulcherrima* (bunt), and *Uromyces graminicola* (rust) have been isolated and identified as compatible disease-causing agents of switchgrass (Tiffany and Knaphus, 1995; Etheridge et al., 2001; Krupinsky et al., 2004; Carris et al., 2008; Crouch et al., 2009; Vu et al., 2011; Uppalapati et al., 2013). Thus far, confirmed reports of plant pathogenic bacteria and nematodes of switchgrass are limited or circumstantial (Cassida et al., 2005; Mekete et al., 2010). The absence of field pathogenicity surveys of microbial pathogens on switchgrass hosts indicates that their potential impact on switchgrass production efficiency remains undetermined.

Plant viruses comprise another pathogen group for which little information is available as to their occurrence and importance in switchgrass. Members of the *Luteoviridae* family, including *Barley yellow dwarf virus* (BYDV, genus: *Luteovirus*) and *Cereal yellow dwarf virus* (CYDV, genus: *Polerovirus*) have been identified as compatible pathogens of switchgrass (Garrett et al., 2004). BYDV and CYDV are positive-sense, single-stranded RNA (+ssRNA) viruses that rely on aphid vectors for plant-to-plant transmission. Multiple strains of these viruses have been identified and characterized by their strain-specific association with key aphid vectors. BYDV strains MAV and PAV and CYDV strain RPV are known pathogens of switchgrass in the field and rely on persistent transmission by multiple species of aphid vectors including the grain aphid (*Sitobion avenae*), the bird cherry-oat aphid (*Rhopalosiphum padi*), and rose grain aphid (*Metopolophium dirhodum*) (Gray and Gildow, 2003; Garrett et al., 2004). Additional +ssRNA viruses of switchgrass include *Sugarcane mosaic virus* (SCMV, genus: *Potyvirus*) and Switchgrass mosaic virus (SwMV, genus: putative *Marafivirus*) (Agindotan et al., 2010; Agindotan et al., 2013c). Recently, high-throughput sequencing analyses indicated the presence of partial sequences related to eight RNA viruses and one DNA virus in diverse families (Agindotan et al., 2013a). Together, these studies suggest that pathogenic viruses of switchgrass are likely present in the field, but their prevalence in cultivated switchgrass and their impact on switchgrass growth are largely unknown.

Panicum mosaic virus (PMV) was discovered in Kansas in 1953 and described as the first viral pathogen of switchgrass (Sill and Pickett, 1957). PMV also infects St. Augustinegrass (*Stenotaphrum secondatum*), a turfgrass, causing St. Augustine Decline disease, as first reported in the early 1960s (Batten and Scholthof, 2004a). PMV infects residential St. Augustinegrass lawns in states along the Gulf Coast region of the United States and, recently, in New South Wales, Australia (Batten and Scholthof, 2004a; Thomas and Steele, 2011). PMV has also been identified in St. Augustinegrass in Oklahoma, Kansas, Nebraska, Wisconsin, North and South Carolina (Batten and Scholthof, 2004a; Thomas and Steele, 2011). In addition to switchgrass and St. Augustinegrass, PMV infects pearl (*Pennisetum glaucum*), proso (*Panicum miliaceum*), and foxtail (*Setaria italica*) millets; maize (*Zea mays*); centipedegrass (*Eremochloa ophiuroides*); and crabgrass (*Digitaria sanguinalis*) (Batten and Scholthof, 2004a).

Experimental model hosts of the virus include *Brachypodium distachyon* (Brachypodium) and *Setaria viridis* (Setaria) (Mandadi and Scholthof, 2012; Mandadi et al., 2014).

PMV is a +ssRNA virus and the type member of the genus *Panicovirus* in the *Tombusviridae* (Turina et al., 1998; Turina et al., 2000). The 4,326 nucleotide (nt) genomic RNA is encapsidated by a 26-kD capsid protein (CP) to form 30 nm icosahedral virions. An unusual feature of PMV is that the virus supports the accumulation of a satellite virus (SPMV) (Masuta et al., 1987; Turina et al., 1998; Scholthof, 1999). SPMV, an 826 nt +ssRNA, encodes a 17.5-kDa CP that is assembled into 16-nm icosahedral virions. By definition, a satellite virus like SPMV is dependent on its helper virus (PMV) for replication and systemic movement in the host plant. The mixed infection of PMV+SPMV is characterized by exacerbated host symptoms and more rapid systemic accumulation of the viruses than observed during infections by PMV alone (Scholthof, 1999; Mandadi and Scholthof, 2012). Despite the observed severity and prevalence of this pathosystem in St. Augustinegrass and the significant overlap in the geographic distributions of PMV and cultivated switchgrass, there have been no reports or surveys investigating the emergence of the PMV disease complex in switchgrass populations.

Because cropping systems for switchgrass as a biofuel are still being developed, comprehensive pathogen surveys are required in order to proactively assess the potential pathogen-associated threats to large-scale production. Here we report on plant viruses present in three previously established genetic and breeding experimental field nurseries in eastern Nebraska. The nurseries were designed prior to this survey to aid in the development and ultimate release of bioenergy switchgrass cultivars. A pathogenicity assessment in these established experimental fields was performed to determine potential cultivar-specific pathogen problems, which may inform future decisions regarding the selection of optimum switchgrass cultivar for lignocellulosic feedstock. Findings from this three-year study, from 2012 to 2014, identified PMV and PMV+SPMV as the most prevalent infection types in experimental switchgrass populations. Additionally, this viral disease complex was consistently associated with enhanced field symptomatology in susceptible switchgrass populations.

4.3 RESULTS

4.3.1 Prevalence and Distribution of Virus-associated Symptoms in Switchgrass Breeding Plots in 2012

Typical virus-like symptoms observed on switchgrass plants in the field included mild to severe chlorotic mottling or mosaic of the foliage, as well as stunting of most or all tillers of individual plants (Figure 4.1). Surprisingly, nearly 60% of the switchgrass populations in the two experiments PV1103 and PV1104, each containing more than 1700 plants of a single population, were symptomatic (Table 4.2). Of the plants in the PV1103 and PV1104 nurseries, 12% and 24%, respectively, exhibited high disease severity ratings (DSR 4 or 5).

In contrast, disease incidence varied markedly among the five switchgrass populations in experiment PV0910, each with roughly 300 plants.

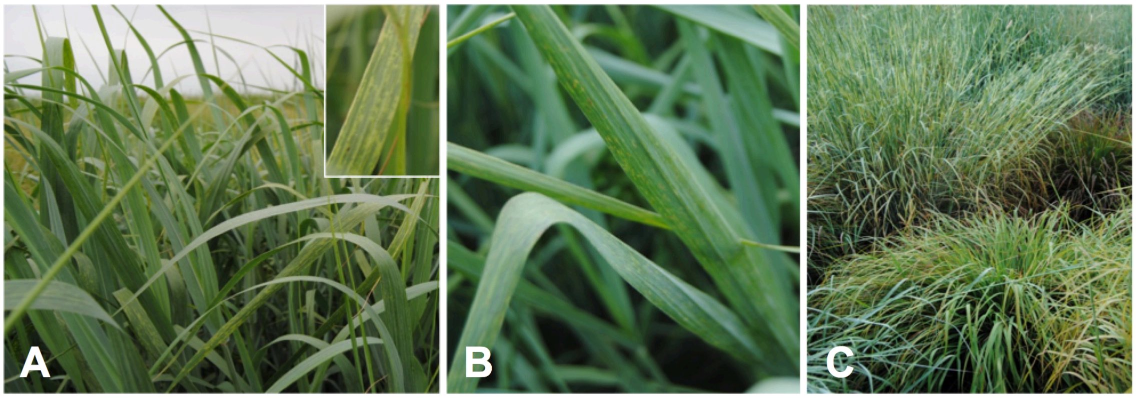

Figure 4.1. Virus-like symptoms in switchgrass populations in 2012. Chlorotic mottling and mosaic symptoms were frequently observed on switchgrass canopy tissues, as shown on the foliage of Kanlow (A) and Kanlow N1 (B) individuals. The inset image in (A) depicts the chlorotic mosaic pattern from an individual of the Kanlow population. Typical stunting of above-ground portions of plants associated with virus infection were also prominent, as shown for an individual of the Kanlow variety, seen in the picture foreground, compared with a Kanlow plant with normal growth in the background (C).

DSR	Associated disease characteristics
1	No visual symptoms associated with viral infection
2	Indistinct mottling or mosaic, or distinct mottling or mosaic in less than 10% of the canopy
3	Distinct mottling or mosaic in greater than 10% but less than 50% of the canopy
4	Distinct mottling or mosaic in over 50% of the canopy
5	Distinct mottling or mosaic in over 50% of the canopy, with additional stunting

Table 4.1. Disease severity rating (DSR) system for virus symptoms on switchgrass plants.

Experimental field or population	Total no. plants evaluated	No. symptomatic plants (% of total)	No. plants with high or severe symptoms* (% of total)
PV1103	1718	991 (58%)	200 (12%)
PV1104	1788	1050 (59%)	436 (24%)
PV0910			
Summer	324	222 (69%)	60 (20%)
KxS	291	137 (47%)	22 (8%)
Kanlow	350	71 (20%)	1 (<1%)
Kanlow N1	356	80 (22%)	2 (1%)
Kanlow High Yield	364	79 (22%)	3 (1%)

Table 4.2. Incidence of virus-associated symptoms in switchgrass populations in Nebraska field experiments in 2012. *Disease severity ratings (DSR) of 4 or 5.

The highest disease incidence (69%) was found in Summer, whereas Kanlow and the two Kanlow-derived populations (Kanlow N1 and Kanlow High Yield) exhibited disease incidences of approximately 20%. Incidences of plants with a DSR of 4 or 5 also differed between Summer (20%) and the Kanlow-derived populations (<1%). The KxS population, based on crosses between Kanlow and Summer, from PV0910 was intermediate between that of the Summer and the Kanlow germplasm populations, with respect to total disease incidence and the incidence of plants with high to severe symptoms. Despite the high percentage of symptomatic plants, there were no obvious visual spatial patterns for symptomatic individuals or for symptom severity within a population. A representative example of the distribution of symptomatic individuals and the associated DSRs is illustrated for a portion of field PV1104 (Supplementary Figure 4.1A). Together, these results reveal that virus-associated symptoms, such as chlorotic mottling, mosaic, and stunting were highly prevalent among individuals in the switchgrass experimental fields, particularly in certain switchgrass populations.

4.3.2 Detection of Viruses in Switchgrass Samples

With the high incidence of virus-associated symptoms observed in 2012 in the switchgrass experiments, we next sought to identify potential causal agents. In total, 139 individual plants were sampled and analyzed via DAS ELISA for BYDV-MAV, BYDV-PAV, CYDV-RPV, PMV, and SCMV and WSMV. Of the samples collected, 78% (109 samples) were positive for PMV (Table 4.3). Four other viruses were detected in 14% (20 samples) of all samples tested.

Virus(es) detected	Number of plants	Percentage of total plants tested
No virus detected	34	24%
Single virus detected		
PMV	81	58%
CYDV-RPV	8	6%
SCMV	7	5%
BYDV-MAV	1	1%
BYDV-PAV	2	1%
Multiple viruses detected		
PMV+SPMV	19	14%
PMV+SCMV	5	4%
PMV+CYDV-RPV	4	3%
PMV+BYDV-PAV	2	1%
PMV+CYDV-RPV+SCMV	1	1%

Table 4.3. Incidences of single- and multiple-virus infections among symptomatic switchgrass plants sampled in 2012. Each of 139 samples were tested by DAS ELISA for the presence of *Panicum mosaic virus* (PMV), *Barley yellow dwarf virus* strains MAV and PAV (BYDV-MAV, -PAV), *Cereal yellow dwarf virus* strain RPV (CYDV-RPV), and *Sugarcane mosaic virus* (SCMV). Only PMV-positive samples were tested for the presence of its satellite virus (SPMV) by immunoblot analysis.

Additionally, 24% (34 samples) did not give a positive ELISA reaction for the tested viruses. WSMV was not detected in any samples by DAS ELISA.

Subsequent immunoblot analyses of the 109 PMV-positive samples revealed that 19 (14% of the total samples) were also positive for SPMV (PMV+SPMV). From the ELISA results, 12 PMV-infected plants (9% of all samples) were co-infected with viruses other than SPMV. None of these 12 individuals tested positive for the presence of SPMV. Overall, these results demonstrate that PMV, alone or in a co-infection with SPMV or with other unrelated viruses, was the predominant virus detected among symptomatic switchgrass samples in the experimental fields in 2012.

4.3.3 PMV and SPMV Incidence in 2013

During the 2013 harvest cycle, the same experimental fields that were surveyed in 2012 (PV1103, PV1104, and PV0910) were assessed for PMV and PMV+SPMV incidence. We used leaf tissue from plants selected randomly, without regard to symptomology. PMV was assayed by DAS ELISA. Samples that were negative by ELISA were retested for PMV by RT-PCR. All PMV-positive samples were tested for SPMV by RT-PCR. Of 56 plants sampled from PV1103, 2 (4%) tested positive for PMV alone, 27 (48%) tested positive for PMV+SPMV, and 26 (46%) were negative for PMV (Figure 4.2). Of 53 plants sampled from PV1104, none were positive for PMV alone, 41 samples (76%) had both PMV and SPMV, and 12 (23%) of the plants tested negative for PMV.

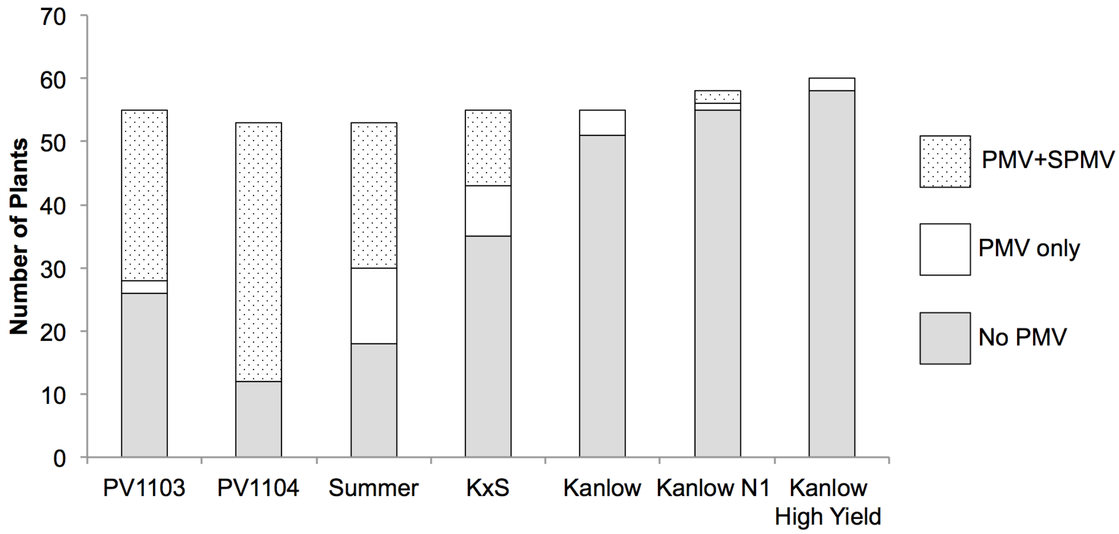

Figure 4.2. Incidence of *Panicum mosaic virus* (PMV) and its co-infecting satellite virus (PMV+SPMV) among randomly sampled switchgrass plants during the 2013 growing season. Leaf samples were collected from more than 50 plants in fields PV1103 and PV1104, and each of the five named switchgrass populations that were planted in field PV0910. Samples were tested for the presence of PMV by double antibody sandwich enzyme-linked immunosorbent assay (DAS ELISA) and for SPMV by reverse transcription polymerase chain reaction (RT-PCR).

Experimental field PV0910 contained five switchgrass populations planted in three clonal replicate blocks, each replicate block contained genetically identical plants to the other replicates. This field provided us with an opportunity to determine if specific populations being developed for desirable bioenergy traits differed in susceptibility to infection by PMV alone or the co-infection of PMV+SPMV. It is not known whether selective breeding measures have an impact on host susceptibility or tolerance to pathogens. To evaluate this, more than 50 plants in each population were randomly sampled and tested for PMV and SPMV in 2013. Less than 10% of the sampled plants from Kanlow and the two Kanlow-derived populations were positive for PMV or PMV+SPMV (Figure 4.2). In contrast, Summer and KxS populations had 66% and 36% of the sampled plants, respectively, infected with PMV alone or with PMV+SPMV. In both the Summer and KxS populations, nearly twice as many plants were infected with PMV+SPMV as were infected by PMV alone.

Together, these results reveal that the incidence of PMV and SPMV in 2013 varied among switchgrass populations. Summer and KxS appeared more prone to infection by PMV than populations derived from Kanlow. Furthermore, with the exception of infected plants in the Kanlow and Kanlow High Yield varieties, PMV was detected more often as a co-infection with SPMV than as a single infection.

4.3.4 Relationships Between PMV and PMV+SPMV Infection and Disease Severity

It is well established that PMV- and PMV+SPMV-infected Brachypodium and

Setaria host plants exhibit symptoms including chlorosis, necrosis, and stunting, and that co-inoculation of those hosts with PMV and SPMV can result in heightened symptom expression over PMV alone (Mandadi and Scholthof, 2012; Mandadi et al., 2014). However, it is not known whether such symptomology is recapitulated in PMV- and PMV+SPMV-infected switchgrass plants under field conditions. Thus, we were interested in the relation between virus presence and disease symptom severity.

In 2013, randomly-selected plants in PV1103, PV1104, and each of the five populations in PV0910 were sampled for virus presence and severity of virus-associated symptoms. Each plant was assigned a DSR (Table 4.1). Examination of the percentages of plants with no virus, PMV alone, or PMV+SPMV within each DSR category, with few exceptions, sampled plants with DSRs of 3 or higher were infected by either PMV alone or PMV+SPMV. However, a portion of PMV- and PMV+SPMV-infected plants, from 1.7% (Kanlow High Yield) to 24.5% (Summer), were symptomless (Figure 4.3). With the exception of two plants (KxS), DSRs of 4 and 5 were most often associated with plants that were co-infected with PMV and SPMV. Higher percentages of plants infected by PMV+SPMV, however, exhibited only mild to moderate symptoms (DSRs of 2 and 3, respectively). With the exception of one individual (KxS), all plants infected with PMV alone were associated with DSRs of 3 or lower.

The data also was analyzed by comparing mean DSRs between three virus categories (no virus, PMV only, PMV+SPMV) for each switchgrass population. In the PV0910 KxS population the mean DSR for plants infected by PMV alone was significantly higher (P=0.03) than plants with no PMV, but there was no significant difference in mean DSRs between plants infected by PMV+SPMV and plants with no virus (Table 4.4). In contrast, analysis of results from PV1103, PV1104, and PV0910 Summer populations revealed the mean DSRs for plants with PMV+SPMV to be higher ($P < 0.003$) than the mean DSRs for plants with no virus. The mean DSRs for plants with no virus and for those with PMV alone were not significantly different in Summer in experimental field PV0910; there were no plants in PV1104 having PMV alone. In the comparison of mean DSRs for 'PMV alone' with mean DSRs for 'PMV+SPMV', there was a significant difference only in Summer in PV0910, in which the mean DSR for plants infected with PMV+SPMV was higher than that of plants infected with PMV alone. Because of the low numbers of infected plants in the PV0910 Kanlow-derived populations, there were no significant effects of virus infection on DSRs in those populations.

Together, these results demonstrate that infection of switchgrass in the field by PMV and PMV+SPMV can lead to a range of DSRs. While the occurrence of virus symptoms under field conditions is closely related to infection by either PMV alone or PMV+SPMV, virus infection does not always lead to symptom expression. Furthermore, co-infection by PMV and SPMV does not always cause symptoms more severe than infection by PMV alone.

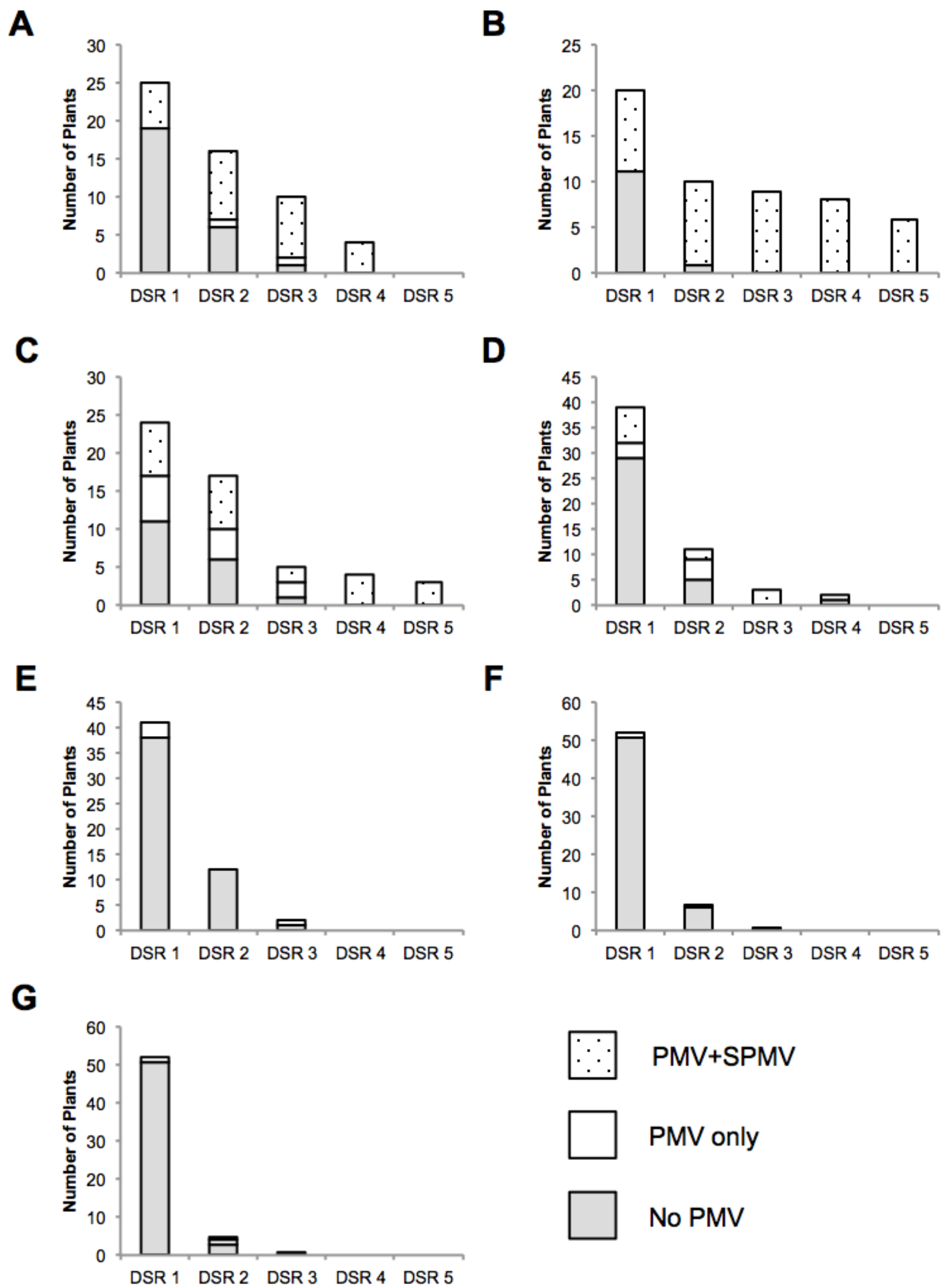

Figure 4.3. Relationship between presence of *Panicum mosaic virus* (PMV) and its co-infecting satellite virus (PMV+SPMV) and disease severity rating (DSR) of randomly sampled switchgrass in 2013. DSR 1 denotes no symptoms, while DSR 5 represents the highest symptom severity (Table 1). Individuals from fields PV1103 (A), PV1104 (B); and five populations in field PV0910: Summer (C), Kanlow x Summer (KxS) (D), Kanlow (E), Kanlow High Yield (F), and Kanlow N1 (G). Absence of a data bar indicates that no plants were in that virus infection or DSR category.

	No virus		PMV alone		PMV+SPMV	
Experimental Field or population	No. plants	Mean DSR	No. plants	Mean DSR	No. plants	Mean DSR
PV1103	26	1.3	2	2.5*	27	2.4**
PV1104	12	1.1	nd	nd	41	2.9**
PV0910						
Summer	18	1.4	12	1.7	23	2.5**#
Kanlow x Summer (KxS)	35	1.2	8	1.9*	12	1.7
Kanlow	51	1.3	4	1.5	nd	nd
Kanlow High Yield	58	1.1	2	1.5	nd	nd
Kanlow N1	55	1.1	1	2.0	2	1.5

Table 4.4. Mean disease severity ratings (DSR) among switchgrass plants with no virus detected, with PMV alone, and with PMV+SPMV. Plants were randomly sampled in 2013 from two Nebraska breeding nurseries (PV1103 and PV1104) and from five switchgrass populations in experimental field PV0910.
* and ** indicate significant difference from ‘No virus’ at P=0.05 and P=0.01, respectively, based on comparison of least squares means (ls-means) using SAS ProcMixed.
# indicates significant difference (P=0.05) between ls-means of ‘PMV alone’ and ‘PMV+SPMV’.
nd (no data) indicates an absence of plants in that category.

4.3.5 Year to Year Dynamics for PMV and SPMV

Switchgrass plants cultivated for bioenergy purposes are harvested annually for eight to ten years (Vogel, 2004; McLaughlin and Kszos, 2005). Thus, we were interested in determining the spread of PMV and SPMV and the persistence of these viruses in infected plants over annual harvest cycles. A subset of the sampled switchgrass individuals from two fields, PV1103 and PV1104, were assayed for PMV and PMV+SPMV for two harvest years (2012 to 2013; 2013 to 2014). A third subset was re-sampled from PV0910 for one harvest year (2013 to 2014). Plants for the 2012-2013 resampling experiment were different plants than those selected for the 2013-2014 assays. Included in each set were plants that did not test positive for PMV in the previous year, those that tested positive for PMV alone, and those that tested positive for PMV+SPMV. The three sets were analyzed together, with a pooled total population of 102 plants. Among the 35 plants that previously did not test positive for the presence of PMV, 19 (54%) remained virus-free in the following year, three (9%) tested positive for PMV alone, and 13 (37%) tested positive for the presence of both PMV and SPMV (Table 4.5). Surprisingly of the 27 plants that previously tested positive for PMV alone, 11 (41%) tested negative for the presence of either virus, and 16 (59%) tested positive for PMV+SPMV. None of the plants tested positive for PMV alone in the next year. Lastly, most (90%) of the 40 plants that previously tested positive for co-infection of PMV+SPMV remained positive for both viruses in the subsequent year, whereas only two plants each were virus free or positive for PMV alone.

Year 1	Number of Plants (Year 1)	Year 2	Number of Plants (Year 2)	Percentage of Year 1 Plants
No PMV	35	No PMV	19	54%
		PMV only	3	9%
		PMV+SPMV	13	37%
PMV only	27	No PMV	11	41%
		PMV only	0	0%
		PMV+SPMV	16	59%
PMV+SPMV	40	No PMV	2	5%
		PMV only	2	5%
		PMV+SPMV	36	90%

Table 4.5. Annual change in the occurrence of PMV and SPMV in individual switchgrass plants. Plants (n=102) were selected based on their disease category (No PMV, PMV only, or PMV+SPMV) in year 1 (2012 or 2013). These plants were sampled for virus presence or absence in year 2 (2013 or 2014, respectively).

Taken together, these results indicate that PMV and PMV+SPMV can spread to new susceptible hosts between harvest cycles, and that those plants infected with both viruses will likely remain infected throughout future years of cultivation. It appears, however, that some plants infected only with PMV can become virus free over a single year, suggesting that the virus was below detectable levels or the plant may have cleared the virus infection.

4.4 DISCUSSION

PMV was first reported almost six decades ago in Kansas in switchgrass breeding plots with little attention to virus-infections since this initial finding. However, with switchgrass receiving renewed attention in the twenty-first century as a bioenergy crop, it is important to determine which pathogens are present and if they are negatively affecting plant health. Here, we report the first survey of multiple viruses in switchgrass from three established experimental breeding fields in Nebraska. From our investigations, we found a frequently observed association between virus-like symptoms and viral infections. The predominant viral pathogen present in these nurseries was PMV, either as a single infection or in a co-infection with its satellite virus and other viruses. This is the first report of co-infections of PMV+SPMV in cultivated switchgrass in the field. It also is the first report of PMV in co-infections with unrelated viruses in switchgrass hosts. The biological significance of these viral co-infection combinations, and any effects it has on switchgrass production, is an area that deserves further attention.

In 2012, switchgrass plants were specifically identified, sampled, and tested based on symptoms that are often associated with virus infection (e.g., chlorotic mosaic or mottling, stunting, or necrosis.). One limitation of the 2012 experimental design is that the symptomatic plants were only tested for six suspected viruses and SPMV. As a result, any additional viruses present in the symptomatic plants, and viruses that infected the switchgrass hosts without inducing symptoms, were not detected. The randomized sampling in 2013 was designed to provide an overall estimation of PMV and SPMV incidence for all three fields. It should be noted that these three breeding plots are not, and should not be treated as, representatives for all switchgrass populations. However, the variety of genetic backgrounds for the different switchgrass populations in the three nurseries investigated in this study allows for some conclusions to be drawn about the natural incidence of virus infections for diverse switchgrass varieties.

Although PMV was first identified as a pathogen of switchgrass in 1953 and in St. Augustinegrass a decade later, the virus has been primarily studied in the laboratory, with few follow-up field surveys (Sill and Pickett, 1957; Cabrera and Scholthof, 1999; Batten and Scholthof, 2004a). Therefore, it was quite unprecedented to find PMV and SPMV as the predominant viral pathogens in switchgrass in this study. Several of the viruses identified in field samples are arthropod-transmitted (BYDV, CYDV, and SCMV). Arthropod-transmitted viruses are typically regarded as high-risk pathogens in agricultural settings due to their ability to spread quickly to new hosts over long distances (Jones, 2006). SwMV, transmitted by the leafhopper *Graminella aureovittata,* may also be considered a risk (Agindotan et al., 2013b). In this study, we did not test for the presence of SwMV and, therefore, the involvement of SwMV in these switchgrass fields is unknown. Mechanical transmission is the only known mechanism for plant-to-plant spread of PMV and SPMV. It is likely that mechanical transmission of PMV and SPMV plays an important role in virus spread given the perennial nature of the crop as well as the procedures associated with switchgrass harvesting and maintenance (Vogel, 2004).

Using a combination of random and targeted sampling approaches, we found that PMV alone and PMV+SPMV can spread to previously uninfected hosts in between harvest cycles. The co-infection of PMV+SPMV is more often detected together than PMV alone. Higher overall DSRs in the field are generally associated with PMV and PMV+SPMV infections across multiple genetically diverse switchgrass cultivars. Switchgrass populations Summer and KxS appeared to be more susceptible to infection by PMV or PMV+SPMV and more severe disease phenotypes were evident when compared to uninfected plants of the same cultivar.

In terms of viral pathogenesis and the unique PMV+SPMV disease synergism, it is interesting that PMV was found more often in a co-infection with SPMV in our random sampling of plants in breeding nurseries during the 2013 season than as a single infection (Figure 4.2). The precise molecular advantages for PMV and SPMV to coexist within the host cell are still largely unknown. The striking synergistic disease symptoms associated with PMV+SPMV infections of other grasses suggests that this might have significant negative implications for switchgrass production (Scholthof, 1999), especially in a cropping system where a single perennial plant is expected to be productive for multiple years. A limitation of the current study is that the 2013 sampling data was only focused on the incidence of PMV and SPMV as specific causal agents of disease. As a result, we cannot determine whether or not the sampled plants in 2013 were infected with additional viruses. Plants that tested negative for PMV may have been infected with an additional virus(es) which may have influenced the DSR. Given the sampling results from 2012 (Table 4.3), a portion of the plants sampled in 2013 might be infected by additional viruses. However, due to the design of this project, these data are not available.

In our investigation of the temporal dynamics of infection by PMV and PMV+SPMV, a number of uninfected plants tested positive for PMV and SPMV in the following year (Table 4.5). It seems likely that the viruses spread to new hosts during the mechanical fall harvesting and spring cultivation processes (Vogel, 2004). Additionally, it is possible that interactions between switchgrass roots in the soil can cause microabrasions in the root epidermal tissue that may allow for virus spread. Alternatively, a yet unidentified soil-borne vector could spread the viruses. Previous experiments have demonstrated that certain Brachypodium accessions infected with PMV and SPMV accumulate higher titers of the viral CPs in the root tissues, compared to other infected accessions (J. D. Pyle and K-B.G. Scholthof, unpublished data). This would suggest that differences in host factors might allow for altered accumulation of virus particles or other viral complexes in the root tissues. However, there is currently no experimental evidence to support this mode of PMV or SPMV transmission. Given that switchgrass plants are expected to remain in the ground for sequential harvesting over the course of 8-10 years, it is important to consider the possible modes of transmission for viruses like PMV and SPMV, which could potentially account for widespread reductions in biomass yields in a matter of a few years.

In the same re-sampling study, other individuals that previously tested positive for PMV were negative for the virus when re-tested in the next year (Table 4.5). It is generally accepted that once a virus causes a systemic infection, the host plant will likely remain infected throughout the duration of its life. Therefore, one possible explanation for the absence of the virus in samples from previously infected plants is that PMV alone is less effective than PMV+SPMV in spreading systemically into the foliage from overwintering crown and root tissues. Additionally, we have previously observed that slight modifications to environmental conditions (e. g., day length, light intensity, and temperature) can result in altered accumulation of detectable viral CPs, specifically in the case of SPMV (Cabrera and Scholthof, 1999; Mandadi and Scholthof, 2012; Mandadi et al., 2014). However, there is the possibility that antiviral RNA silencing and other host-mediated defense responses may result in clearing of the virus infection (Alvarado and Scholthof, 2009; Mandadi and Scholthof, 2012, 2013). Additionally, we cannot rule out the possibility of experimental or sample error, which may have resulted in the lack of PMV detection in these samples. Currently, there is a lack of available information pertaining to systemic viral movement within infected switchgrass hosts. This information could clarify the significance of winterkill on systemic viral movement within the plant, and the potential ability of the host to clear the virus infection. The possible interactions between host, viral, and environmental factors may explain the unusual findings for the apparent virus clearing in year 2, presented in Table 4.5.

Investigation of the potential factors involved may be important for our understanding of switchgrass antiviral responses and possible disease control mechanisms.

Another significant finding from this study pertains to the relationships that we identified between virus incidence, switchgrass cultivar, and increase in average DSR. Switchgrass varieties have been bred and selected for numerous desired traits and it is clear from the results of this study that some cultivars are more susceptible to virus infection than others. Our results indicate that the Kanlow parental variety may contain genomic features that confer tolerance against viral pathogens compared to populations with the Summer background. Segregation of the tolerance trait can be observed in the KxS switchgrass population that exhibited intermediate susceptibility and disease severity compared to the parent strains. The tolerance-imparting genetic loci in Kanlow against PMV should be investigated further as a possible parental resource for the development of switchgrass varieties that are less susceptible to the PMV disease complex, either through selective breeding methods or genetic engineering approaches.

Recent transcriptome analyses of field-grown Kanlow switchgrass revealed the upregulated expression of multiple WRKY transcription factors involved in pathogen response under field conditions, compared to the Summer variety (Palmer et al., 2014). Additionally, the gene expression levels for enzymes in the phenylpropanoid biosynthesis pathway, and accumulation of their downstream metabolite products are higher in the Kanlow cultivar compared to Summer (Palmer et al., 2014). Overall, the results from transcriptomic and metabolomic analyses suggests that Kanlow may be primed for defense against invading pathogens, including viruses, compared to the

Summer cultivar.

These genetic differences in switchgrass types in response to virus infection, suggest that in the future particular attention should be paid to Kanlow and other lowland germplasm as viable solutions towards improving the performance of switchgrass as a bioenergy crop. This study provides the first framework for our understanding of major viral pathogen problems for cultivated switchgrass and reveals PMV and PMV+SPMV as agents of concern for pathogen-associated losses in the field and reduced production efficiency for biofuel applications.

4.5 MATERIALS AND METHODS

4.5.1 Establishing and Maintaining Switchgrass Breeding Nurseries

Switchgrass plants for the field nurseries were established from greenhouse-grown switchgrass seedlings with a 16 hr light/8 hr dark photoperiod. The seedlings were grown in Ray Leach SC7 Cone-tainers (Steuwe & Sons, Inc., Tangent, OR) in a 1:1:1 potting mixture of loam soil:peat:perlite by volume. Switchgrass plants at the 2-3 leaf stage were transplanted into each respective experimental field plot.

The field plots were located at the University of Nebraska Agricultural Research and Extension Center located near Mead, NE (41.166103^{o} N, 96.482938^{o} W). These nurseries were PV0910, PV1103, and PV1104 with PV indicating *P. virgatum* (switchgrass), the first two numbers indicating the establishment year and the following two numbers indicating the sequential experiment number for that year. Field nurseries PV1103 and PV1104 were adjacent to one another in an area located approximately 2 km from PV0910. The three fields contained transplanted switchgrass plants grown in rows spaced 1.1 m apart. In PV0910, plants within rows were also spaced 1.1 m apart. In PV1103 and PV1104, plants in half-sib families or check strain plots were spaced 0.5 m apart. The switchgrass cultivars, experimental strains, and half-sib families that were in these fields are summarized in Supplementary Table 4.1. Each of the five cultivars or experimental strains in experiment PV0910 was treated as a distinct population. All of the plants in PV1103 were considered to be a single population in this study, as were all plants in PV1104.

Within the PV0910 field, soil between plants and rows were cultivated with 0.6 m-wide roto-tillers creating 0.4 m x 0.4 m mini-plots containing individual plants. In PV1103 and PV1104, roto-tillers were used between rows and hand weeding was used between plants within a plot. Nurseries were fertilized annually with 112 kg N per ha. In addition to tillage, the following herbicide mixture was applied to the field nurseries post transplanting and annually each spring: Metolachor [2-chloro-N-(2-ethyl-6methylphenyl)-N-(2-methoxy-1-methyl) acetamide], Atrazine (6-chloro-N-ethyl-N-isopropyl-1,3,5,-triazine-2,4-diamine) and 2,4-D (2,4-dichlorophenoxyacetic acid) at 1.1, 2.2, and 1.1 kg ai/ha, respectively. All nurseries were harvested in 2012 and PV1103 and PV1104 were also harvested in 2013. Harvests were made after a killing frost with a flail type forage plot harvester. In years when plants were not harvested in the fall, the nurseries were mowed or burned each spring to remove the accumulated biomass from the previous year.

4.5.2 Field Survey and Sampling Techniques

A preliminary inspection of established switchgrass nurseries was conducted in May 2012. From this initial inspection, three nurseries were identified with noticeable symptoms suggestive of virus infection. These nurseries were subsequently inspected and sampled during the 2012, 2013, and 2014 seasons. In 2012, inspection and sampling of symptomatic plants in PV1103 and PV1104 (one-year old nurseries) and PV0910 (a three-year old nursery), was conducted to assess virus symptom incidence and severity and for diagnosis of the causal agent(s). To provide a measure for the degree of symptom expression, we developed a visual disease severity rating (DSR) in which a 1 to 5 score was assigned to each plant based on a subjective scale of chlorotic mottling or mosaic of the foliage tissues and stunting of plants (Table 4.1). Each sample was placed in a plastic bag and kept on ice for transport to the University of Nebraska-Lincoln campus where the samples were stored at −20°C while processing plant material, and at −75°C for long-term storage.

In 2013, the second year of this study, randomly selected plants from plots PV0910, PV1103, and PV1104 were sampled to determine the incidence of infection by PMV alone and co-infections by PMV+SPMV, and if there were any relationships between virus infection, switchgrass cultivar/strain, and symptom severity. More than 50 plants were selected at random from each of the five populations in experiment PV0910 (over 250 plants total). Similarly, over 50 plants were identified randomly from each of experiments PV1103 and PV1104, with the plants in each of these two experiments representing single, distinct populations. Sampling and symptom severity scoring was performed for all three fields during the summer months, from May to August.

Field samples were obtained by grasping and tearing 2-3 leaves (ca. 15 cm tissue) at random from the top portion of the plant. There was no attempt to select leaves based on observable symptoms. All leaves from a single sampling event for each individual plant were pooled together, representing one sample for processing. Data from each experiment or switchgrass population was analyzed separately to investigate the relationships between virus presence and disease symptom severity. Two methods of analysis were used, the first being the calculation of the percentages of plants with no virus, PMV alone, or PMV+SPMV among plants within a DSR category (1-5). In the second method, a mean DSR was calculated from all plants within a virus category. Because of the disparity in number of measurements used in calculating mean DSR values, ProcMixed (SAS 9.3, SAS Institute, Cary, NC) was used in means comparison by generating least squares means (ls-means) and testing differences among ls-means for statistical significance.

Three sets of plants were selected for two rounds of targeted resampling in 2013 and 2014 to investigate changes in virus presence from one year to the next. In this instance, resampling refers to plants that were sampled the preceding year (2012 and/or 2013). The absence or presence of PMV and SPMV in plants resampled in 2013 and 2014 was determined previously during the 2012 and 2013 growing seasons, respectively. In 2013 a set consisted of 27 plants resampled from nurseries PV1103 and PV1104. In 2014 a set of 24 plants was re-sampled from PV1103 and PV1104. A third set, also collected in 2014, consisted of 51 plants re-sampled from Summer, and Kanlow x Summer (KxS) populations in experiment PV0910.

4.5.3 Serological Virus Detection from Switchgrass Samples

Switchgrass leaf samples collected in 2012 were analyzed using double-antibody sandwich enzyme-linked immunosorbent assay (DAS ELISA) kits (AC Diagnostics, Fayetteville, AR) specific for PMV, SCMV, *Wheat streak mosaic virus* (WSMV), CYDV-RPV, and BYDV-MAV and -PAV serotypes. In 2013 and 2014, DAS ELISA was used to assay switchgrass samples for PMV. For DAS ELISA, leaf tissue was ground in a 1:10 ratio with the manufacturer-provided sample buffer containing phosphate-buffered saline [10 mM sodium phosphate, pH 7.5, 0.15 M NaCl (PBS) with 0.05% Tween-20 (PBST)], and the extracts tested in duplicate wells following methods specified by the manufacturer. One hour after adding the substrate, optical density (OD) readings were taken at 405 nm. Negative controls included the negative control supplied in the DAS ELISA kits and tissue extracts from two switchgrass seedlings, cultivated in a growth chamber. All field and control samples were replicated at least twice for each ELISA plate. A negative-positive threshold was calculated for each plate from the average negative control OD values, plus two standard deviations from the mean. If a sample produced reactions in both of its wells that exceeded the negative-positive threshold, the sample was considered to be positive for the serological presence of the corresponding virus. Most of the samples were well above (positive reading) or well below (negative reading) the established negative-positive threshold. Samples with reactions that varied considerably between duplicate wells or which exhibited reactions close to the negative-positive threshold were retested by PMV-specific DAS ELISA or by RT-PCR.

All samples collected in 2012 that were positive for PMV in DAS ELISA were retested for PMV and SPMV by immunoblot analyses as described previously (Mandadi et al., 2014). Tissue samples previously homogenized in PBST were centrifuged at 10,000 X *g* for 5 minutes. The supernatants containing soluble proteins were mixed in a 1:1 ratio with 5X Laemmli total protein extraction buffer. The prepared samples were boiled for 5 min, separated on 12.5% polyacrylamide-sodium dodecyl sulfate gels by electrophoresis (SDS-PAGE) (BioRad, Hercules, CA), then transferred to nitrocellulose membranes. Membranes were incubated in blocking solution [5% milk in Tris-buffered saline (TBS) (10 mM Tris, pH 7.4, 0.15 M NaCl) plus 0.05% Tween-20 (TBST)] for 1 hour at 25°C on a shaker, then incubated with primary rabbit polyclonal antibody solutions for either PMV (1:5,000 dilution) or SPMV (1:2,000 dilution) in blocking solution overnight at 4°C. Following incubation with the primary antibody, the membranes were washed three times on a shaker: one quick rinse with TBST, two 5 min washes at 25°C in TBST. Next, the membranes were incubated at 25°C with the horseradish peroxidase (HRP)-conjugated goat anti-rabbit secondary antibody (Thermo Scientific) (1:10,000 dilution) in blocking solution. Membranes were then rinsed with TBST and washed for 5 minutes in TBST at 25°C, rinsed in TBS, and then developed using ECL Prime chemiluminescent reagents (Amersham) and exposed to X-ray film (Agfa).

4.5.4 RNA Extraction and RT-PCR Analysis

Total RNA was extracted from leaf samples using the Direct-zol RNA MiniPrep kit (Zymo Research, Irvine, CA) and TRI reagent (Ambion, Grand Island, NY). The homogenized PBST switchgrass leaf tissue samples prepared for DAS ELISA also was suitable for total RNA isolation. For the initial phenol extraction, 50 μL of leaf sample homogenate was combined with 400 μL of the TRI reagent. All steps following the TRI reagent extraction were conducted according to the manufacturer's protocol. RNA quality was visually assessed by electrophoresis on a 1% agarose gel and ethidium bromide staining. Total cDNA was prepared using SuperScript III Reverse Transcriptase (Life Technologies, Grand Island, NY) as described by the manufacturer. All first-strand cDNA synthesis reactions were primed with either the reverse SPMV or PMV primers. The generated cDNA samples were used as templates in PCR using Taq DNA polymerase. The primers used for RT-PCR diagnostics of PMV and SPMV were specific for the open reading frames of the PMV CP (forward primer: 5′-ATGAATCGCAATGGAGCTAC-3′; reverse primer: 5′-TTATGCGCTAACCCCACTGA-3′) and SPMV CP (forward primer: 5′-ATGGCTCCTAAGCGTTCCA-3′; reverse primer: 5′-TTATGAAGACTGAAGCTCGC-3′).

5. CONCLUSION

5.1 COMPARATIVE VIROMICS FOR THE MONOCOTS

Our comparative viromics study was prompted by the clear need for model monocot hosts that were suitable for molecular virology work in the laboratory. In particular, we were focused on establishing compatible pathosystems between host grasses and viral pathogens, in order to effectively study both the host response to infection, and molecular pathogenesis of the virus. Brachypodium and Setaria have recently emerged in the plant biology and plant pathology communities, and are currently used for functional genomics, molecular plant biology, evolutionary biology, and agricultural translation studies (Xu et al., 2013; Covshoff et al., 2014; Brutnell et al., 2015; Chochois et al., 2015; Fitzgerald et al., 2015; Van Eck and Swartwood, 2015). Our initial study (Section 2) promoted the incorporation of Brachypodium and Setaria as models for grass virus biology, and revealed new findings regarding conserved and distinct C_3 and C_4 antiviral host responses.

A major finding from the comparative viromics study was the conserved antagonistic SA-JA/ET crosstalk across Brachypodium and Setaria during diverse viral infections, similar to what has been shown for dicot hosts. Although this was not entirely unexpected, there is little evidence currently in the literature to suggest that the pathway responses to biotic pathogens are conserved among the grasses. These findings advance our understanding of the monocot innate hormone signaling responses to diverse compatible viral pathogens.

Another important finding from this study was the down-regulation of *PAD4* during multiple viral infections in both Brachypodium and Setaria. Given the known role of this signaling component in viral resistance in other systems (Chandra-Shekara et al., 2004), *PAD4* should be investigated as a critical host factor for determining the outcome of disease. Perhaps the down-regulation of *PAD4* is a general mechanism triggered by viral, or other biotic pathogens, to overcome the host defense system and initiate a successful infection.

Interestingly, this study revealed the surprising finding that structurally-related viral pathogens induce distinct differences in the expression of host signaling components. This was specifically noted for WSMV and FoMV, both of which accumulate flexuous rod virions in the cytoplasm of infected host cells, and led us to the proposal of the vMAMPs hypothesis. The existence of vMAMPs, including secondary RNA structures, virion structural properties, and viral CP symmetries, is a well-established concept in the field of mammalian virology (Parker et al., 2005; Kendall et al., 2008; Chintakuntlawar et al., 2010; Hyde et al., 2014; Chan and Gack, 2015; Sparrer and Gack, 2015). Future studies in plant should consider this concept, and investigate the host factors involved with the specific recognition of conserved viral features.

5.2 NEW FINDINGS FOR HELPER-SATELLITE INTERACTIONS

On the virus side of the story, we provide new details about the biological activity of a satRNA of PMV in multiple laboratory and field host grasses (Section 3). We provide evidence that satS interacts and interferes with its PMV helper virus in a host-dependent manner, characterized by the attenuation of host symptoms, acquisition of helper virus RNA, and differential impact on helper virus systemic accumulation. These results are strikingly similar to the previously described interaction between the genomic RNA of TCV and its satRNA, satC (Simon and Howell, 1986; Simon et al., 1988; Simon et al., 2004). However the main difference here is that the satS-PMV chimera accumulation in host plants results in an overall attenuation of the disease, which is opposite of the TCV-satC pathosystem.

These findings raise many questions about the role(s) of satS in native infections, as PMV is often found associated with both SPMV and satRNAs in turf and crop grasses. Additionally, our current findings from switchgrass, along with previous reports on the binding and encapsidation properties of the SPCP, suggest that SPMV and the satRNA species may exist as a "package deal" (pun intended) during co-infections. Given the synergistic interaction between PMV and SPMV, and the apparent antagonistic interaction PMV and satS, this would suggest that PMV might retain and utilize its satellite agents for the specific modulation of host symptoms and physiology in a host- and environment-dependent manner. We know from previous reports that the environment plays a role in both the development of host symptoms and the accumulation of viral components for the *Panicovirus* disease complex (Cabrera and Scholthof, 1999; Batten and Scholthof, 2004b; Mandadi and Scholthof, 2012; Mandadi et al., 2014). Much of the interactions between viral, subviral, and host factors, along with the influence of environmental factors, remain to be determined. Elucidating the roles of these factors in the development of disease would allow for the development of tolerant or resistant grass varieties, and enhance our overall understanding of viral and subviral pathogenesis.

5.3 POLYADENYLATION OF VIRAL RNAS: A MOLECULAR ARMS RACE

We also report the novel finding that viral and subviral RNAs that lack a known poly(A) sequence become polyadenylated *de novo* in infected host cells (Section 3). Contrary to our initial hypothesis, it appears that these polyadenylated RNAs resemble byproducts of a poly(A)-mediated RNA degradation pathway, rather than an acquired beneficial sequence for the virus (Dreyfus and Régnier, 2002; Li et al., 2014). These findings may represent the ongoing battle of viral RNAs against cytoplasmic 3′-5′ exonucleases. Alternatively, specific host factors could recognize invading viral RNAs, targeting them for polyadenylation and subsequent degradation or activating downstream defense responses, as demonstrated in mammalian systems (Chan and Gack, 2015; Sparrer and Gack, 2015). Each of these possible scenarios could also be associated with the detection of conserved vMAMPs, as discussed earlier.

Many open questions remain about the role of viral and subviral RNA polyadenylation in the infection cycle and progression of disease, including where the RNAs are polyadenylated, the host factors involved, and the biological significance to the virus (packaging, replication, cell-to-cell movement, etc.).

5.4 THE PANICOVIRUS DISEASE COMPLEX IN SWITCHGRASS

As a final component of this study, we report on the re-emergence of PMV, in association with SPMV, as the primary virus pathogen of cultivated biofuel switchgrass in Nebraska (Section 4). PMV and SPMV were the predominant viral/subviral pathogens detected in selected fields, compared with other known viruses of switchgrass. Infections by PMV and PMV+SPMV were primarily associated with the Summer and Summer-based switchgrass varieties, compared to the less susceptible Kanlow-based varieties. The infected plants in these highly susceptible Summer varieties displayed more severe disease phenotypes in the field. We also report that PMV and SPMV can spread to previously uninfected switchgrass hosts from year-to-year, likely as a result of the mechanical harvesting process.

From an economic standpoint, these field data represent the most significant portion of this study, especially if the U.S. plans to continue developing switchgrass as a primary bioenergy crop. Our findings, combined with recently available transcriptomic and metabolomic data for Kanlow and Summer varieties, suggest that the Kanlow genetic background should be incorporated in the development of future varieties with broad tolerance to viral, and possibly additional biotic pathogens (Palmer et al., 2014). The Kanlow-based plants consistently displayed low DSRs in the field, even during infection. These findings also extend the pathogenic threat of PMV and SPMV beyond the known problems of turfgrass, and suggest that future studies should be conducted to gain a better understanding of factors that affect native virus infection cycles, including plant-to-plant transmission, additional host reservoirs, and virus population dynamics.

REFERENCES

Agindotan, B.O., Domier, L.L., Gray, M.E., and Bradley, C.A. 2013a. Eight new viruses identified in bioenergy switchgrass. Phytopathology 103(Suppl. 2):S2.3.

Agindotan, B.O., Ahonsi, M.O., Domier, L.L., Gray, M.E., and Bradley, C.A. 2010. Application of sequence-independent amplification (SIA) for the identification of RNA viruses in bioenergy crops. J. Virol. Methods 169:119-128.

Agindotan, B.O., Prasifka, J.R., Gray, M.E., Dietrich, C.H., and Bradley, C.A. 2013b. Transmission of Switchgrass mosaic virus by *Graminella aureovittata*. Can. J. Plant Pathol. 35:384-389.

Agindotan, B.O., Okanu, N., Oladeinde, A., Voigt, T., Long, S., Gray, M., and Bradley, C. 2013c. Detection of Switchgrass mosaic virus in *Miscanthus* and other grasses. Can. J. Plant Pathol. 35:81-86.

Albar, L., Bangratz-Reyser, M., Hébrard, E., Ndjiondjop, M.-N., Jones, M., and Ghesquière, A. 2006. Mutations in the eIF(iso)4G translation initiation factor confer high resistance of rice to *Rice yellow mottle virus*. Plant J. 47:417-426.

Allan, A.C., Lapidot, M., Culver, J.N., and Fluhr, R. 2001. An early *Tobacco mosaic virus*-induced oxidative burst in tobacco indicates extracellular perception of the virus coat protein. Plant Physiol. 126:97-108.

Alvarado, V.Y., and Scholthof, H.B. 2009. Plant responses against invasive nucleic acids: RNA silencing and its suppression by plant viral pathogens. Sem. Cell Dev. Biol. 20:1032-1040.

An, C., and Mou, Z. 2011. Salicylic acid and its function in plant immunity. J. Integ. Plant Biol. 53:412-428.

Andino, R., and Domingo, E. 2015. Viral quasispecies. Virology 479 - 480:46-51.

Arvidsson, S., Kwasniewski, M., Riano-Pachon, D., and Mueller-Roeber, B. 2008. QuantPrime - a flexible tool for reliable high-throughput primer design for quantitative PCR. BMC Bioinformatics 9:465.

Ascencio-Ibáñez, J.T., Sozzani, R., Lee, T.-J., Chu, T.-M., Wolfinger, R.D., Cella, R., and Hanley-Bowdoin, L. 2008. Global analysis of Arabidopsis gene expression uncovers a complex array of changes impacting pathogen response and cell cycle during geminivirus infection. Plant Physiol. 148:436-454.

Barr, J.N., and Fearns, R. 2010. How RNA viruses maintain their genome integrity. J. Gen. Virol. 91:1373-1387.

Batten, J., and Scholthof, K.-B.G. 2004a. St. Augustine decline. Pages 800-802 in: Viruses and virus diseases of *Poaceae* (*Gramineae*), H. Lapierre and P. Signoret, eds. INRA, Paris.

Batten, J., Turina, M., and Scholthof, K.-B. 2006a. *Panicovirus* accumulation is governed by two membrane-associated proteins with a newly identified conserved motif that contributes to pathogenicity. Virol. J. 3:12.

Batten, J.S., and Scholthof, K.-B.G. 2004b. Panicum mosaic-St. Augustine decline. Pages 796-802 in: Viruses and virus diseases of *Poaceae* (*Gramineae*), H. Lapierre and P.-A. Signoret, eds. INRA, Paris.

Batten, J.S., Desvoyes, B., Yamamura, Y., and Scholthof, K.-B.G. 2006b. A translational enhancer element on the 3′-proximal end of the *Panicum mosaic virus* genome. FEBS Lett. 580:2591-2597.

Bennetzen, J.L., Schmutz, J., Wang, H., Percifield, R., Hawkins, J., Pontaroli, A.C., Estep, M., Feng, L., Vaughn, J.N., Grimwood, J., Jenkins, J., Barry, K., Lindquist, E., Hellsten, U., Deshpande, S., Wang, X., Wu, X., Mitros, T., Triplett, J., Yang, X., Ye, C.-Y., Mauro-Herrera, M., Wang, L., Li, P., Sharma, M., Sharma, R., Ronald, P.C., Panaud, O., Kellogg, E.A., Brutnell, T.P., Doust, A.N., Tuskan, G.A., Rokhsar, D., and Devos, K.M. 2012. Reference genome sequence of the model plant Setaria. Nat. Biotech. 30:555-561.

Bouton, J.H. 2007. Molecular breeding of switchgrass for use as a biofuel crop. Curr. Opin. Genet. Dev. 17:553-558.

Bragg, J.N., and Jackson, A.O. 2004. Barley stripe mosaic. Pages 456-457 in: Viruses and Virus Diseases of *Poaceae* (*Gramineae*), H. Lapierre and P. Signoret, eds. INRA, France.

Bragg, J.N., Jiajie, W., Gordon, S.P., Guttman, M.E., Thilmony, R., Lazo, G.R., Gu, Y.Q., Vogel, J.P., and Hazen, S.P. 2012. Generation and characterization of the Western Regional Research Center Brachypodium T-DNA insertional mutant collection. PLOS ONE 7:1-14.

Brenchley, R., Spannagl, M., Pfeifer, M., Barker, G.L.A., D'Amore, R., Allen, A.M., McKenzie, N., Kramer, M., Kerhornou, A., Bolser, D., Kay, S., Waite, D., Trick, M., Bancroft, I., Gu, Y., Huo, N., Luo, M.-C., Sehgal, S., Gill, B., Kianian, S., Anderson, O., Kersey, P., Dvorak, J., McCombie, W.R., Hall, A., Mayer, K.F.X., Edwards, K.J., Bevan, M.W., and Hall, N. 2012. Analysis of the bread wheat genome using whole-genome shotgun sequencing. Nature 491:705-710.

Brkljacic, J., Grotewold, E., Scholl, R., Mockler, T., Garvin, D.F., Vain, P., Brutnell, T., Sibout, R., Bevan, M., Budak, H., Caicedo, A.L., Gao, C., Gu, y., Hazen, S.P., Holt, B.F., Hong, S.-Y., Jordan, M., Manzaneda, A.J., Mitchell-Olds, T., Mochida, K., Mur, L.A.J., Park, C.-M., Sedbrook, J., Watt, M., Zheng, S.J., and Vogel, J. 2011. Brachypodium as a model for the grasses: Today and the future. Plant Physiol. 157:3-13.

Brodhun, F., and Feussner, I. 2011. Oxylipins in fungi. FEBS J. 278:1047-1063.

Brutnell, T.P., Bennetzen, J.L., and Vogel, J.P. 2015. *Brachypodium distachyon* and *Setaria viridis*: Model genetic systems for the grasses. Annu. Rev. Plant Biol. 66:465-485.

Brutnell, T.P., Wang, L., Swartwood, K., Goldschmidt, A., Jackson, D., Zhu, X.-G., Kellogg, E., and Van Eck, J. 2010. *Setaria viridis*: A model for C4 photosynthesis. Plant Cell 22:2537-2544.

Buzen, F.G., Niblett, C.L., Hooper, G.R., Hubbard, J., and Newman, M.A. 1984. Further characterization of *Panicum mosaic virus* and its associated satellite virus. Phytopathology 74:313-318.

Cabrera, O., and Scholthof, K.-B.G. 1999. The complex viral etiology of St. Augustine Decline. Plant Dis. 83:902-904.

Cabrera, O., Roossinck, M.J., and Scholthof, K.-B.G. 2000. Genetic diversity of panicum mosaic virus satellite RNAs in St. Augustinegrass. Phytopathology 90:977-980.

Cao, S., Siriwardana, C., Kumimoto, R., and Holt, B. 2011. Construction of high quality Gateway entry libraries and their application to yeast two-hybrid for the monocot model plant *Brachypodium distachyon*. BMC Biotechnol. 11:53.

Carris, L.M., Castlebury, L.A., and Zale, J. 2008. First report of *Tilletia pulcherrima* bunt on switchgrass (*Panicum virgatum*) in Texas. Plant Dis. 92:1707-1707.

Cascone, P.J., Carpenter, C.D., Li, X.H., and Simon, A.E. 1990. Recombination between satellite RNAs of *Turnip crinkle virus*. EMBO J. 9:1709-1715.

Cassida, K.A., Kirkpatrick, T.L., Robbins, R.T., Muir, J.P., Venuto, B.C., and Hussey, M.A. 2005. Plant-parasitic nematodes associated with switchgrass (*Panicum* *virgatum* L.) grown for biofuel in the south central United States. Nematropica 35:1-10.

Chan, Y.K., and Gack, M.U. 2015. RIG-I-like receptor regulation in virus infection and immunity. Curr. Opin. Virol. 12:7-14.

Chandra-Shekara, A.C., Navarre, D., Kachroo, A., Kang, H.-G., Klessig, D., and Kachroo, P. 2004. Signaling requirements and role of salicylic acid in HRT- and rrt-mediated resistance to *Turnip crinkle virus* in Arabidopsis. Plant J. 40:647-659.

Chern, M., Fitzgerald, H.A., Canlas, P.E., Navarre, D.A., and Ronald, P.C. 2005. Overexpression of a rice NPR1 homolog leads to constitutive activation of defense response and hypersensitivity to light. Mol. Plant Microbe Interact. 18:511-520.

Chintakuntlawar, A.V., Zhou, X., Rajaiya, J., and Chodosh, J. 2010. Viral capsid Is a pathogen-associated molecular pattern in adenovirus keratitis. PLOS Pathog. 6:e1000841.

Chochois, V., Vogel, J., P., Rebetzke, G., J, and Watt, M. 2015. Variation in adult plant phenotypes and partitioning among seed and stem-borne roots across *Brachypodium distachyon* accessions to exploit in breeding cereals for well-watered and drought environments. Plant Physiol.

Covshoff, S., Burgess, S., Kneřová, J., and Kümpers, B.C. 2014. Getting the most out of natural variation in C4 photosynthesis. Photosynth. Res. 119:157-167.

Crouch, J.A., Beirn, L.A., Cortese, L.M., Bonos, S.A., and Clarke, B.B. 2009. Anthracnose disease of switchgrass caused by the novel fungal species *Colletotrichum navitas*. Mycol. Res. 113:1411-1421.

Cui, Y., Lee, M.Y., Huo, N., Bragg, J., Yan, L., Yuan, C., Li, C., Holditch, S.J., Xie, J., Luo, M.-C., Li, D., Yu, J., Martin, J., Schackwitz, W., Gu, Y.Q., Vogel, J.P., Jackson, A.O., Liu, Z., and Garvin, D.F. 2012. Fine mapping of the *Bsr1 Barley stripe mosaic virus* resistance gene in the model grass *Brachypodium distachyon*. PLOS ONE 7:e38333.

Desnues, C., and Raoult, D. 2012. Virophages question the existence of satellites. Nat. Rev. Micro. 10:234-234.

Desvoyes, B., and Scholthof, K.-B.G. 2000. RNA: protein interactions associated with satellites of panicum mosaic virus. FEBS Lett. 485:25-28.

Dodds, J.A. 1998. Satellite tobacco mosaic virus. Annu. Rev. Phytopathol. 36:295-310.

Dodds, P.N., and Rathjen, J.P. 2010. Plant immunity: towards an integrated view of plant–pathogen interactions. Nat. Rev. Genet. 11:539-548.

Domingo, E., Sheldon, J., and Perales, C. 2012. Viral quasispecies evolution. Microbiol. Mol. Biol. R. 76:159-216.

Donald, R.G.K., and Jackson, A.O. 1994. Hordeiviruses. Pages 661-664 in: Encyclopedia of Virology, R.G. Webster and A. Granoff, eds. Academic Press Inc., San Diego.

Dong, X. 2004. NPR1, all things considered. Curr. Opin. Plant Biol. 7:547-552.

Draper, J., Mur, L.A.J., Jenkins, G., Ghosh-Biswas, G.C., Bablak, P., Hasterok, R., and Routledge, A.P.M. 2001. *Brachypodium distachyon*. A new model system for functional genomics in grasses. Plant Physiol. 127:1539-1555.

Dreher, T.W. 1999. Functions of the 3′-untranslated regions of positive strand RNA viral genomes. Annu. Rev. Phytopathol. 37:151-174.

Dreyfus, M., and Régnier, P. 2002. The poly(A) tail of mRNAs: Bodyguard in eukaryotes, scavenger in bacteria. Cell 111:611-613.

Eckardt, N.A. 2008. Grass genome evolution. Plant Cell 20:3-4.

Engelberth, J., Viswanathan, S., and Engelberth, M. 2011. Low concentrations of salicylic acid stimulate insect elicitor responses in *Zea mays* seedlings. J. Chem. Ecol. 37:263-266.

Etheridge, J.V., Davey, L., and Christian, D.G. 2001. First report of *Rhizoctonia cerealis* causing sharp eyespot in *Panicum virgatum* in the UK. Plant Pathol. 50:807.

FAO. (2009). Global agriculture towards 2050. In High-Level Expert Forum (Rome).

Feys, B.J., Moisan, L.J., Newman, M.-A., and Parker, J.E. 2001. Direct interaction between the Arabidopsis disease resistance signaling proteins, EDS1 and PAD4. EMBO J. 20:5400-5411.

Fitzgerald, T.L., Powell, J.J., Schneebeli, K., Hsia, M.M., Gardiner, D.M., Bragg, J.N., McIntyre, C.L., Manners, J.M., Ayliffe, M., Watt, M., Vogel, J.P., Henry, R.J., and Kazan, K. 2015. Brachypodium as an emerging model for cereal–pathogen interactions. Ann. Bot. 115:717-731.

French, R., and Stenger, D.C. 2003. Evolution of *Wheat streak mosaic virus*: Dynamics of population growth within plants may explain limited variation. Annu. Rev. Phytopathol. 41:199-214.

French, R., and Stenger, D.C. 2004. Wheat streak mosaic. Pages 602-604 in: Viruses and Virus Diseases of *Poaceae* (*Gramineae*), H. Lapierre and P. Signoret, eds. INRA, France.

Gadagkar, S.R., Rosenberg, M.S., and Kumar, S. 2005. Inferring species phylogenies from multiple genes: Concatenated sequence tree versus consensus gene tree. J. Exp. Zool. 304B:64-74.

Gallie, D. 1996. Translational control of cellular and viral mRNAs. Pages 145-158 in: Post-Transcriptional Control of Gene Expression in Plants, W. Filipowicz and T. Hohn, eds. Springer Netherlands.

Garrett, K.A., Dendy, S.P., Power, A.G., Blaisdell, G.K., Alexander, H.M., and McCarron, J.K. 2004. Barley yellow dwarf disease in natural populations of dominant tallgrass prairie species in Kansas. Plant Dis. 88:574-574.

Gerwick, W.H. 1994. Structure and biosynthesis of marine algal oxylipins. BBA-Lipid Lipid Met. 1211:243-255.

Goodstein, D.M., Shu, S., Howson, R., Neupane, R., Hayes, R.D., Fazo, J., Mitros, T., Dirks, W., Hellsten, U., Putnam, N., and Rokhsar, D.S. 2012. Phytozome: a comparative platform for green plant genomics. Nucleic Acids Res. 40:D1178-D1186.

Graham-Rowe, D. 2011. Agriculture: Beyond food versus fuel. Nature 474:S6-S8.

Grass Phylogeny Working Group II. 2012. New grass phylogeny resolves deep evolutionary relationships and discovers C4 origins. New Phytol. 193:304-312.

Gray, S., and Gildow, F.E. 2003. *Luteovirus*-aphid interactions. Annu. Rev. Phytopathol. 41:539-566.

Guilford, P.J., Beck, D.L., and Forster, R.L.S. 1991. Influence of the poly(A) tail and putative polyadenylation signal on the infectivity of *White clover mosaic potexvirus*. Virology 182:61-67.

Hagborg, W.A.F. 1954. Dwarfing of wheat and barley by the barley stripe-mosaic (false stripe) virus. Can. J. Bot. 32:24-37.

Hanssen, I.M., Peter van Esse, H., Ballester, A.-R., Hogewoning, S.W., Parra, N.O., Paeleman, A., Lievens, B., Bovy, A.G., and Thomma, B.P.H.J. 2011. Differential tomato transcriptomic responses induced by *Pepino mosaic virus* isolates with differential aggressiveness. Plant Physiol. 156:301-318.

Hill, J., Nelson, E., Tilman, D., Polasky, S., and Tiffany, D. 2006. Environmental, economic, and energetic costs and benefits of biodiesel and ethanol biofuels. Proc. Natl. Acad. Sci. USA 103:11206-11210.

Hill, K.R., Hajjou, M., Hu, J.Y., and Raju, R. 1997. RNA-RNA recombination in Sindbis virus: roles of the 3' conserved motif, poly(A) tail, and nonviral sequences of template RNAs in polymerase recognition and template switching. J. Virol. 71:2693-2704.

Hillman, B.I., Carrington, J.C., and Morris, T.J. 1987. A defective interfering RNA that contains a mosaic of a plant virus genome. Cell 51:427-433.

Hong, S.-Y., Seo, P.J., Yang, M.-S., Xiang, F., and Park, C.-M. 2008. Exploring valid reference genes for gene expression studies in *Brachypodium distachyon* by real-time PCR. BMC Plant Biol. 8:112-112.

Hu, C.-C., Hsu, Y.-H., and Lin, N.-S. 2009. Satellite RNAs and satellite viruses of plants. Viruses 1:1325-1350.

Huang, Z., Yeakley, J.M., Garcia, E.W., Holdridge, J.D., Fan, J.-B., and Whitham, S.A. 2005. Salicylic acid-dependent expression of host genes in compatible Arabidopsis-virus interactions. Plant Physiol. 137:1147-1159.

Hull, R. 2002. Chapter 14 - Viroids, Satellite Viruses and Satellite RNAs. Pages 593-626 in: Matthews' Plant Virology (Fourth Edition), R. Hull, ed. Academic Press, London.

Hunt, A., Xing, D., and Li, Q. 2012. Plant polyadenylation factors: Conservation and variety in the polyadenylation complex in plants. BMC Genomics 13:641.

Hyde, J.L., Gardner, C.L., Kimura, T., White, J.P., Liu, G., Trobaugh, D.W., Huang, C., Tonelli, M., Paessler, S., Takeda, K., Klimstra, W.B., Amarasinghe, G.K., and Diamond, M.S. 2014. A viral RNA structural element alters host recognition of nonself RNA. Science 343:783-787.

International Brachypodium Initiative. 2010. Genome sequencing and analysis of the model grass *Brachypodium distachyon*. Nature 463:763-768.

International Committee on Taxonomy of Viruses. (2012). Ninth Report of the International Committee on Taxonomy of Viruses, A.M.Q. King, M.J. Adams, E.B. Carstens, and E.J. Lefkowitz, eds (London).

Jackson, A.O., Lim, H.-S., Bragg, J., Ganesan, U., and Lee, M.Y. 2009. Hordeivirus replication, movement, and pathogenesis. Annu. Rev. Phytopathol. 47:385-422.

Jakubiec, A., Yang, S.W., and Chua, N.-H. 2012. Arabidopsis DRB4 protein in antiviral defense against *Turnip yellow mosaic virus* infection. Plant J. 69:14-25.

Jia, M.-A., Li, Y., Lei, L., Di, D., Miao, H., and Fan, Z. 2012. Alteration of gene expression profile in maize infected with a double-stranded RNA fijivirus associated with symptom development. Mol. Plant Pathol. 13:251-262.

Jones, R.A.C. 2006. Control of plant virus diseases. Adv. Virus Res. 67:205-244.

Jupin, I., Bouzoubaa, S., Richards, K., Jonard, G., and Guilley, H. 1990. Multiplication of *Beet necrotic yellow vein virus* RNA 3 lacking a 3′ poly(A) tail is accompanied by reappearance of the poly(A) tail and a novel short U-rich tract preceding it. Virology 178:281-284.

Kachroo, P., Yoshioka, K., Shah, J., Dooner, H.K., and Klessig, D.F. 2000. Resistance to *Turnip crinkle virus* in Arabidopsis is regulated by two host genes and is salicylic acid dependent but NPR1, ethylene, and jasmonate independent. Plant Cell 12:677-690.

Kendall, A., McDonald, M., Bian, W., Bowles, T., Baumgarten, S.C., Shi, J., Stewart, P.L., Bullitt, E., Gore, D., Irving, T.C., Havens, W.M., Ghabrial, S.A., Wall, J.S., and Stubbs, G. 2008. Structure of flexible filamentous plant viruses. J. Virol. 82:9546-9554.

Krupinsky, J.M., Berdahl, J.D., Schoch, C.L., and Rossman, A.Y. 2004. Leaf spot on switchgrass (*Panicum virgatum*), symptoms of a new disease caused by *Bipolaris oryzae*. Can. J. Plant Pathol. 26:371-378.

Krupovic, M., and Cvirkaite-Krupovic, V. 2011. Virophages or satellite viruses? Nat. Rev. Micro. 9:762-763.

Larkin, M.A., Blackshields, G., Brown, N.P., Chenna, R., McGettigan, P.A., McWilliam, H., Valentin, F., Wallace, I.M., Wilm, A., Lopez, R., Thompson, J.D., Gibson, T.J., and Higgins, D.G. 2007. Clustal W and Clustal X version 2.0. Bioinformatics 23:2947-2948.

Lee, A., Cho, K., Jang, S., Rakwal, R., Iwahashi, H., Agrawal, G.K., Shim, J., and Han, O. 2004. Inverse correlation between jasmonic acid and salicylic acid during early wound response in rice. Biochem. Biophys. Res. Commun. 318:734-738.

Lee, D.-S., Nioche, P., Hamberg, M., and Raman, C.S. 2008. Structural insights into the evolutionary paths of oxylipin biosynthetic enzymes. Nature 455:363-368.

Lee, M.Y., Yan, L., Gorter, F.A., Kim, B.Y.T., Cui, Y., Hu, Y., Yuan, C., Grindheim, J., Ganesan, U., Liu, Z., Han, C., Yu, J., Li, D., and Jackson, A.O. 2012. *Brachypodium distachyon* line Bd3-1 resistance is elicited by the *Barley stripe mosaic virus* triple gene block 1 movement protein. J. Gen. Virol. 93:2729-2739.

Lee, T.A., JR., and Toler, R.W. 1973. Purification and characterization of the virus causing St. Augustine Decline (SAD). Phytopathology 63:444.

Letunic, I., and Bork, P. 2007. Interactive Tree Of Life (iTOL): an online tool for phylogenetic tree display and annotation. Bioinformatics 23:127-128.

Li, P., and Brutnell, T.P. 2011. *Setaria viridis* and *Setaria italica*, model genetic systems for the Panicoid grasses. J. Exp. Bot. 62:3031-3037.

Li, W., Zhang, Y., Zhang, C., Pei, X., Wang, Z., and Jia, S. 2014. Presence of poly(A) and poly(A)-rich tails in a positive-strand RNA virus known to lack 3′ poly(A) tails. Virology 454–455:1-10.

Li, X.H., Heaton, L.A., Morris, T.J., and Simon, A.E. 1989. *Turnip crinkle virus* defective interfering RNAs intensify viral symptoms and are generated *de novo*. Proc. Natl. Acad. Sci. USA 86:9173-9177.

Livak, K.J., and Schmittgen, T.D. 2001. Analysis of relative gene expression data using real-time quantitative PCR and the $2^{-\Delta\Delta CT}$ method. Methods 25:402-408.

Love, A.J., Geri, C., Laird, J., Carr, C., Yun, B.-W., Loake, G.J., Tada, Y., Sadanandom, A., and Milner, J.J. 2012. *Cauliflower mosaic virus* protein P6 inhibits signaling responses to salicylic acid and regulates innate immunity. PLOS ONE 7:e47535.

Mandadi, K.K., and Scholthof, K.-B.G. 2012. Characterization of a viral synergism in the monocot *Brachypodium distachyon* reveals distinctly altered host molecular processes associated with disease. Plant Physiol. 160:1432-1452.

Mandadi, K.K., and Scholthof, K.-B.G. 2013. Plant immune responses against viruses: How does a virus cause disease? Plant Cell 25:1489-1505.

Mandadi, K.K., Pyle, J.D., and Scholthof, K.-B.G. 2014. Comparative analysis of antiviral responses in *Brachypodium distachyon* and *Setaria viridis* reveals conserved and unique outcomes among C3 and C4 plant defenses. Mol. Plant Microbe Interact. 27:1277-1290.

Martín-Benito, J., and Ortín, J. 2013. Influenza virus transcription and replication. Adv. Virus Res. 87:113-137.

Masuta, C., Zuidema, D., Hunter, B.G., Heaton, L.A., Sopher, D.S., and Jackson, A.O. 1987. Analysis of the genome of satellite panicum mosaic virus. Virology 159:329-338.

McLaughlin, S.B., and Kszos, L.A. 2005. Development of switchgrass (*Panicum virgatum*) as a bioenergy feedstock in the United States. Biomass Bioenerg. 28:515-535.

Mekete, T., Reynolds, K., Lopez-Nicora, H.D., Gray, M.E., and Niblack, T.L. 2010. Plant-parasitic nematodes are potential pathogens of *Miscanthus* × *giganteus* and *Panicum virgatum* used for biofuels. Plant Dis. 95:413-418.

Miller, W.A., Wang, Z., and Treder, K. 2007. The amazing diversity of cap-independent translation elements in the 3′-untranslated regions of plant viral RNAs. Biochem. Soc. Trans. 35:1629-1633.

Monis, J., Sopher, D.S., and Jackson, A.O. 1992. Biologically active cDNA clones of panicum mosaic virus satellites. Phytopathology 82:1175.

Moon, S.L., Barnhart, M.D., and Wilusz, J. 2012. Inhibition and avoidance of mRNA degradation by RNA viruses. Curr. Opin. Microbiol. 15:500-505.

Mur, L.A.J., Kenton, P., Atzorn, R., Miersch, O., and Wasternack, C. 2006. The outcomes of concentration-specific interactions between salicylate and jasmonate signaling include synergy, antagonism, and oxidative stress leading to cell death. Plant Physiol. 140:249-262.

Mur, L.A.J., Allainguillaume, J., Catalán, P., Hasterok, R., Jenkins, G., Lesniewska, K., Thomas, I., and Vogel, J. 2011. Exploiting the Brachypodium Tool Box in cereal and grass research. New Phytol. 191:334-347.

Murant, A.F., and Mayo, M.A. 1982. Satellites of plant viruses. Annu. Rev. Phytopathol. 20:49-68.

Navia, D., Mendonça, R., Skoracka, A., Szydło, W., Knihinicki, D., Hein, G., da Silva Pereira, P., Truol, G., and Lau, D. 2013. Wheat curl mite, *Aceria tosichella*, and transmitted viruses: an expanding pest complex affecting cereal crops. Exp. Appl. Acarol. 59:95-143.

Niblett, C.L., and Paulsen, A.Q. 1975. Purification and further characterization of *Panicum mosaic virus*. Phytopathology 65:1157-1160.

Ouyang, S., Zhu, W., Hamilton, J., Lin, H., Campbell, M., Childs, K., Thibaud-Nissen, F., Malek, R.L., Lee, Y., Zheng, L., Orvis, J., Haas, B., Wortman, J., and Buell, C.R. 2007. The TIGR rice genome annotation resource: improvements and new features. Nucleic Acids Res. 35:D883-D887.

Pacheco, R., García-Marcos, A., Manzano, A., de Lacoba, M.G., Camañes, G., García-Agustín, P., Díaz-Ruíz, J.R., and Tenllado, F. 2012. Comparative analysis of transcriptomic and hormonal responses to compatible and incompatible plant-virus interactions that lead to cell death. Mol. Plant Microbe Interact. 25:709-723.

Palmer, N.A., Saathoff, A.J., Tobias, C.M., Twigg, P., Xia, Y., Vogel, K.P., Madhavan, S., Sattler, S.E., and Sarath, G. 2014. Contrasting metabolism in perenniating structures of upland and lowland switchgrass plants late in the growing season. PLOS ONE 9:e105138.

Parker, L., Kendall, A., Berger, P.H., Shiel, P.J., and Stubbs, G. 2005. *Wheat streak mosaic virus* - Structural parameters for a Potyvirus. Virology 340:64-69.

Pathak, K.B., and Nagy, P.D. 2009. Defective interfering RNAs: Foes of viruses and friends of virologists. Viruses 1:895-919.

Pearson, W.R. 1991. Searching protein sequence libraries: Comparison of the sensitivity and selectivity of the Smith-Waterman and FASTA algorithms. Genomics 11:635-650.

Perry, A. 2012. Biofuel prospects with prairie perennials. Agr. Res. 60:7-9.

Petty, I.T.D., Hunter, B.G., Wei, N., and Jackson, A.O. 1989. Infectious *Barley stripe mosaic virus* RNA transcribed *in vitro* from full-length genomic cDNA clones. Virology 171:342-349.

Pieterse, C.M.J., Van der Does, D., Zamioudis, C., Leon-Reyes, A., and Van Wees, S.C.M. 2012. Hormonal modulation of plant immunity. Annu. Rev. Cell Dev. Biol. 28:489-521.

Postnikova, O., and Nemchinov, L. 2012. Comparative analysis of microarray data in Arabidopsis transcriptome during compatible interactions with plant viruses. Virology J. 9:101.

Qi, D., Omarov, R.T., and Scholthof, K.-B.G. 2008. The complex subcellular distribution of satellite panicum mosaic virus capsid protein reflects its multifunctional role during infection. Virology 376:154-164.

Qiu, W., and Scholthof, K.-B.G. 2000. In vitro- and in vivo-generated defective RNAs of satellite panicum mosaic virus define cis-acting RNA elements required for replication and movement. J. Virol. 74:2247-2254.

Qiu, W., and Scholthof, K.-B.G. 2001. Defective interfering RNAs of a satellite virus. J. Virol. 75:5429-5432.

Raju, R., Hajjou, M., Hill, K.R., Botta, V., and Botta, S. 1999. *In vivo* addition of poly(A) tail and AU-rich sequences to the 3′ terminus of the Sindbis virus RNA genome: a novel 3′-end repair pathway. J. Virol. 73:2410-2419.

Redinbaugh, M., and Pratt, R. 2009. Virus resistance. Pages 251-270 in: Handbook of Maize: Its Biology, J.L. Bennetzen and S.C. Hake, eds. Springer, New York, U.S.A.

Reinisch, K.M., and Wolin, S.L. 2007. Emerging themes in non-coding RNA quality control. Curr. Opin. Struct. Biol. 17:209-214.

Robertson, N.L., and French, R. 2004. Foxtail mosaic. Pages 765-766 in: Viruses and virus diseases of *Poaceae* (*Gramineae*), H. Lapierre and P.-A. Signoret, eds. INRA, Paris.

Rubino, L., Burgyan, J., Grieco, F., and Russo, M. 1990. Sequence analysis of *Cymbidium ringspot virus* satellite and defective interfering RNAs. J. Gen. Virol. 71:1655-1660.

Saeed, A.I., Sharov, V., White, J., Li, J., Liang, W., Bhagabati, N., Braisted, J., Klapa, M., Currier, T., Thiagarajan, M., Sturn, A., Snuffin, M., Rezantsev, A., Popov, D., Ryltsov, A., Kostukovich, E., Borisovsky, I., Liu, Z., Vinsavich, A., Trush, V., and Quackenbush, J. 2003. TM4: A free, open-source system for microarray data management and analysis. Biotechniques 34:374-378.

Salzman, R.A., Brady, J.A., Finlayson, S.A., Buchanan, C.D., Summer, E.J., Sun, F., Klein, P.E., Klein, R.R., Pratt, L.H., Cordonnier-Pratt, M.-M., and Mullet, J.E. 2005. Transcriptional profiling of sorghum induced by methyl jasmonate, salicylic acid, and aminocyclopropane carboxylic acid reveals cooperative regulation and novel gene responses. Plant Physiol. 138:352-368.

Sanderson, M.A., Reed, R.L., McLaughlin, S.B., Wullschleger, S.D., Conger, B.V., Parrish, D.J., Wolf, D.D., Taliaferro, C., Hopkins, A.A., Ocumpaugh, W.R., Hussey, M.A., Read, J.C., and Tischler, C.R. 1996. Switchgrass as a sustainable bioenergy crop. Bioresource Technol. 56:83-93.

Satoh, K., Kondoh, H., Sasaya, T., Shimizu, T., Choi, I.-R., Omura, T., and Kikuchi, S. 2010. Selective modification of rice (*Oryza sativa*) gene expression by *Rice stripe virus* infection. J. Gen. Virol. 91:294-305.

Schmer, M.R., Vogel, K.P., Mitchell, R.B., and Perrin, R.K. 2008. Net energy of cellulosic ethanol from switchgrass. Proc. Natl. Acad. Sci. USA 105:464-469.

Schmid, M., Speiseder, T., Dobner, T., and Gonzalez, R.A. 2014. DNA virus replication compartments. J. Virol. 88:1404-1420.

Scholthof, K.-B.G. 1999. A synergism induced by satellite panicum mosaic virus. Mol. Plant Microbe Interact. 12:163-166.

Scholthof, K.-B.G., Jones, R.W., and Jackson, A.O. 1999. Biology and Structure of Plant Satellite Viruses Activated by Icosahedral Helper Viruses. Pages 123-143 in: Satellites and Defective Viral RNAs, P.K. Vogt and A.O. Jackson, eds. Springer Berlin Heidelberg.

Schwessinger, B., and Ronald, P.C. 2012. Plant innate immunity: Perception of conserved microbial signatures. Annu. Rev. Plant Biol. 63:451-482.

Shimizu, T., Satoh, K., Kikuchi, S., and Omura, T. 2007. The repression of cell wall- and plastid-related genes and the induction of defense-related genes in rice plants infected with *Rice dwarf virus*. Mol. Plant Microbe Interact. 20:247-254.

Shpaer, E.G., Robinson, M., Yee, D., Candlin, J.D., Mines, R., and Hunkapiller, T. 1996. Sensitivity and selectivity in protein similarity searches: A comparison of Smith–Waterman in hardware to BLAST and FASTA. Genomics 38:179-191.

Sill, W.H., and Pickett, R.C. 1957. A new disease of switchgrass, *Panicum virgatum*. Plant Dis. Reptr. 41:241-249.

Simon, A.E., and Howell, S.H. 1986. The virulent satellite RNA of *Turnip crinkle virus* has a major domain homologous to the 3' end of the helper virus genome. EMBO J. 5:3423-3428.

Simon, A.E., Roossinck, M.J., and Havelda, Z. 2004. Plant virus satellite and defective interfering RNAs: New paradigms for a new century. Annu. Rev. Phytopathol. 42:415-437.

Simon, A.E., Engel, H., Johnson, R.P., and Howell, S.H. 1988. Identification of regions affecting virulence, RNA processing and infectivity in the virulent satellite of *Turnip crinkle virus*. EMBO J. 7:2645-2651.

Slomovic, S., Fremder, E., Staals, R.H.G., Pruijn, G.J.M., and Schuster, G. 2010. Addition of poly(A) and poly(A)-rich tails during RNA degradation in the cytoplasm of human cells. Proc. Natl. Acad. Sci. U.S.A. 107:7407-7412.

Smith, T.F., and Waterman, M.S. 1981. Identification of common molecular subsequences. J. Mol. Biol. 147:195-197.

Somma, D., Lobkowicz, H., and Deason, J. 2010. Growing America's fuel: an analysis of corn and cellulosic ethanol feasibility in the United States. Clean Techn Environ Policy 12:373-380.

Sparrer, K.M.J., and Gack, M.U. 2015. Intracellular detection of viral nucleic acids. Curr. Opin. Microbiol. 26:1-9.

Spoel, S.H., Koornneef, A., Claessens, S.M.C., Korzelius, J.P., Van Pelt, J.A., Mueller, M.J., Buchala, A.J., Métraux, J.-P., Brown, R., Kazan, K., Van Loon, L.C., Dong, X., and Pieterse, C.M.J. 2003. NPR1 modulates cross-talk between salicylate- and jasmonate-dependent defense pathways through a novel function in the cytosol. Plant Cell 15:760-770.

Stewart, C.L., Yuen, G.Y., Vogel, K., Pyle, J.D., and Scholthof, K.-B.G. 2013. *Panicum mosaic virus*-A potential threat to biofuel switchgrass production. Phytopathology 103:138-138.

Stewart, C.L., Pyle, J.D., Jochum, C.C., Vogel, K.P., Yuen, G., and Scholthof, K.-B.G. 2015. Multi-year pathogen survey of biofuel switchgrass breeding plots reveals high prevalence of infections by *Panicum mosaic virus* and its satellite virus. Phytopathology In press.

Sun, X., and Simon, A.E. 2003. Fitness of a *Turnip crinkle virus* satellite RNA correlates with a sequence-nonspecific hairpin and flanking sequences that enhance replication and repress the accumulation of virions. J. Virol. 77:7880-7889.

Thaler, J.S., Humphrey, P.T., and Whiteman, N.K. 2012. Evolution of jasmonate and salicylate signal crosstalk. Trends Plant Sci. 17:260-270.

Thomas, J.E., and Steele, V. 2011. First report of *Panicum mosaic virus* in buffalo grass (*Stenotaphrum secundatum*) from Australia. Australasian Plant Dis. Notes 6:16-17.

Tiffany, L.H., and Knaphus, G. (1995). Fungus pathogens of prairie plants in Iowa. In 14th Annual North American Prairie Conference, pp. 49-54.

Trottet, M., and Gouis, J.L. 2004. Manipulation of resistance genes. Pages 180-186 in: Viruses and Virus Diseases of Poaceae (Gramineae), H. Lapierre and P. Signoret, eds. INRA, France.

Turina, M., Desvoyes, B., and Scholthof, K.-B.G. 2000. A gene cluster encoded by *Panicum mosaic virus* is associated with virus movement. Virology 266:120-128.

Turina, M., Maruoka, M., Monis, J., Jackson, A.O., and Scholthof, K.-B.G. 1998. Nucleotide sequence and infectivity of a full-length cDNA clone of *Panicum mosaic virus*. Virology 241:141-155.

Uppalapati, S.R., Serba, D.D., Ishiga, Y., Szabo, L.J., Mittal, S., Bhandari, H.S., Bouton, J.H., Mysore, K.S., and Saha, M.C. 2013. Characterization of the rust fungus, *Puccinia emaculata*, and evaluation of genetic variability for rust resistance in switchgrass populations. Bioenerg. Res. 6:458-468.

Van Eck, J., and Swartwood, K. 2015. *Setaria viridis*. Pages 57-67 in: Agrobacterium Protocols, K. Wang, ed. Springer New York.

van Leeuwen, H.C., Liefhebber, J.M.P., and Spaan, W.J.M. 2006. Repair and polyadenylation of a naturally occurring Hepatitis C virus 3′ nontranslated region-shorter variant in selectable replicon cell lines. J. Virol. 80:4336-4343.

Ventelon-Debout, M., Nguyen, T.T.H., Wissocq, A., Berger, C., Laudie, M., Piégu, B., Cooke, R., Ghesquière, A., Delseny, M., and Brugidou, C. 2003. Analysis of the transcriptional response to *Rice yellow mottle virus* infection in *Oryza sativa* indica and japonica cultivars. Mol. Genet. Genom. 270:253-262.

Verhage, A., van Wees, S.C.M., and Pieterse, C.M.J. 2010. Plant immunity: It's the hormones talking, but what do they say? Plant Physiol. 154:536-540.

Vogel, J., and Hill, T. 2008. High-efficiency *Agrobacterium*-mediated transformation of *Brachypodium distachyon* inbred line Bd21-3. Plant Cell Rep. 27:471-478.

Vogel, J.P., Gu, Y.Q., Twigg, P., Lazo, G.R., Laudencia-Chingcuanco, D., Hayden, D.M., Donze, T.J., Vivian, L.A., Stamova, B., and Coleman-Derr, D. 2006. EST sequencing and phylogenetic analysis of the model grass *Brachypodium distachyon*. Theor. Appl. Genet. 113:186-195.

Vogel, K.P. 2004. Switchgrass. Pages 561-588 in: Warm-Season (C4) Grasses, L.E. Moser, B.L. Burson, and L.E. Sollenberger, eds. American Society of Agronomy-Crop Science Society of America-Soil Science Society of America.

Vu, A.L., Dee, M.M., Gualandi, R.J., Huff, S., Zale, J., Gwinn, K.D., and Ownley, B.H. 2011. First report of leaf spot caused by *Bipolaris spicifera* on switchgrass in the United States. Plant Dis. 95:1191-1191.

Weichert, H., Stenzel, I., Berndt, E., Wasternack, C., and Feussner, I. 1999. Metabolic profiling of oxylipins upon salicylate treatment in barley leaves - preferential induction of the reductase pathway by salicylate. FEBS Lett. 464:133-137.

Weiner, A.M., and Maizels, N. 1987. tRNA-like structures tag the 3' ends of genomic RNA molecules for replication: implications for the origin of protein synthesis. Proc. Natl. Acad. Sci. USA 84:7383-7387.

White, K.A., and Morris, T.J. 1999. Defective and Defective Interfering RNAs of Monopartite Plus-strand RNA Plant Viruses. Pages 1-17 in: Satellites and Defective Viral RNAs, P. Vogt and A. Jackson, eds. Springer Berlin Heidelberg.

Whitham, S.A., Yang, C., and Goodin, M.M. 2006. Global impact: elucidating plant responses to viral infection. Mol. Plant Microbe Interact. 19:1207-1215.

Xu, J., Li, Y., Ma, X., Ding, J., Wang, K., Wang, S., Tian, Y., Zhang, H., and Zhu, X.-G. 2013. Whole transcriptome analysis using next-generation sequencing of model species *Setaria viridis* to support C4 photosynthesis research. Plant Mol. Biol. 83:77-87.

Yuan, Y., Zhong, S., Li, Q., Zhu, Z., Lou, Y., Wang, L., Wang, J., Wang, M., Li, Q., Yang, D., and He, Z. 2007. Functional analysis of rice NPR1-like genes reveals that OsNPR1/NH1 is the rice orthologue conferring disease resistance with enhanced herbivore susceptibility. Plant Biotechnol. J. 5:313-324.

Zhang, C., Cascone, P.J., and Simon, A.E. 1991. Recombination between satellite and genomic RNAs of *Turnip crinkle virus*. Virology 184:791-794.

Zhou, N., Tootle, T.L., Tsui, F., Klessig, D.F., and Glazebrook, J. 1998. PAD4 functions upstream from salicylic acid to control defense responses in Arabidopsis. Plant Cell 10:1021-1030.

Zhu, S., Jeong, R.-D., Venugopal, S.C., Lapchyk, L., Navarre, D., Kachroo, A., and Kachroo, P. 2011. SAG101 forms a ternary complex with EDS1 and PAD4 and is required for resistance signaling against *Turnip crinkle virus*. PLOS Pathog. 7:e1002318.

APPENDIX A

SUPPLEMENTARY FIGURES

Page

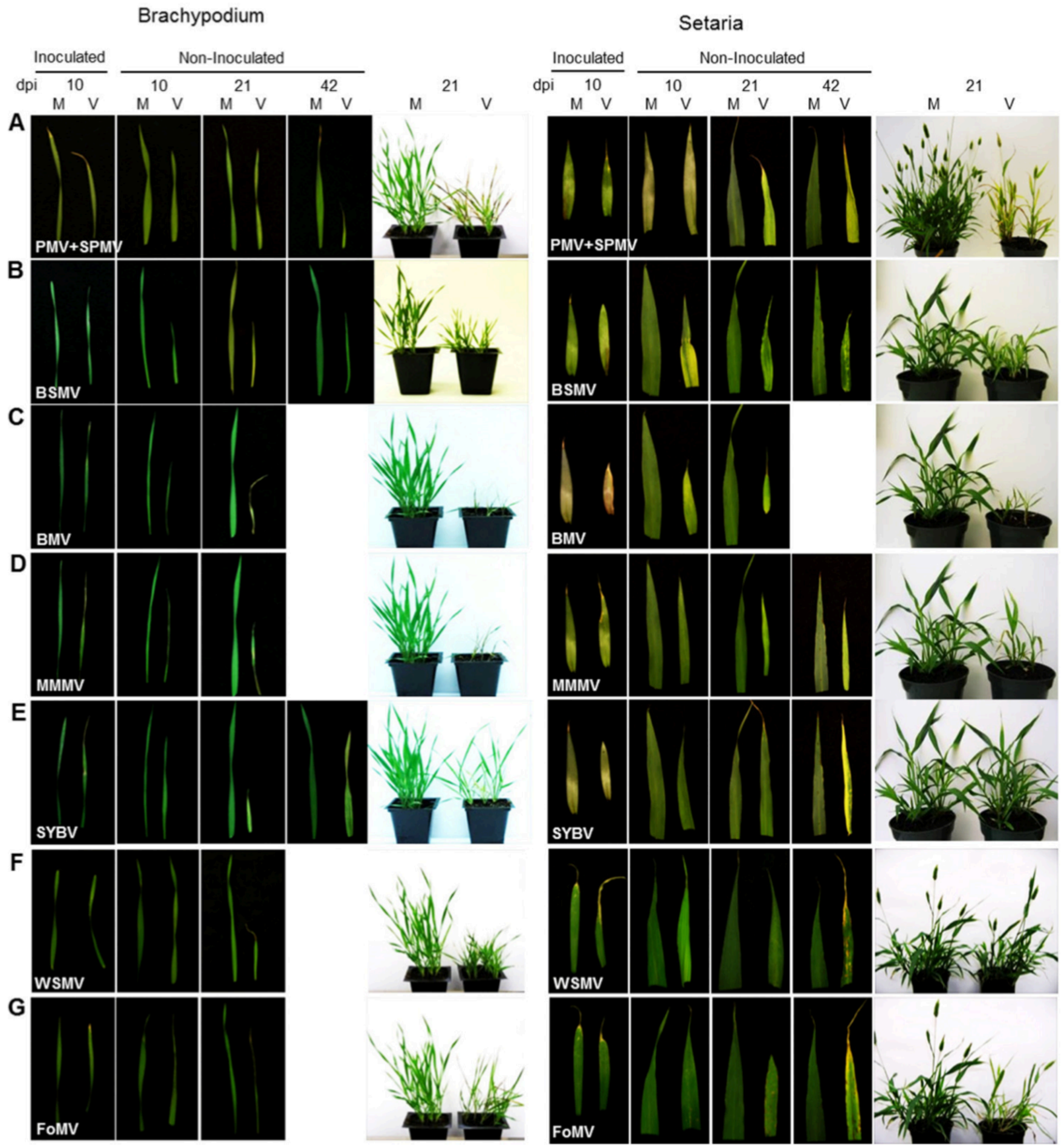

Supplementary Figure 2.1. Typical disease symptoms of virus-infected Brachypodium and Setaria. Symptoms induced by (A) PMV+SPMV, (B) BSMV, (C) BMV, (D) MMMV, (E) SYBV, (F) WSMV, and (G) FoMV at 10 (Stage I), 21 (Stage II) and 42 (Stage III) days post-inoculation (dpi). All viruses, with the exception of SYBV, caused prominent chlorosis and necrosis of leaves and severe stunting of plant height. Stage I is characterized by mild to no visible chlorosis on leaves, stage II with mild to severe chlorosis on leaves, and stage III with prominent chlorosis and necrosis on leaves, stunting, and reduced seed-set for most viruses. BMV-infected plants survived only until stage II. "M" represents mock-inoculated plants and "V" indicates virus-infected plants.

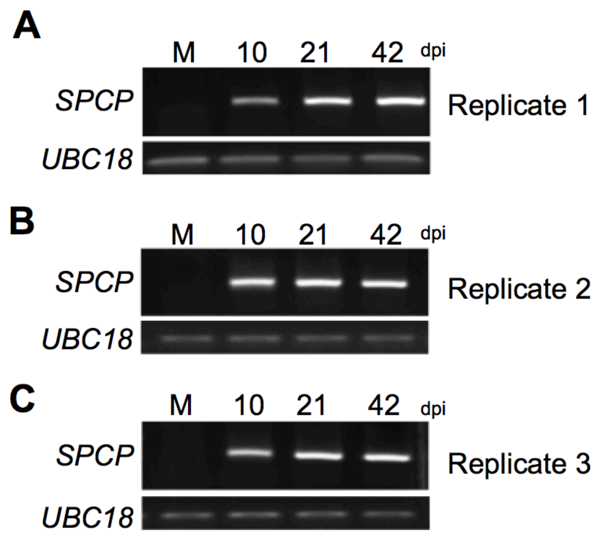

Supplementary Figure 2.2. RT-PCR detection of SPMV RNA accumulation at infection stages I (10 dpi), II (21 dpi) and III (42 dpi) in mock-inoculated and PMV+SPMV-infected Brachypodium in the three biological replicates (A-C). The primers used for RT-PCR are specific to the open reading frame for the SPMV capsid protein (SPCP). "M" represents cDNA from mock-inoculated samples at stage III. Brachypodium *UBIQUITIN18* (*UBC18*) was used to monitor template cDNA quantities used for the different samples.

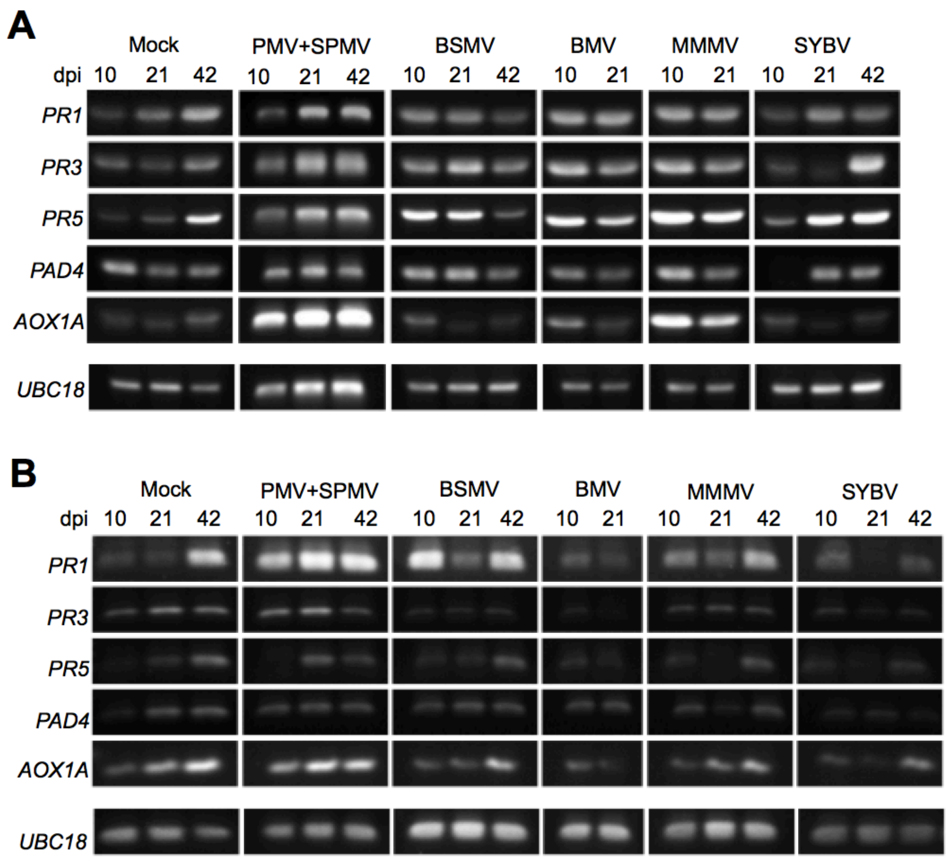

Supplementary Figure 2.3. Preliminary RT-PCR tests of defense marker gene expression at infection stages I (10 dpi), II (21 dpi) and III (42 dpi) for mock-inoculated, PMV+SPMV-, BSMV-, BMV-, MMMV-, and SYBV-infected (A) Brachypodium, and (B) Setaria. For Brachypodium, the BMV- and MMMV-infected plants did not survive through stage III. For Setaria, BMV-infected plants did not survive through stage III. *UBIQUITIN18* (*UBC18*) was used to monitor template cDNA quantities used for the different samples. WSMV and FoMV infections had not been established at the time of these preliminary analyses.

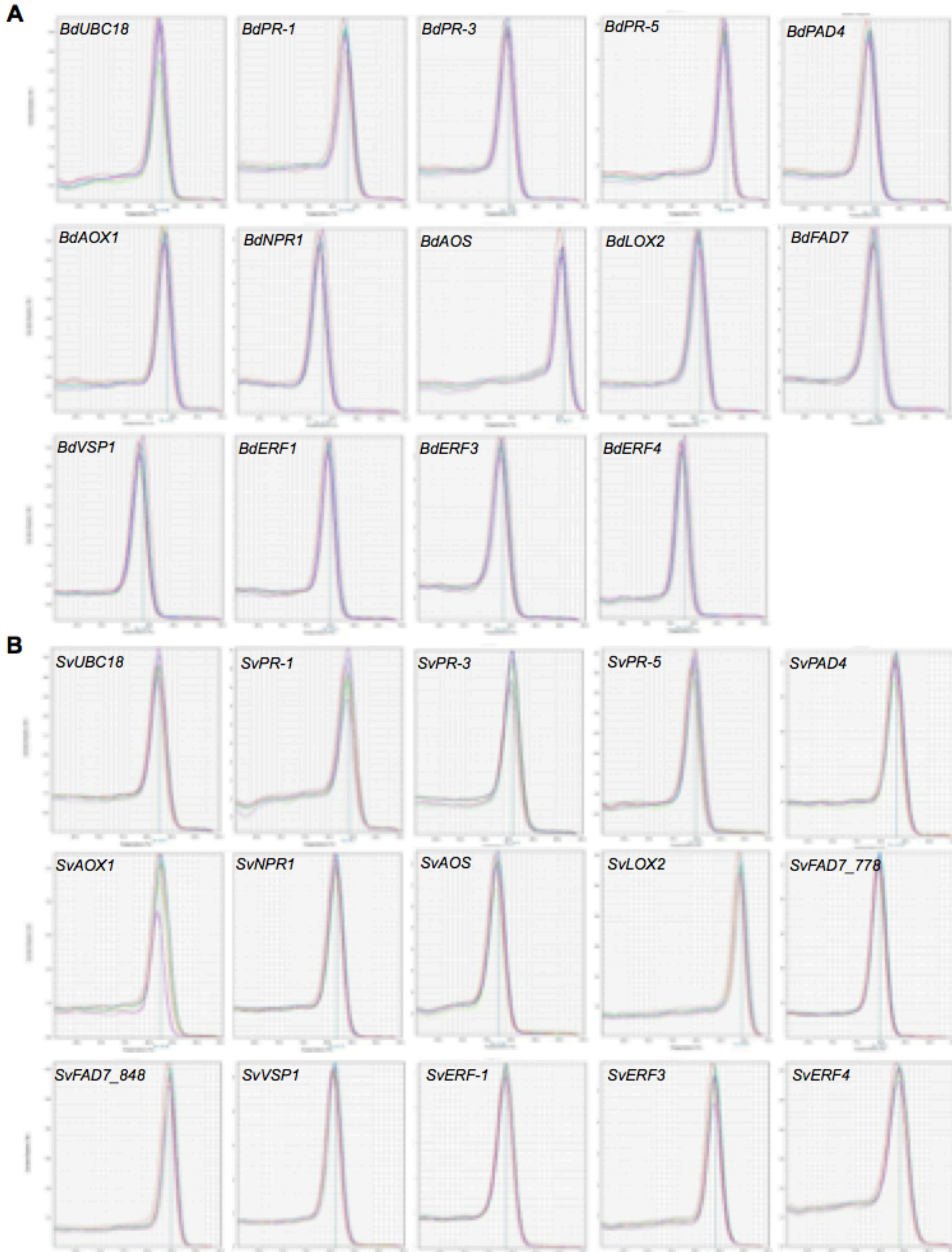

Supplementary Figure 2.4. Quality control and specificity of (q) RT-PCR analyses. The post-amplification dissociation curve analysis of (q) RT-PCR reactions show single product peaks with no primer-dimer and/or non-specific amplicons in mock and virus-infected samples for individual genes in (A) Brachypodium and (B) Setaria. The melting temperature of the PCR products is plotted on the X-axis and the derivative reporter fluorescence on the Y-axis.

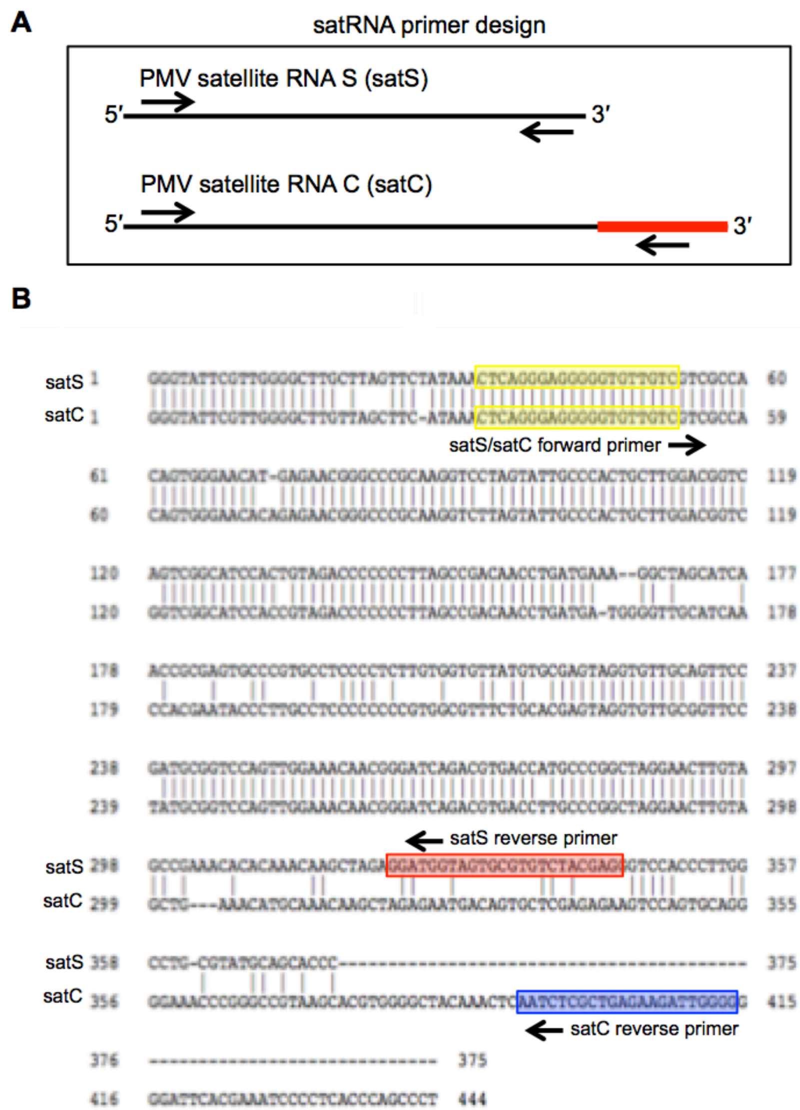

Supplementary Figure 3.1. Model for satS- and satC-specific primer design for RT-PCR analysis. The approximate positions of the forward and reverse primers are illustrated by arrows on the genomic RNA representations of satS and satC (A). The red line for satC indicates the region of sequence similarity with the terminal 3′-end of the PMV genomic RNA. A sequence alignment of satS and satC is shown to illustrate the regions of sequence similarity, and the primer binding regions (B). A region of sequence identity in the 5′-region of the satS/satC genomic RNA (yellow) was selected for design of the satS/satC forward primer. The reverse primer sequence regions for satS (red) and satC (blue) were selected based on sequences unique to each satRNA.

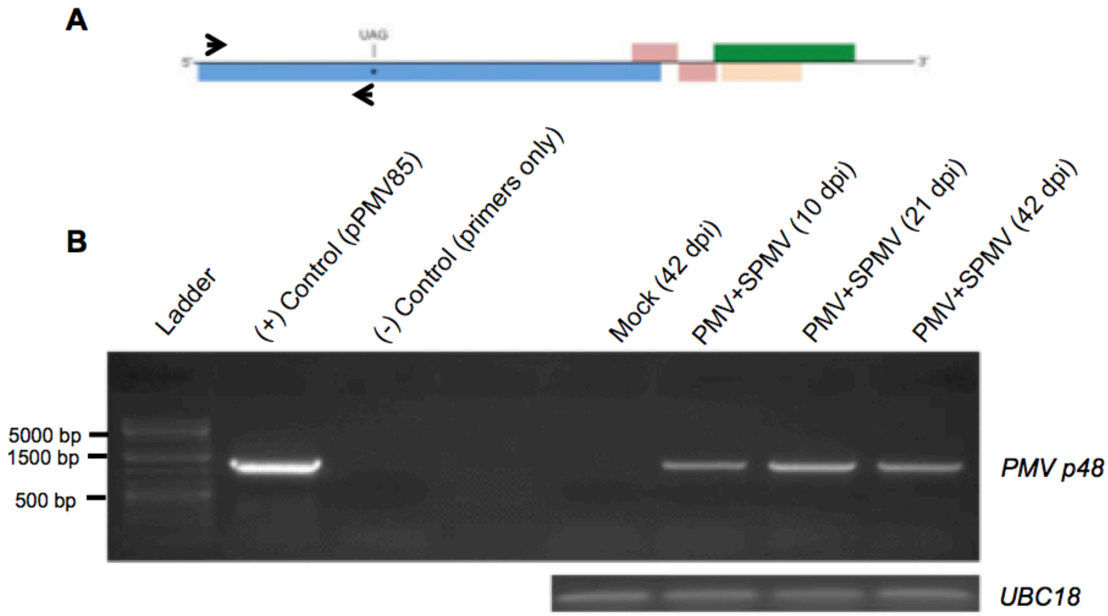

Supplementary Figure 3.2. RT-PCR analysis of the *PMV p48* ORF from oligo-dT primed cDNA samples. Total RNA was isolated from Mock-inoculated and PMV+SPMV-infected Brachypodium at 10, 21, and 42 dpi, as part of a previous study (Mandadi, et al. 2014). Total cDNA was prepared for each sample using oligo-dT primers for first-strand synthesis. A model of the PMV genomic RNA and ORFs is shown in A. The arrows indicate the forward and reverse primer binding regions for amplification of the *p48* ORF. *PMV p48* was amplified by RT-PCR, using the pPMV85 cDNA plasmid as a positive control (B). *UBIQUITIN18* (*UBC18*) was used to monitor template cDNA quantities used for the different Mock- and PMV+SPMV-infected samples.

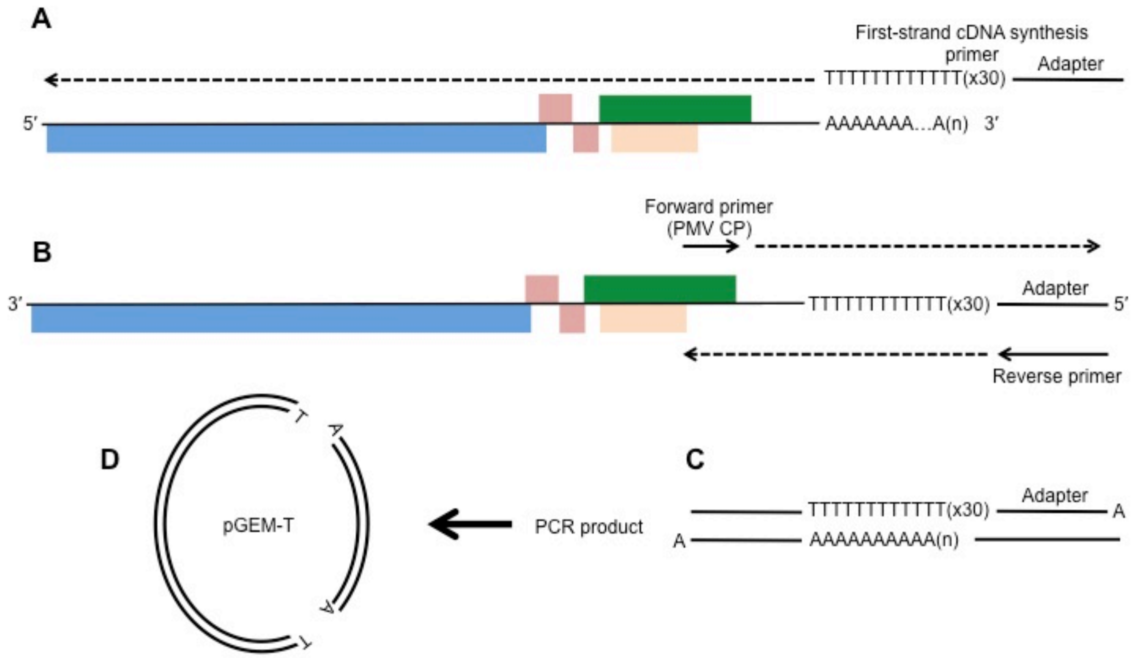

Supplementary Figure 3.3. Strategy for cloning of the polyadenylated viral and subviral RNAs. A hypothetical representation of a polyadenylated RNA genome of PMV is depicted for visualization. First-strand cDNA synthesis (A) will be performed using an oligo-dT primer designed with a 25 nucleotide 5′-overhang adapter sequence. PCR amplification (B) will be performed using PMV-, SPMV-, and satRNA-specific forward primers and the universal adapter reverse primer. PCR products (C) will be ligated into T-overhang pGEM-T vectors (D) for sequencing.

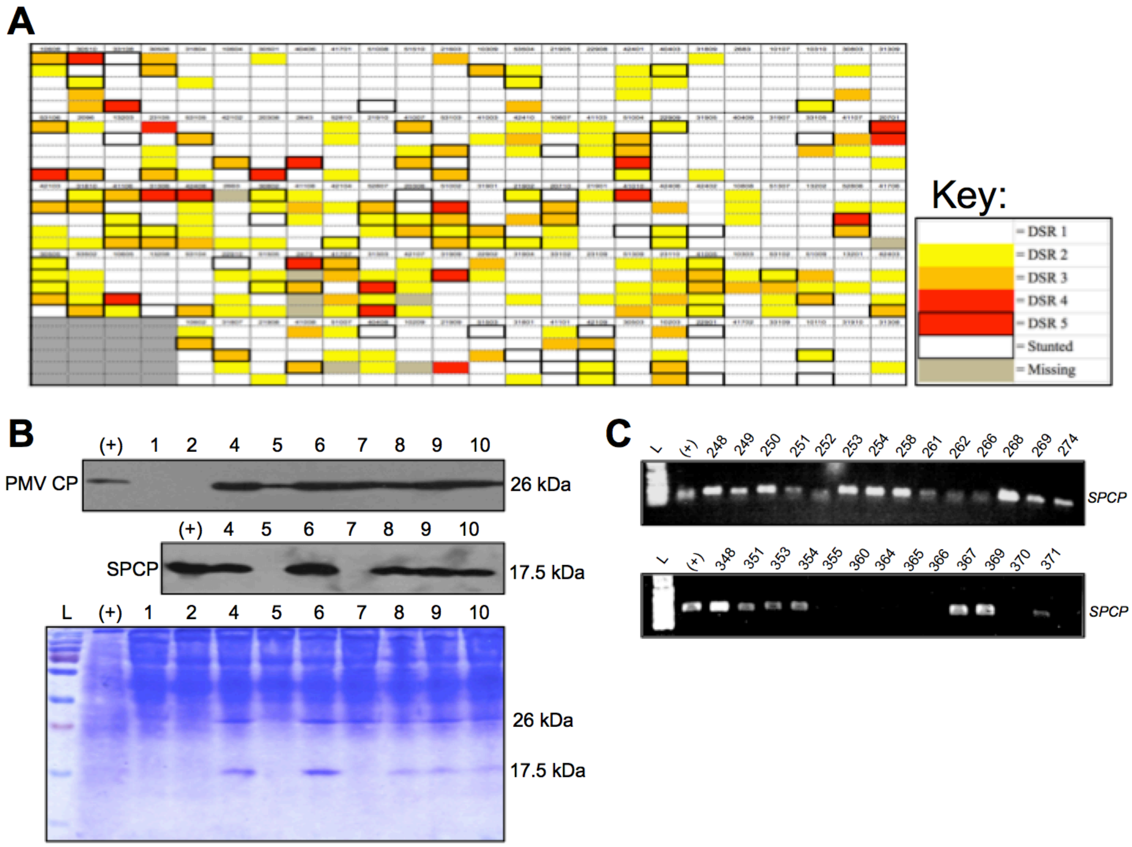

Supplementary Figure 4.1. Field distribution of symptomatic switchgrass and virus diagnostics. A representative field plot of switchgrass individuals with varying disease severity ratings (DSRs) is illustrated for Block 3 of field PV1104 in 2012 (A). Samples from 2012 were tested for the presence of *Panicum mosaic virus* (PMV) and its satellite virus (SPMV) via immunoblotting (B). Immunoblotting was performed using antibodies specific to either the PMV or SPMV capsid proteins (PMV CP, SPCP). Sample numbers shown in B (1, 2, 4-10) represent select switchgrass individuals from field PV1103 in 2012. A polyacrylamide gel stained with Coomassie Brilliant Blue R-250 is shown to represent approximate equal protein loading among samples, and to provide a visualization of the PMV CP (26 kDa) and SPCP (17.5 kDa) accumulation within infected samples. Randomly sampled switchgrass individuals in 2013 and 2014 were tested for the presence of SPMV via reverse transcription polymerase chain reaction (RT-PCR) (C). The SPCP open reading frame was amplified using virus-specific primers. The PCR products were visualized on 1% agarose gels stained with ethidium bromide. Sample numbers shown in C represent select switchgrass individuals tested in 2014. Lanes labeled with “L” contain either a protein (B) or DNA (C) molecular weight ladder. Lanes labeled with “(+)” contain samples from PMV+SPMV-infected positive control plants.

APPENDIX B

SUPPLEMENTARY TABLES

Gene	Primer	Sequence (5′ to 3′)
PR1	Bradi1g57580.1_F	AGCTCTGGCATCATCAGCATCC
	Bradi1g57580.1_R	CGTTGTGTGGGTCCAGGAAATC
PR3	Bradi3g48230.1_F	GCTCGGCTGATTGTTCAACACG
	Bradi3g48230.1_R	TTGCCCGAACCACAAATATGCC
PR5	Bradi1g13060.1_F	CCGACCGATTACTCCAGGTTCTTC
	Bradi1g13060.1_R	TAATTAGCTCGCTCGCTCGCTTG
PAD4	Bradi4g23367.1_F	GCGAGAGAAGGTATGAGCTGTTTG
	Bradi4g23367.1_R	TGGTGCAGCCAGTAAAGGTTCC
AOX1A	Bradi5g20547.1_F	ACTACGCCTCGGACATCCATTAC
	Bradi5g20547.1_R	AGGCATCGACCGTCCATTTGAG
NPR1	Bradi2g05870.1_F	TGCAATGGCTGGTGATTGTCTACG
	Bradi2g05870.1_R	ATATCCTCGCCAAGGCAACTCG
AOS	Bradi3g01110.1_F	AACAATGGTGCGATCGGCTTCG
	Bradi3g01110.1_R	CCGTGGGACCTCAAGGTAAAGTTC
LOX2	Bradi3g07010.1_F	GCGGCGTTCGAGAAGTTCAATG
	Bradi3g07010.1_R	GTCCTGGTTATTGTTTCGCTCGTC
FAD7	Bradi1g16580.1_F	CATCATGGCCACAACGACAAGC
	Bradi1g16580.1_R	CACGCAGATAGCTCCATTCCTTTC
VSP1-like	Bradi1g51330.1_F	CGTCACGGTGGACAATCTCAAG
	Bradi1g51330.1_R	AGCTGCTGCCCTCAATATAAGCC
ERF1	Bradi3g50490.1_F	TGGTGCCGTGTGAAATTTGTCG
	Bradi3g50490.1_R	CAGATTTCGCTGCACCACTTGC
ERF3	Bradi5g25570.1_F	AGGATTTGCGCCAAATTGTGCAG
	Bradi5g25570.1_R	ATCCAAGAGGGCGTGCAAAGAG
ERF4-like	Bradi2g52370.1_F	CGTTGAGATGAGCGGAACCTTG
	Bradi2g52370.1_R	TTCAACGACGGACGGAATCGAC
UBC18	Bradi4g00660.1_F	ACAGCAATGGCCACATCTGTTTAG
	Bradi4g00660.1_R	TTGTCTTGCGGACGTTGCTTTG

Supplementary Table 2.1. Brachypodium defense marker genes in SA, JA, and ET signaling used in this study. The gene descriptions were deduced from peptide ortholog analysis with inferred Arabidopsis protein sequences on Phytozome (Goodstein et al., 2012), as well as phylogenetic analysis (Mandadi and Scholthof, 2012). Brachypodium genes that were difficult to characterize as an ortholog or had multiple homologs with high similarity to their respective Arabidopsis orthologs (e.g., *VSP1* and *ERF4*) are indicated as “-like”.

Gene	Primer	Sequence (5′ to 3′)
PR1 (66.1%)	Si031297m_F	TCTTCATCACCTGCAACTACAACC
	Si031297m_R	GTATTCATTGAGGCGGCAGTCG
PR3 (72.2%)	Si018061m_F	ATGTCATGTGCGTGGTGTGAGG
	Si018061m_R	ATCAGAACGGCGCACGCTATAC
PR5 (73.6%)	Si037366m_F	AGCTCCGCGTAGAGCAACTAATC
	Si037366m _R	TGGAGGATGGAAGCCATTTCTGC
PAD4-like (57.7%)	Si026081m_F	ACTACGACGCGTTCAAGAAGCAG
	Si026081m_R	AGCTTGAACCGGCACATGTTGG
AOX1A-like (86.7%)	Si010539m_F	GTCAACCACTTCGCATCGGACATC
	Si010539m_R	ACCAGTCCTGATCTGCTAAGCAAC
NPR1 (79.6%)	Si000814m_F	AGGTTCCATGACCTGCAAGACG
	Si000814m_R	AACGGGCTGACCTGTCATTCTC
AOS (78.3%)	Si016973m_F	GGAGCGCAATGAGCAATTGAGG
	Si016973m_R	TTATCAGCGGCTGGATCGGAAC
LOX2 (78.1%)	Si016269m_F	CTTCTTCACCGTCAAGTCGTACC
	Si016269m_R	CGTTGTACACGTCGTAGTCGTAG
FAD7_778-like (70.1%)	Si035778m _F	TGGCTGGTCTCACCTTTGTGATG
	Si035778m_R	TCCAGCCAAGCAACAAATACCAAG
FAD7_848-like (71.7%)	Si011848m_F	ACTACAGGGAGCCACAGAAGTC
	Si011848m_R	CTGCTGCAGTGTTCAAGGTGTG
VSP1-like (72.2%)	Si036789m_F	AGATGGAAGCAGAAGGGTACAGG
	Si036789m _R	AGCACTCATGGAAGAGCCAAGC
ERF1 (74.7 %)	Si017941m_F	TGTCGTATTGGTGCGTCATCGC
	Si017941m_R	ACGGAGAAGCTTCCGATTTCAACC
ERF3 (28.3 %)	Si023330m_F	TCAGAACGACGAACAGCTTGCC
	Si023330m_R	CGTGTCGCACATCATCCTATCCTG
ERF4-like (76.5%)	Si002729m _F	TTTCCGTTCAAGGGCTACCCTGTC
	Si002729m_R	CGCCTGTTCGTAGAAGAAGTACGG
UBC18 (93.8%)	Si023498m_F	GTTGTCTAGTTCGCCAGCAAAGC
	Si023498m_R	TCCCATTGCGGCAGTTCCTAAC

Supplementary Table 2.2. Setaria defense marker genes in SA, JA, and ET signaling used in the study. The percentage similarity of the predicted Setaria proteins with the orthologous Brachypodium proteins are indicated in parenthesis. *S. viridis* gene primers were designed based on the annotated genome sequence of its highly syntenic, domesticated relative, *S. italica* (Bennetzen et al., 2012). All primers were verified for specific matches to the *S. viridis* raw sequence libraries using SRA-BLAST analyses and were further tested by RT-PCR. Setaria genes that were difficult to characterize as an ortholog (e.g., *PAD4, AOX1A, VSP1*, and *ERF4*) or had multiple homologs (e.g., *FAD7*) with high similarity to their respective Brachypodium orthologs are indicated as "-like".

Primer	Use in this study	Sequence (5′ to 3′)
PMV_CP_F	RT-PCR detection	ATGAATCGCAATGGAGCTAC
PMV_CP_R	RT-PCR detection	TTATGCGCTAACCCCACTGA
PMV_p8_F	RT-PCR detection	ATGTCTACTGTTGAGACTCC
PMV_p8_R	RT-PCR detection	CTAGAAATTGAAGTTGAAAG
PMV_p6.6_F	RT-PCR detection	ATGGCGACCGGCAAGTGCTA
PMV_p6.6_R	RT-PCR detection	TCATTTCTGGATCTCAATGT
PMV_p48_F	RT-PCR detection	ATGGAGTCGCTCATACAGCACA
PMV_p48_R	RT-PCR detection	CTACTTGGCAAACCTCAGACCC
PMV_polyA_F	Polyadenylation cloning	ATCAGTGGGGTTAGCGCATAA
SPCP_F	RT-PCR detection	ATGGCTCCTAAGCGTTCC
SPCP_R	RT-PCR detection	TTATGAAGACTGAAGCTCGC
SPMV87_F	RT-PCR detection	ATGGCTCCTAAGCGTTCCA
SPMV297_F	RT-PCR detection	GATGTATAACGCGCGCCTGTAT
SPMV297_R	RT-PCR detection	ATACAGGCGCGCGTTATACATC
SPMV541_R	RT-PCR detection	TTATGAAGACTGAAGCTCGC
Bd_UBC18_F	RT-PCR control	ACAGCAATGGCCACATCTGTTTAG
Bd_UBC18_R	RT-PCR control	TTGTCTTGCGGACGTTGCTTTG
Pv_UBC18_F	RT-PCR control	ATGACGAGCTCCTCCTCTCCT
Pv_UBC18_R	RT-PCR control	AACCACCATCTGGTCTCCTTC
satS/C_F	RT-PCR detection, satS cloning	CTCAGGGAGGGGGTGTTGTC
satS_R	RT-PCR detection	CTCGTAGACACGCACTACCATC
satC_R	RT-PCR detection, satS cloning	CCCCAATCTTCTCAGCGAGATT
OligodT_adapter	Polyadenylation cloning	AAGCAGTGGTATCAACGCAGAGTACT TTTTTTTTTTTTTTTTTTTTTTTTTTTTTT
Adapter_R	Polyadenylation cloning	AAGCAGTGGTATCAACGCAGAGTAC
M13_F	Polyadenylation/satS sequencing	GTAAAACGACGGCCAG
M13_R	Polyadenylation/satS sequencing	CAGGAAACAGCTATGAC

Supplementary Table 3.1. List of DNA primers used in this study. Primer names are listed in the left column, with the trailing _F and _R indicating forward and reverse primers, respectively. Primers used for "RT-PCR detection" were utilized in multiple experiments for amplification of the PMV, SPMV, and satS/satC genomic RNAs accordingly. Additional primers were used as RT-PCR cDNA controls (Bd/PvUBC18) and for cloning and sequencing of the satS-PMV chimeras and polyadenylated PMV RNAs.

Experiment	Cultivar or experimental strain in each experiment or nursery	Breeding history of experimental strain or population type
PV0910		
Genetic study nursery of 150 clonally replicated (r=3) spaced plants of five switchgrass strains	**Kanlow**	Released lowland tetraploid cultivar
	Kanlow N1	Population based on 72 Kanlow genotypes that survived a minimum of 2 winters at the ARDC with minimal winter injury and had good vigor.
	Kanlow N1 Early Mat-High Yield C1 = **Kanlow High Yield**	Population based on early maturing plants in the Kanlow N1 cycle 1 selection nursery.
	NE Summer = **Summer**	Nebraska re-generation of the upland tetraploid cultivar Summer.
	Kanlow X Summer HP1 High Yield C1= **KxS**	F3 progeny of cross between select Kanlow (male) x Summer (female) plants
PV1103		
KxS HP1 NETO2 C3 selection nursery; replicated plots (r=3) of five spaced plants	111 half-sib families.	Half-sib families were produced by harvesting seed from individual genotypes in the KxS NETO2 C2 polycross nursery
	Check strains:	
	Kanlow	
	KxS HP1 C0	Progeny of Kanlow (male) x Summer (female) plants that had gone through 2 generations of random mating and increase to stabilize the population.
	Liberty	Released cultivar developed from KxS HP1 C0 by one breeding generation with selection for high index NETO2 (ethanol selection index 2). Experimental name was KxS HP1 NETO2 C1. NETO2 index selected for high biomass yield with low lignin concentration.
	NE Summer	
	Shawnee	Released upland octaploid cultivar
PV1104		
Summer Late Mat HYLD C3 selection nursery; replicated plots (r=4) of five spaced plants	89 half-sib families.	Half-sib families were produced by harvesting seed from individual genotypes in the Summer Late Mat HYLD C2 polycross nursery
	Check strains:	
	Kanlow	
	Liberty	
	NE Summer	
	Shawnee	
	Summer Late Mat-HYLD C1	Population based on plants from Summer selected for late maturity, high biomass yield, and overall vigor.

Supplementary Table 4.1. Switchgrass cultivars and experimental strains evaluated for viruses in the USDA-ARS breeding nurseries at the University of Nebraska Agriculture Research and Development Center (ARDC) located near Ithaca, NE. Cultivar or strain names in bold are the names used in referring to populations planted in PV0190.

	No PMV	PMV only	PMV+SPMV
PV1103	26	2	27
PV1104	12	0	41
PV0910			
Summer	18	12	23
KxS	35	8	12
Kanlow	51	4	0
Kanlow N1	55	1	2
Kanlow High Yield	58	2	0

Supplementary Table 4.2. Incidence of *Panicum mosaic virus* (PMV) and its co-infecting satellite virus (PMV+SPMV) among randomly sampled switchgrass plants during the 2013 growing season. Leaf samples were collected from more than 50 plants in breeding nurseries PV1103 and PV1104 and the five named switchgrass populations that were planted in PV0910 (Supplementary Table 4.1) and tested for the presence of PMV by double antibody sandwich enzyme-linked immunosorbent assay (DAS ELISA) and for SPMV by reverse transcription polymerase chain reaction (RT-PCR). The numerical values shown here are represented as stacked bar graphs in Figure 2.

PV1103	DSR 1	DSR 2	DSR 3	DSR 4	DSR 5
No PMV	19	6	1	0	0
PMV only		1	1	0	0
PMV+SPMV	6	9	8	4	0
PV1104	**DSR 1**	**DSR 2**	**DSR 3**	**DSR 4**	**DSR 5**
No PMV	11	1	0	0	0
PMV only	0	0	0	0	0
PMV+SPMV	9	9	9	8	6

PV0910 (5 Cultivars)

Summer	DSR 1	DSR 2	DSR 3	DSR 4	DSR 5
No PMV	11	6	1	0	0
PMV only	6	4	2	0	0
PMV+SPMV	7	7	2	4	3
Kanlow X Summer	**DSR 1**	**DSR 2**	**DSR 3**	**DSR 4**	**DSR 5**
No PMV	29	5	0	1	0
PMV only	3	4	0	1	0
PMV+SPMV	7	2	3	0	0
Kanlow	**DSR 1**	**DSR 2**	**DSR 3**	**DSR 4**	**DSR 5**
No PMV	38	12	1	0	0
PMV only	3	0	1	0	0
PMV+SPMV	0	0	0	0	0
Kanlow High Yield	**DSR 1**	**DSR 2**	**DSR 3**	**DSR 4**	**DSR 5**
No PMV	51	6	1	0	0
PMV only	1	1	0	0	0
PMV+SPMV	0	0	0	0	0
Kanlow N1	**DSR 1**	**DSR 2**	**DSR 3**	**DSR 4**	**DSR 5**
No PMV	51	3	1	0	0
PMV only	0	1	0	0	0
PMV+SPMV	1	1	0	0	0

Supplementary Table 4.3. Relationship between presence of *Panicum mosaic virus* (PMV) and its co-infecting satellite virus (PMV+SPMV) and disease severity rating (DSR) of randomly sampled switchgrass in 2013. DSR 1 denotes no symptoms, DSR 5 the highest symptom severity. Individuals from switchgrass breeding nursery fields PV1103, PV1104, and five populations in field PV0910: Summer, Kanlow x Summer, Kanlow, Kanlow High Yield, and Kanlow N1 (Supplementary Table 4.1). The numerical values shown here are represented as stacked bar graphs A-G in Figure 3.